UNIVERSITY OF TURKU

Petrography and emplacement mechanism of the Tanhua mafic complex in Central Lapland greenstone belt

Geology/ Faculty of Science
Master's thesis

Author:
Patrik Jänkävaara

Supervisors:
PhD Esa Heilimo
PhD Jukka Konnunaho

29.9.2023
Turku

Master's thesis

Subject: Geology
Author: Patrik Jänkävaara
Title: Petrography and emplacement mechanism of the Tanhua mafic complex in Central Lapland greenstone belt
Supervisors: PhD Esa Heilimo and PhD Jukka Konnunaho
Number of pages: 68 pages
Date: 29.9.2023

The Tanhua mafic complex consists of three different mafic intrusions (Kylälampi, Kannusvaara, and Markkinaselkä) in ca. 54 km^2 area. The complex locates ca. 45 km from Sodankylä towards NE. The country rocks contain Paleoproterozoic supracrustal rocks of Central Lapland Greenstone Belt (CLGB) as quarzites and mafic vulcanic rocks. The Tanhua mafic complex contains elevated concentrations of Co and Cu.

The conducted petrographic studies aimed at determining the main rock types of the Tanhua mafic complex and resulted in sub-division into three main rock types: gabbros, diorites and tonalites. Based on detailed petrographic studies, gabbros could be futher subdivided to four groups: gabbros, oxide gabbros, remained mottled gabbros and biotitized mottled gabbros. All rocks of the Tanhua mafic complex are metamorphosed in middle amphibole facies and post-magmatic hydrothermal alterations including albitization, scapolitization and biotitization have been significant.

The benchtop micro–X-Ray Fluorescence (XRF) instrument was used to support petrographic studies and determine the localization of Co- and Zr-bearing minerals within the Tanhua mafic complex. The results indicates that Co is present in mineral lattice of pyrite where Co^{2+}-ions replaces Fe^{2+}-ions. Zr locates in the zircon mineral, which commonly occur together with plagioclase. Sulphides, mainly pyrite and chalcopyrite as well as magnetite, occur as dissemination and veinlets in the Tanhua mafic complex.

In this work, I propose that multiple magma pulses have formed the Tanhua mafic complex. Chilled margins together with cross-cutting relationships of rock units are the most important evidence for the presence of multiple magma pulses of the Tanhua mafic complex. Also, the stratigraphy of the Tanhua mafic complex supports the multiple magma pulses as the Tanhua mafic complex lacks typical layered structure of layered intrusions and rock units appear in disorder with multiple chilled margins representing magma flows. The abundant magnetite indicates elevated Fe contents which designates that the magma pulses originated from the same magma chamber. The S and Co are probably not magmatic in origin but rather from country rocks and their enrichment would be associated with hydrothermal fluids. The source of Co might be Paleoproterozoic metavulcanic rocks, and the possible source of S is Paleoproterozoic schist occurring either below or above of the Tanhua mafic complex.

Key words: Tanhua, Central Lapland Greenstone Belt, petrography, gabbro, mafic intrusion, cobalt, multiple magma pulses, alteration.

Pro gradu-tutkielma

Oppiaine: Geologia
Kirjoittaja: Patrik Jänkävaara
Otsikko: Tanhua mafisen compleksin petrografia ja syntymekanismi Keski-Lapin vihreäkivi vyöhykkeellä
Ohjaajat: FT Esa Heilimo ja FT Jukka Konnunaho
Sivumäärä: 68
Päivämäärä: 29.9.2023

Tanhuan mafinen kompleksi sisältää kolme erillistä mafista intruusiota (Kylälampi, Kannusvaara ja Markkinaselkä) noin 54 km^2 alueella. Se sijaitsee noin 45 km Sodankylästä koilliseen. Sivukivi koostuu Paleoproterotsooisista pintasyntyisistä kivistä, jotka kuuluvat Keski-Lapin vihreäkivi vyöhykkeeseen kuten kvartsiiteista ja mafisista vulkaniiteista. Tanhuan mafinen kompleksi sisältää kohonneita pitoisuuksia kobolttia ja kuparia.

Petrografisilla tutkimuksilla selvitettiin Tanhuan mafisen kompleksin pääkivilajit. Kivilajit jaettiin kolmeen pääkivilajiin, gabroihin, dioriitteihin ja tonaliitteihin. Yksityiskohtaisten petrografisten turkimusten perusteella gabrot voidaan vielä jakaa neljään alatyyppiin, gabrot, oksidi gabrot, säilyneet ”mottled” gabrot, sekä biotiittiutuneet ”mottled” gabrot. Kaikki Tanhuan mafisen kompleksin kivet ovat metamorfoituneet keskiasteen amfiboliitti fasieksessa ja post-magmaattinen hydroterminen muuttuninen, kuten albiittiutuminen, scaboliittiutuminen sekä biotiittiutuminen, on ollut merkittävää.

Pöytä mikro-röntgenflouresenssi (XRF) instrumenttia käytettiin petrografisten tutkimusten tukena sekä koboltin (Co) ja zirkonin (Zr) esiintymisen selvittämiseen Tanhuan mafisen kompleksin kivilajien mineraaleissa. Co esiintyy pyriitin kidehilassa, kun Co^{2+}-ioni korvaa Fe^{2+}-ionin. Zr on sitoutuneena zirkoni mineraaliin, jota esiintyy usein yhdessä plagioklaasin kanssa. Sulfidit, pääasiassa pyriitti ja kuparikiisu, esiintyvät pirotteena sekä suonina ja kapeina juonina Tanhuan mafisessa kompleksissa, kuten magnetiittikin.

Tässä työssä esitän, että useampi magmaattinen pulssi on muodostanut Tanhuan mafisen kompleksin. Jäähtymissaumat yhdessä kivilajiyksiköiden välisien leikkaussuhteiden kanssa ovat tärkein todiste useiden magmaattisten pulssien esiintymiselle Tanhuan mafisessa kompleksissa. Myös Tanhuan mafisen kompleksin stratigrafia tukee useita magmaattisia pulsseja, koska kerrosintruusioiden tyypillinen kerroksellinen rakenne puuttuu ja kivilajiyksiköt esiintyvät epäjärjestyksessä, siten että useita nopeasti jäähtyneitä kontakteja on säilynyt todisteena magma virroista. Runsas magnetiitin esiintyminen on osoitus magman Fe pitoisuudesta, joka viittaa siihen, että useat magmapulssit ovat lähtöisin samasta magmasäiliöstä. S ja Co eivät todennäköisesti ole magmaattista alkuperää vain ovat tulleet sivukivestä ja niiden rikastuminen on liittynyt hydrotermisiin fluideihin. Koboltin alkuperä voisi olla paleoproterosooinen metavulkaniitti, ja mahdollinen rikin lähde on paleoproterosooinen liuskekivi, joko Tanhuan mafisen kompleksin alla tai päällä.

Avainsanat: Tanhuan, Keksi-Lapin vihreäkivi vyöhyke, petrografia, gabro, mafinen intruusio, koboltti, useat magmapulssit, muuttuminen.

Table of contents

1 Introduction

Mafic-ultramafic intrusions vary from narrow dykes to large, layered intrusions up to more than 60000 km^2 in size. Some of the intrusions are formed from basaltic magma and can be found in different geotectonic environments (eg. Begg et al., 2018). Mafic-ultramafic intrusions contain important metallogenies e.g. platinum group element (PGE) metals, nickel (Ni), copper (Cu) and cobalt (Co). Some of these metals are listed as critical raw materials by EU and are important in green transition as these metals are required for batteries (Mondal & Griffin, 2018; European Commission, 2023). Co is used in batteries for electric cars and cell phones as well as in superalloys. It is challenging to replace, and the majority of Co is excavated from Democratic Republic of Congo, where exist problems with child labour and political instability (Yilanci et al. 2022).

The Central Lapland Greenstone Belt (CLGB) contains various economical mineral deposits (Figs. 1 and 2) hosted by mafic-ultramafic intrusions like Cu-Ni-PGE-Co deposits of Kevitsa (Mutanen, 2005; Brownscombe et al., 2015) and komatiite-related Cu-Ni-PGE-Co deposit of Sakatti (Santaguida et al., 2015; Makkonen et al., 2017). Koitelainen mafic-ultramafic intrusion locates also in CLGB, and contains Cr, PGE, and Fe-Ni-V mineralizations (Mutanen, 1997). The Tanhua mafic complex locates in northern Finland ca. 45 km NE from Sodankylä (Fig. 1). It is metamorphosed and partly hydrothermally modified group of mafic intrusions, that have positive magnetic characteristics (Vartiainen, 1971; Korvuo, 1975; 1977). The age of the intrusion is ca. 2.15-2.11 Ga based on U-Pb and Pb-Pb analyses (Huhma et al., 2018). The Tanhua mafic complex is related to CLGB and is surrounded by supracrustal metasedimentary and metavulcanic rocks (Köykkä et al., 2019). There are other mafic-ultramafic sulphide deposits associated with hydrothermally altered gabbros with elevated Co in CLGB as Hietakero mafic deposit (Konnunaho et al., 2018).

The Tanhua mafic complex contains mainly gabbros, which vary from oxide gabbros to non-magnetic gabbros, but also, intermediate, and felsic rocks are present in intrusions. The grain size of the Tanhua mafic complex varies from fine to coarse. The majority of the rocks of the Tanhua mafic complex are altered. Common alterations are albitization and biotitization. The Tanhua mafic complex in partly mineralized and contains disseminated and veined sulphides. Whole-rock compositions indicate that the mineralized part of the Tanhua gabbro contains Co up to 3000 ppm and Cu up to 1.4 wt% with low concentration of V (Konnunaho et al., 2022).

The aims of this study are: 1) Describe petrography of the lithological units within the Tanhua mafic complex and further sub-divide them into representative rock types. 2) Confirm the proposed multiple magma pulses theory for the forming process for the Tanhua mafic complex by Konnonaho (Personal communication 23.2.2022). 3) Point out cobalt and zircon bearing minerals in the Tanhua mafic complex. Additionally, I also propose emplacement mechanism of the Tanhua mafic complex. The mineralogy of the Tanhua mafic complex is compared to other mafic-ultramafic intrusion in northern Finland. In terms of methodology, I have used petrography and benchtop micro-X-ray fluorescence (XRF) instrument. I used MOVE and ArcMap softwares to presenting the cross-sections and maps.

Figure 1. Simplified map of mineralized mafic-ultramafic intrusions in Northern Finland. Coordinate system ETRS-TM35FIN Abbreviations, CLGB– Central Lapland Greenstone Belt, TNB–Tornio-Näränkävaara Belt, KGB – Karasjok Greenstone Belt. (FODD)

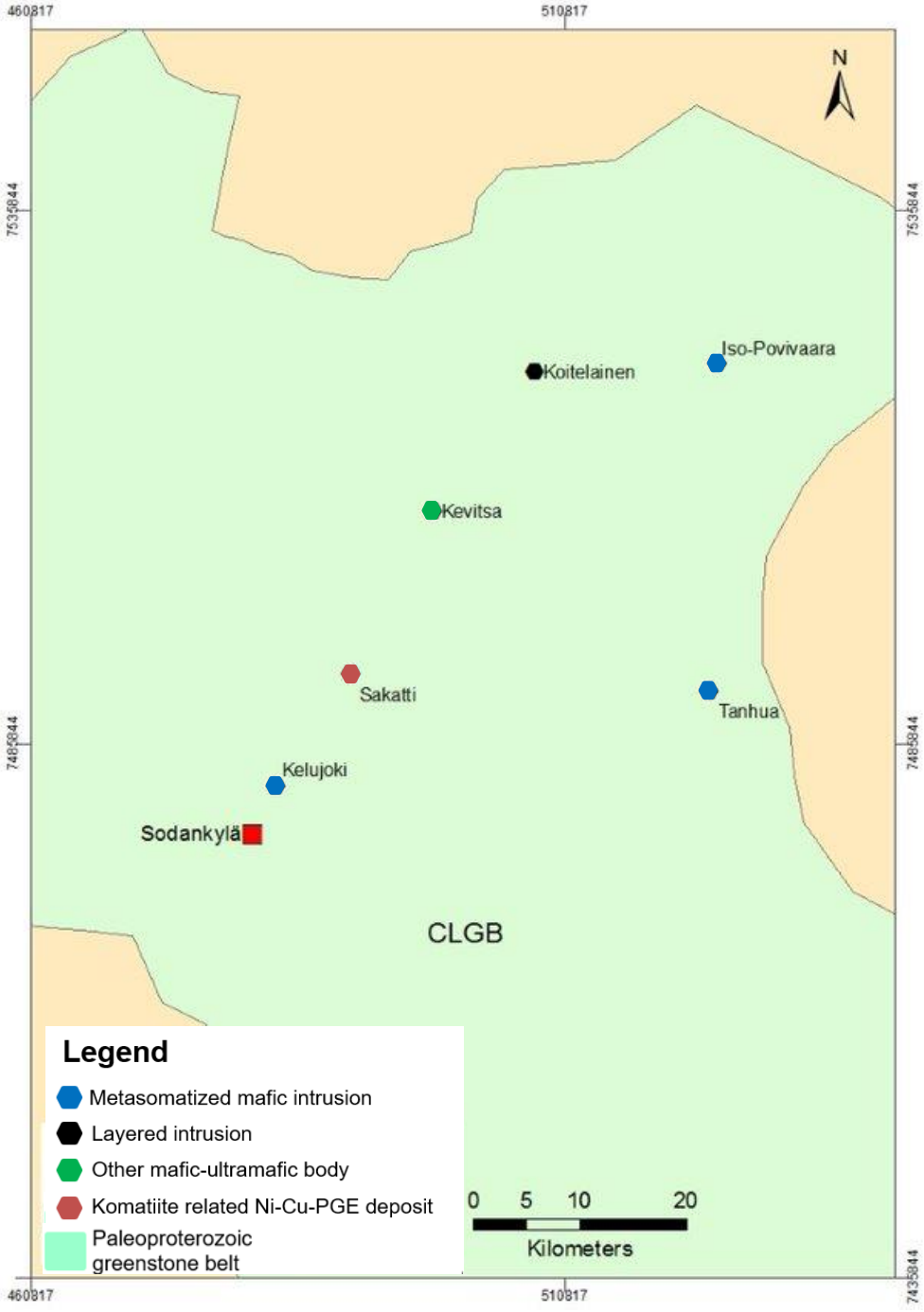

Figure 2. Simplified map presenting location of Kelujoki and Iso-Povivaara. Coordinate system ETRS-TM35FIN. Abbreviations, CLGB–Central Lapland Greenstone Belt. (FODD)

2 Mafic-ultramafic intrusions

2.1 General

Mafic-ultramafic intrusions are often studied around the world due to their economic potential. The mafic-ultramafic intrusions host orthomagmatic ore deposits and the metallogeny associated with mafic-ultramafic intrusion are typically Ni-Cu-Co-PGE and Cr-V-Ti-F. In addition, P as economical amounts can be present in V-Fe-Ti rich deposits (eg. Ripley & Li, 2018). Globally different types of mafic-ultramafic intrusions have been studied. Some intrusions are well fractionated as large, layered intrusions and Alaska-type intrusions (Irvine, 1998; Thakurta, 2018). Some intrusions are weakly fractionated as narrow dyke-shape intrusions. The size of the mafic-ultramafic can be from minor dyke <10 m^2 (Vuollo & Huhma, 2005) to up to large igneous bodies >60000 km^2 (VanTongeren, 2018).

2.1.1 Cumulus texture

Cumulate textures are common in layered mafic-ultramafic intrusion but also in other mafic-ultramafic intrusions (eg. Irvine, 1998; Thakurta, 2018). Cumulate textures (Fig. 3) are formed when mafic-ultramafic magma crystallizes and the first mineral to crystallize forms large euhedral grains and the rest of the magma fills the remaining interstitial spaces between the early crystallized grains. Orthocumulate textures are formed when the remaining magma cannot be in interaction with large magma chamber and therefore the remaining interstitial spaces are filled with other mineral than the euhedral mineral which may only have minor additional growth. Adcumulate textures require that remaining magma has interaction with a larger magma chamber and therefore the composition of the remaining magma changes and may bring material to increase the growth of cumulated minerals and therefore the interstitial space is minor. Poikilitic textures contain large oikocryst that occupies interstitial spaces and cumulated minerals occur as poikilitic minerals (Fig. 3; Wager, 1963; Irvine, 1980). The large cumulate minerals are accumulated physically by sinking or floating in magma chamber (Vernon, 2004).

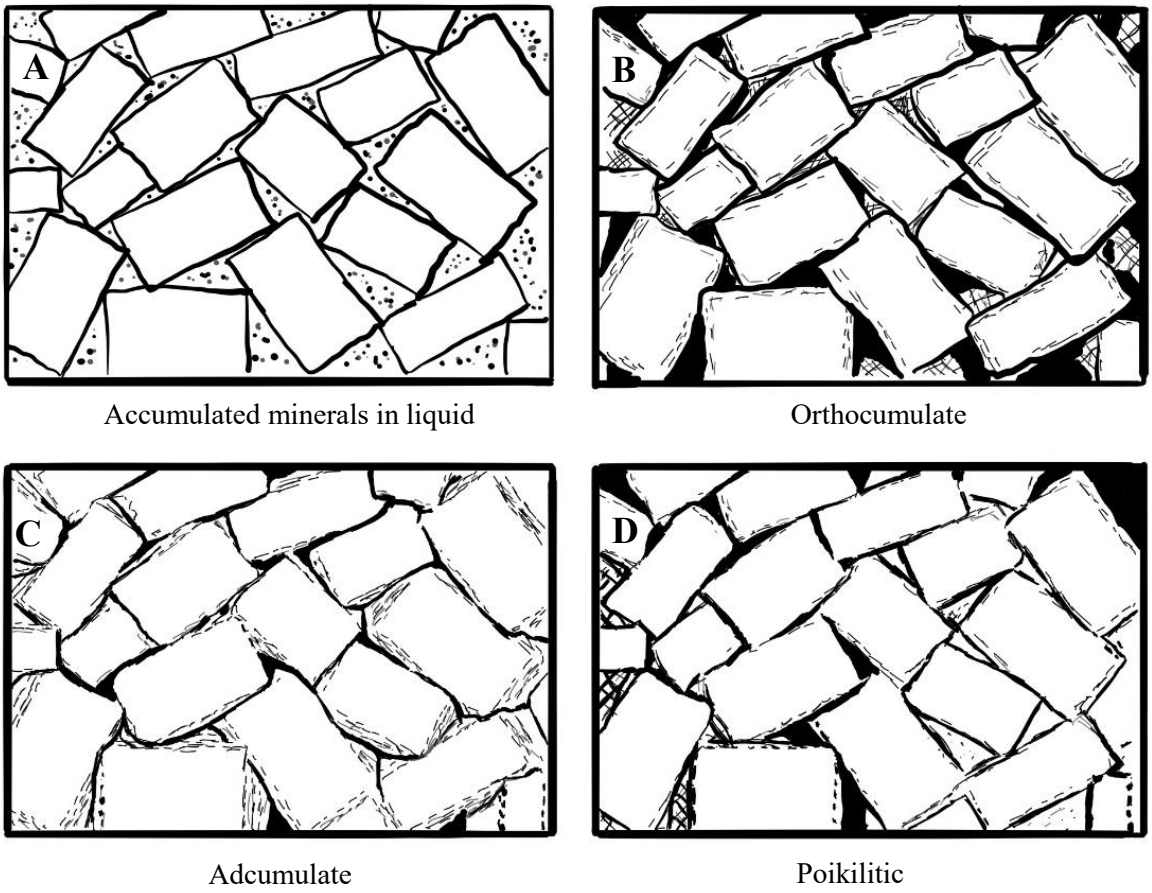

Figure 3. Thematic presentation of different cumulate textures. A) The plagioclase (white mineral) is crystallized first and cumulated. The remaining liquid fulfils the interstitial spaces. B) Orthocumulate texture, the remained magma has been trapped between the cumulated minerals and therefore cannot interact with larger magma chamber. The mineral crystallized from remaining magma is different than the euhedral cumulated mineral. C) Adcumulate, the remaining liquid has contact with larger magma chamber and the magmas has been mixed. Therefore, the euhedral cumulated minerals have been continued to grow with material from larger magma chamber. D) Poikilitic, the interstitial spaces are complete or partly fulfilled with one large oikocryst and the cumulated minerals are inside of this large grain as poikilitic mineral. (Modified after Wager & Brown, 1968)

2.1.2 Formation of mafic-ultramafic intrusion

Different theories to form layered intrusion have been proposed, but the most accepted conventional theory has been that these large intrusions would be formed by one extensive magmatic pulse, which is crystallized, fractionated, and layered in situ in one large magma chamber. The mechanism for differentiation is suggested to be gravitational settling. In this theory, the crystals grown and sink or float and therefore form differentiated layers (Naslund & McBirney, 1996; Irvine et al., 1998). This method is observed to some extend in the Skaergaard intrusion from Greenland, but it does not cover more complex layered intrusions and other methods has been suggested alone or in combination. Other differentiation methods are example recharge and magma mixing, in situ crystallization and convection. It is proposed that

the convection might be effective in both, within the whole magma chamber and the individual layers. The methods depend on different factor of the intrusion as example size, shape, grain size and mineral composition (Naslund & McBirney, 1996).

Recent studies propose that many of plutonic intrusion bodies have been formed by multiple magmatic pulses instead of one extensive magma pulse that would have fractionated in situ. (Annen, 2009; Latypov & Chistyakova, 2009). If the eruption time between two different magma pulses is more than crystallization time of one pulse, magmas from different pulses will not be mixed and in situ fractional differentiation apply to only separate pulses (Annen, 2009). Depending on the eruption time and content of multiple magma pulses, they can form either cyclic layer units or chaotic order of layers (Latopov et al., 2009). The formation of intrusion can take longer time if the intrusion is constructed from multiple magma pulses. Therefore, the age determination (if available) of different parts of the intrusion gives marginally different ages (Annen, 2009; Annen et al., 2015).

2.1.3 Orthomagmatic sulphide and oxide deposits in mafic-ultramafic intrusions

In mafic-ultramafic deposits, Ni, Cu, Co, and PGE are generally associated with sulphides, which are found as dissemination, net-textures, semimassive or massive sulphides, but also low-sulphide PGE deposits exists (eg. PGE reef-type deposits). In strongly differentiated layered intrusion sulphides form horizontal reefs between the layers of the intrusion. These stratiform reefs can be up to ten kilometres in horizontal size in the largest deposits. The thickness of the reefs can be centimetres to more than ten metres and generally if the reef is thin the grade of the reef is higher. In smaller conduit type mafic-ultramafic intrusion the sulphides can be found in different locations. Massive sulphides are situated at the base of the intrusion. Disseminated sulphides commonly locate in middle of the intrusions and additionally the sulphides can be found top of the intrusion. The location varies depending to the size and shape of the intrusion (eg. Maier, 2005; Maier & Groves, 2011; Ripley & Li, 2018). Typical sulphide minerals in mafic-ultramafic intrusions are pyrite, pyrrhotite, chalcopyrite, pentlandite. Oxides bear Fe-Ti-P, Cr and V metals and typically form massive horizontal layers of magnetite or chromite. These deposits are referred as stratiform deposits, and the scale of the mineralized layer varies from centimetres up to 10 metres thick (Ripley & Li, 2018). In the margins of mafic intrusion and the horizontal layers, the marginal border series (MBS) might be formed. This series is not parallel to layering series rather follow the shape of the intrusion. The MBS is crystallized in situ near of the wall of the intrusion. The MBS also contains series of fractioned rocks similar

to the layered series. The economical mineralization of the deposit can also be in MBS of the intrusion as S-enriched magma has been filter pressed out of the main magma (Hoover, 1987a; McBirney, 1996; Irvine et al., 1998). Dissemination is other common form of oxide to be present in mafic-ultramafic deposit as oxide dissemination can be found alone or in the same place together with massive oxides. Chromite layers normally exist alone, but magnetite might exist alone or associate with ilmenite and/or titanomagnetite (Begg et al., 2018; Ripley & Li, 2018).

2.2 Mafic-ultramafic intrusion types

2.2.1 Layered intrusion

Layered intrusions are formed by intrusive body, and it is characterized by clear layers of different rock types (Neuendorf et al., 2011), Many of the most economically important deposit related to mafic intrusion are referred as these layered intrusion such as Skaergaard PGE-Au deposits in Greenland (Irvine et al., 1998; Nielsen et al., 2015), Bushveld PGE-Cr-Ti-V deposits in South Africa (Eales & Cawthorn, 1996), Stillwater PGE-Cr-Ti-V deposits in USA (McCallum, 1996), and the Great Dyke PGE-Cr-Ti-V deposits in Zimbabwe (eg. Wilson, 1996). The layered intrusion internal structure is stratiform as the original orientation of the layer have been horizontal. The variation in layers can be due to e.g., mineralogical, textural or composition. One layer is one distinguishable rock unit from nearby rock, which is parallel with other layers. The variations within the layer are also possible, and similar layers can be repeated in layered series. The formed stratigraphy can be followed from lowest part to upper part of the layered intrusion (Naslund & McBirney, 1996).

2.2.2 Alaska-type intrusions

The Alaska-type intrusion is a zoned mafic-ultramafic intrusion (Neuendorf et al., 2011). This type of intrusion is not a significant source of metals, but studies present that Alaska-type complex can also host Cu-Ni-PGE mineralization like the Duke Island complex in southeastern Alaska (Thakurta et al., 2008a; Thakurta, 2018). Shape of the Alaska-type intrusion can be distinguished as concentric, like Union Bay intrusion in southeast Alaska, although the Alaska-type intrusion does not always present clear layering structure. If the intrusion has concentric structure and all typical rock types are present, the core of concentric structure consists of

dunite. Wehrlite, olivine clinopyroxene and clinopyroxenite are the next concentric layers of larger Alaska-type intrusion, but typically, the structure is not symmetrical or continuous.

These intrusions locate normally in convergent plate-margins and size of intrusion varies from metres to more than 10 kilometres. The cumulus textures are typically found in ultramafic parts of the Alaska-type intrusion suggesting the crystal fractionation and mineral concentration. (Himmelberg & Loney, 1995; Thakurta, 2018)

2.2.3 Other types of mafic-ultramafic intrusions

Numerous different mafic-ultramafic intrusions are known around the Earth. They vary for example on shape, petrography, and formation process (Barnes et al., 2015). The formation process of large Noril'sk Ni-Cu-PGE deposit in north of the Siperia in Russia is not well understood. It has been commonly thought to be related to Siberian flood-basalts, but recent studies indicated that the intrusion is formed from different parental magma than flood-basalts and the ultramafic-mafic intrusion would have formed during multiple magma events (eg. Malitch et al., 2018). One of the biggest Ni-Cu-PGE deposits is Sudbury Igneous Complex in Canada. This mafic-ultramafic deposit is unique due to the formation process as it is proposed to be formed during the meteorite impact. Even though the Sudbury complex is unique, it has some similar aspects example with Noril'sk even the formation process is totally different (eg. Keays & Lightfoot, 2004).

3 Mafic-ultramafic magmatism in Northern Finland

In Northern Fennoscandia, several episodes of mafic magmatism between 2.5 Ga and 1.8 Ga has been described. The mafic magmatism has been episodic with highest activity related at 2.5-2.4 Ga, 2.22 Ga, 2.15 Ga, 2.05 Ga, 2.00 Ga, and 1.8 Ga. These magmatic events are related to rifting and shield-wide extension of the Archean lithosphere (Hanski, 2005; Huhma et al., 2018). Many ultramafic-mafic intrusions formed during these magmatism events containing economical mineral deposits (Maier & Hanski, 2017). The known mafic-ultramafic intrusions in Northern Finland concentrate mainly in two areas, in CLGB and Tornio-Näränkävaara belt (TNB), which locates from Tornio towards Russia in the east (Fig. 1). TNB contains the Kemi, Penikat, Portimo, Koillismaa, and Näränkävaara intrusions. In CLGB there are several mafic-ultramafic intrusions for example Koitelainen, Akanvaara, Kevitsa, Hietakero (Konnunaho et al., 2018) and Palovaara (Hanski et al., 2005; Huhma et al., 2018; Maier & Hanski, 2017). The CLGB also contains komatiite related deposits as e.g. Sakatti, which mainly contain Ni-Cu-PGE mineralizations (eg. Brownscombe et al., 2015; Konnunaho et al., 2015).

3.1 Layered intrusions in Northern Finland

3.1.1 2.5-2.4 Ga magmatism related intrusions

Koitelainen

Mafic-ultramafic layered intrusion of Kemi, Penikat, Portimo, Koillismaa,and Koitelainen are related to magmatism during 2.44 Ga ago (Fig. 1). Koitelainen layered mafic-ultramafic intrusion locates ca. 45 km to NE from the Sodankylä village in Finnish Lapland (Fig. 1) and the intrusion is intruded between Archean basement of granitoid gneiss and Archean or early Proterozoic supracrustal rocks and older gabbroic intrusion. The intrusion is ca. 26 km in width and ca. 29 km in length (Mutanen, 1997). The age of the Koitelainen intrusion is ca. 2.44 Ga estimated from zircon obtained from gabbro pegmatoid and analysed with isotope dilution-thermal ionization mass spectrometry (ID-TIMS) U-Pb dating (Mutanen, 1989; Huhma et al., 2018). The intrusion has clear layered structure, which is cut by ultramafic dykes. The lower zone of the intrusion contains ultramafic rocks formed mainly from olivine-cumulates and above the ultramafic pyroxenites is lower chromite layer hosted by pyroxenite cumulates. In the main zone of the intrusion the main rock unit is gabbroic cumulate consisted of plagioclase, orthopyroxene and clinopyroxene. Minor chromite layer is present in main zone, but it does not extend to cover large area. Upper zone contains various layers of anorthosites, upper chromite

layer and gabbro which consists of plagioclase and pyroxene cumulates. Magnetite is present in upper part of the gabbro, but it is absent in lower part. Above the intrusion locates strongly altered and metamorphosed granophyre which is formed by albite, epidote, hornblende, biotite, and quartz (Mutanen, 1997). Fe-Ti-V content of Koitelainen intrusion is poor, but main zone and magnetite gabbro in upper part of the intrusion contain elevated concentrations of PGE (Mutanen, 1989b). The total amount of resources in Koitelainen is ca. 77 Mt, but only 72 Mt contain Cr3O2 and PGE. Cr3O2 concentration is 21-23% and PGE concentration is about 1.1-1.4 ppm (Appendix 1).

Kemi-Penikat-Portimo

Kemi layered intrusion is stratiform deposit tilted by tectonics. It is formed of lower ultramafic part and upper gabbroic part. The intrusion contains average 40 m thick chromitite layer, which locates in ultramafic part (Huhtelin, 2015). Kemi intrusion contains 130.9 Mt ore with 28.9 % of Cr_3O_2 (Appendix 1). Penikat and Portimo both are layered intrusion, which contain Reef-type (Penikat and Portimo), dissemination, massive sulphide, and offset-type (Portimo) PGE-(Ni-Cu-Co) mineralizations. Portimo is formed by four separated mafic-ultramafic parts, which also contain magmatic marginal series apart from the layered series. These parts have been together and formed one or two larger igneous bodies. In total Portimo contains 381.6 Mt of ore in 12 different deposits. In which PGE concentration varies 0.8 ppm up to 8.4 ppm (Appendix 1). Penikat consists of layered series and marginal series between the footwall and the layered series, which can be divided to five units (Iljina el al., 2015). These five units contain total deposit of 15.4 Mt with PGE concentration variation from 6.7 ppm to 35.3 ppm (Appendix 1). Cr from Kemi layered intrusion has been mined since 1966 (FODD).

Koillismaa

Koillismaa layered intrusion consist also Ni-Cu-Co-PGE metals hosted by sulphides in gabbros of the marginal series. The Koilismaa intursion also contains Fe-Ni-V mineralization in magnetite gabbro in Mustavaara deposit. Koilismaa intursion contains various separated mafic blocks, which would have been originally the same layered mafic intrusion but separated by faults (eg. Karinen, 2010; Karinen et al., 2015). The Koillismaa intrusion contain total of 92.4 Mt of PGE ore with 0.27 ppm to 0.65 ppm concentration and Mustavaara deposit contains resource of 145.9 Mt of 1389 ppm V ore (Appendix 1). V of Mustavaara deposit has mined, but other parts of Koillismaa remains without mine (FODD).

3.2 Other mafic-ultramafic intrusions in northern Finland

3.2.1 Komatiite related sulphide deposits

Sakatti

Sakatti is located 15 km to N from Sodankylä village in Finnish Lapland (Fig. 1); (Brownscombe et al., 2015). The age estimation for Sakatti intrusion is ca. 2.05 Ga (Maier & Hanski, 2017). The intrusion is formed from four separate peridotite bodies, three of whose are Ni-Cu-Co-PGE mineralized. These three separated ore bodies have similar petrography based on hand samples. The Sakatti intrusion contains six main rock types. Two of them contain ore minerals. Peridotite, which consists of olivine cumulates, oikocrystal pyroxene and minor plagioclase. The rock is strongly serpentinized, but primary cumulate textures are still visible. A major part of the ore of Sakatti intrusion is related to olivine cumulates, where the sulphides are found as dissemination, veins, semi-massive, and massive sulphides. Aphanitic unit has vulcanic origin, and it has komatiitic affinity. It is formed by plagioclase-rich picrite which contains phenocryst of olivine and plagioclase. Minor amount of sulphides are found in aphanitic part of the intrusion. The mafic suite, breccia unit, vulcaniclastic unit, and footwall unit do not have mineralization, but are present in the Sakatti area. The mafic suite consists of three different units based on origin and the petrography. The breccia is heterogenous unit which is strongly altered. Vulcaniclastic unit consist of phyllite and is formed by metamorphosed volcano-sedimentary material. The footwall consists of metasediments and is present below the aphanitic unit in part of the intrusion. The stratigraphy of Sakatti intrusion is complex and varies between the different bodies. In the main body the peridotite has an approximately tubular shape and the aphanitic part is mainly located below the peridotite but is present also above the peridotite. Breccia and mafic suite are above the peridotite body (Brownscombe et al., 2015). Sakatti contains 44.4 Mt of ore, which has 0.96% of Ni, 1.9% of Cu, 0.05% of Co and 1.13 ppm of PGE (Appendix 1). There are plans to start mining in Sakatti by AA Sakatti Mining Oy (FODD).

3.2.2 Deposits hosted by other mafic-ultramafic intrusions

Kevitsa

In Finnish Lapland ca. 40 km to N from Sodankylä locates Kevitsa mafic intrusion, which covers an area ca. 35 km^2 (Fig. 1). The age of the intrusion is ca. 2.05 Ga based on U-Pb TIMS studies from zircon from ultramafic cumulates (Huhma et al., 2018). The Kevitsa intrusion is formed from two different parts, ultramafic rocks, and gabbroic rocks together with some komatiite related rocks (eg, Luolavirta, 2018; Puchtel et al., 2020). The ultramafic part local below the gabbroic rock and major part of the intrusion belong to ultramafic part. Even though variation of the composition of the ultramafic part is minor, different rock types can be found. Dominant unit of the ultramafic part of the intrusion consists of poikilitic olivine websterite and it also contains major part of the ore. Olivine pyroxenite variates from olivine websterite in amount of orthopyroxene and are found in same places Although, pyroxene has been strongly altered to amphibole, it is possible to distinguish using thin sections. Plagioclase bearing websterite has orthocumulate texture with more orthopyroxene oikocryst than olivine websterite. This rock type is present in minor amount in the middle of the intrusion. Cumulate pyroxenite has less than 5% of olivine and above pyroxenite there is the gabbroic part of the intrusion. Pyroxene also occurs below and sides of olivine pyroxene or olivine websterite. The intrusion contains also minor amount of strongly serpentized dunite in the middle of the intrusion inside of olivine pyroxene and websterite. Gabbroic rocks locate above the ultramafic rocks. These rocks contain mainly plagioclase with clinopyroxene and minor olivine. The marginal series of the Kevitsa intusion in formed by pyroxene and gabbro together with mafic vulcanic rocks and tuffs. Generally, contacts between different rock type in the Kevitsa intrusion are gradual, but also sharp contact has been found. In the Kevitsa deposit the ore is disseminated and main ore minerals are pentlandite and chalcopyrite. Other ore minerals present in the Kevitsa intrusion are pyrrhotite and magnetite. The ore minerals are located in between cumulate textures of olivine and pyroxene. Minor net-texture and veins of sulphides exist, but these do not have major importance (Santaguida et al., 2015). Total of 138.7 Mt resources exist in the Kevitsa intrusion. The Ni content of the ore is 0.2%, Cu is 1.9% and PGE concentration is 0.216 ppm (Appendix 1). The Kevitsa intrusion has mine since 2011 by Boliden as open pit mine (FODD).

3.2.3 Metasomatized mafic intrusions in Northern Finland

Hietakero

Hietakero mafic-ultramafic intrusion locates ca. 200 km from Sodankylä village (Fig. 1) towards NW in area of municipality Enontekiö. Geologically the area belongs to CLGB. The intrusion contains average of 0.10-0.11 wt.% of Co and 0.31-0.35 wt.% of Cu and 0.20-0.23wt.% of Ni. The country rock of the Hietakero intrusion consist of strongly altered graphite-sulphide schist and felsic to intermediate vulcanic rocks which has tuffigeneous aspect. The rocks of the Hietakero intrusion can be divided three rock units. 1) Gabbroic cumulate is the most common rock type in intrusion and contains different types of gabbros. The main minerals are amphiboles, clinopyroxene, scapolite and plagioclase. 2) Pyroxenitic cumulates are made of clinopyroxene and amphibole together with minor scapolite and plagioclase. 3) Hybrid rocks are different mixed rock of the country rock and intrusion or mixed rock of material from different rock units of the intrusion. All rock of the Hietakero intrusion have been metamorphosed in amphibole facies and have strong hydrothermal alteration. In Hietakero mafic-ultramafic intrusion the mineralization is located in all different rock types and part of it is in country rock. The most common ore minerals are pyrrhotite, Co-bearing pyrite, Co-bearing pentlandite, and chalcopyrite. Sulphides form massive veins, veinlets, patch, net-textures, and minor amount of dissemination and thin veinlets. Magnetite and ilmenite are found as dissemination (Konnunaho et al., 2022).

Kelujoki and Iso-Povivaara

Kelujoki mafic intrusion locates about 5 km towards NNE from Sodankylä. village (Fig. 2). The intrusion is formed by gabbros, which are tilted ca. 60 degrees to S. The mineralization consists of chalcopyrite and Co-bearing pyrite as sulphides are present as dissemination, veins and up to 2 cm accumulations (Karvinen, 1982). Total 1.5 Mt resources with 0.2% of Cu and 0.03% of Co (FODD). Iso-Povivaara is located 60 km from Sodankylä village towards NE (Fig. 2). Iso-Povivaara is intruded to mica and sericite schists, quartzites, and amphibolites. The age determination is 2.14 Ga made from zircon. The intrusion consists of gabbro which contain minor amount of sulphides as chalcopyrite, Co-bearing pyrite and pyrrhotite (Karvinen, 1983).

4 Geological background

4.1 Central Lapland Greenstone Belt

The CLGB is a large Paleoproterozoic greenstone belt (Fig. 1), which extends from Russia crossing Finland and continuing as Karasjok greenstone belt (Fig. 1) in Norway (Orvik et al., 2022). The CLGB is located between the Archean granite-gneiss in east, northeast and west, Lapland Granulite belt in north and Central Lapland Granitoid Complex in south and southwest (Hanski et al., 2005). The CLGB contains mainly supracrustal rocks and its geological evolution consists of five different tectonic basin events after Köykkä et al. (2019), I Early syn-rift, II Syn-rift, III Syn-rift to Early post-rift, IV Passive margin stage and V Foreland basin system. The stages are associated with rifting and development of the epeiric sea. The first three stages took place in 2.5-2.1 Ga, the fourth stage occurred 2.1-1.94/1.92 Ga and the fifth stage 1.94/1.92-1.88 Ga (eg. Köykkä et al., 2019; Köykkä & Luukas, 2021). The northern area of CLGB is metamorphosed under upper greenschist facies conditions. The metamorphic grade increases towards east and from lower amphibolite facies to near of the Archean basement the to the mid-amphibolite facies (Hölttä & Heilimo, 2017). The CLGB contains various epigenetic Au deposits, but the largest is Suurikuusikko (Fig. 1). These Au deposits are classified as orogenic gold (Wyche et al., 2015).

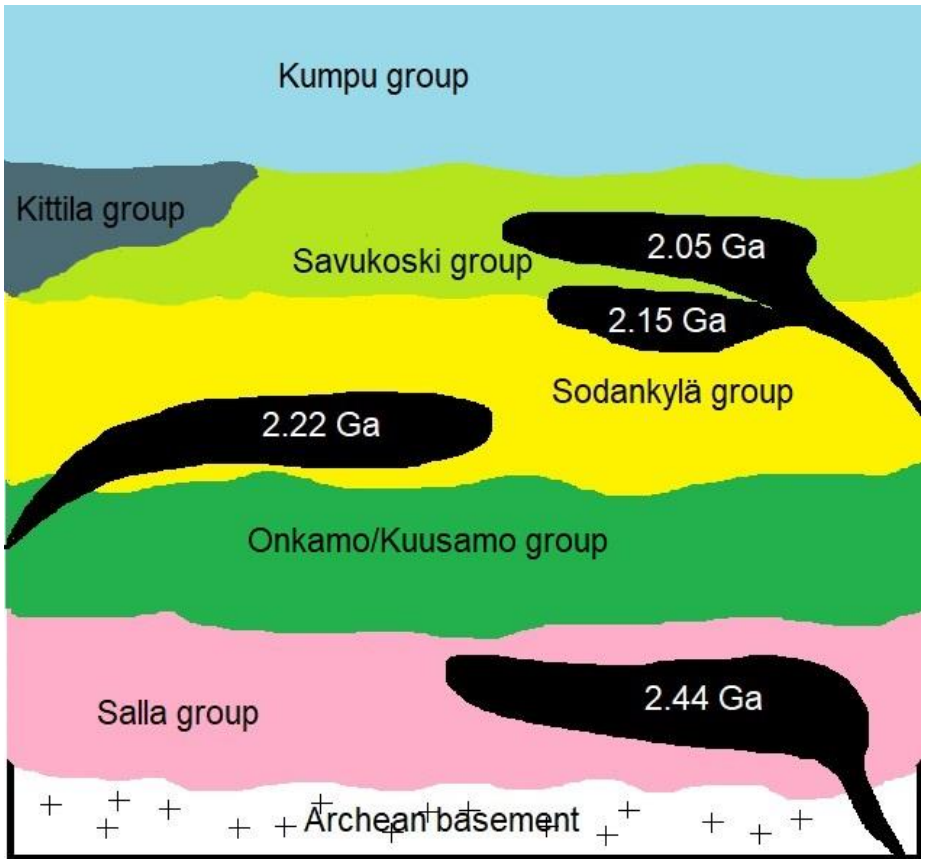

Figure 3. Simplified stratigraphy of CLGB after Köykkä et al. (2019). The subracrustal rocks of CLGB are deposited above the Archean basement. Salla group consists of intermediate to felsic metavulcanic rocks. Kuusamo group contains mainly of mafic to intermediate metavulcanic rocks and ultramafic conglomerates and tuffs. Sodankylä groups consist mostly of quartzites, conglomerates and mica schists. Savukoski group is formed by phyllites, black schists, mafic tuffites, and lavas. Kittilä group is allochthonous mafic metavulcanic rocks. Kumpu group is small group of meta-arkoses, quartzites, conglomerates, siltstones and felsic metavulcanic rocks. The mafic magma has been intruded to supracrustal rocks of CLGB in several episodes.

The CLGB is dominated by supracrustal rocks which are deposited above the Archean basement (Fig. 4). The Paleoproterozoic rocks in CLGB is proposed into 5 to 7 lithostratigraphic groups after Hanski et al. (2005) and Köykkä et al. (2019). The lower most Salla group (Fig. 4) is located in southeastern part of CLGB and are the oldest (2.50-2.44 Ga) supracrustal rocks in the belt, containing intermediate to felsic metavulcanic rocks. Onkamo/Kuusamo group (Fig. 4) supracrustal rock are dispatched to wide are in CLGB. The mafic to intermediate metavulcanic rocks and ultramafic conglomerates and tuffs are deposited (2.44-2.38 Ga) above either Salla group metavulcanic rocks or directly above Archean basement. Sodankylä Group (Fig. 4) is made mainly of supracrustal rocks as quartzites, conglomerates and mica schists and in addition carbonate rocks and mafic metavulcanic rocks. The deposition has occurred 2.28-2.15 Ga above the metavulcanic rock of previous groups or Archean basement. Savukoski group (Fig. 4) supracrustal rocks are formed above the metasedimentary rocks of Sodankylä group during 2.15-2.05 Ga. The supracrustal rocks are

mainly phyllites and black schist, but also mafic tuffites and lavas occur. Kittilä group is formed from mafic metavulcanic rocks in 2.15-2.05 Ga. Kittilä group is located central part of the CLGB and the total are of Kittilä groups is more than 2600 km^2. It is proposed to be allochthonous, as thrust faults separate is from Paleoproterozoic rocks of Sodankylä and Savukoski groups as well as Archean basement (Hanski et al., 2005; Köykkä et al., 2019; Köykkä & Luukas, 2021). Kumpu group occurs in smaller areas than previous groups. This group consists of meta-arkoses, quartzites, conglomerates, siltstones and felsic metavulcanic rocks and are younger than 1.9 Ga (Hanski et al., 2005; Köykkä et al., 2019; Köykkä & Luukas, 2021).

4.2 Geology of the Tanhua area

The Tanhua mafic complex is located in northern Finland (Figs. 1 and 5) near the Tanhua village (ca. 45 km to E from Sodankylä) within the municipality of Savukoski. The complex is formed by three separate intrusions: Kylälampi, Kannusvaara, and Markkinaselkä (Fig. 5). These intrusions may represent an originally coherent large intrusion, which has segmented into separated pieces along faults, or they represent three individual intrusions formed by same type of magmatism. The study area is about 12 km long in NS direction and 4.5 km wide. The Tanhua mafic complex has been intruded to Paleoproterozoic supracrustal rocks of CLGB which are located ca. 5 km from the Archean tonalitic migmatite (Mattila, 1974). Supracrustal rocks surrounding the Tanhua mafic complex belong to the Sodankylä and Savukoski groups of the CLGB. In the area, the most abundant sedimentary rock types from the Sodankylä group are arkose, arkose-quartzite, quartzite, and biotite schist. Mafic and intermediate vulcanic rocks of Sodankylä group are also present in the area. East from the Tanhua mafic complex locates amphibolite, graphite-bearing schist and vulcanic rocks, which define a synformal structure (Mattila, 1973; Konnunaho el al., 2022).

The Tanhua area has been studied by Rautaruukki Oy as a part of V-Ti-Fe exploration project (Mattila, 1973; 1974; Korvuo, 1978). In 1977 Rautaruukki Oy drilled four drillholes, two intersected northern part (i.e., Kylälampi area) and two southern parts of the intrusion (i.e., Kannusvaara area; Fig. 5). The Tanhua mafic complex has so far remained relatively unstudied, and its economical V-Ti-Fe potential was estimated to be poor, and further studies were cancelled (Korvuo, 1977). However, these historical studies showed that the intrusion hosts mineral potential for Co and Cu as the Tanhua mafic complex had conductive parts indicating potential to bear sulphides (Konnunaho et al., 2022).

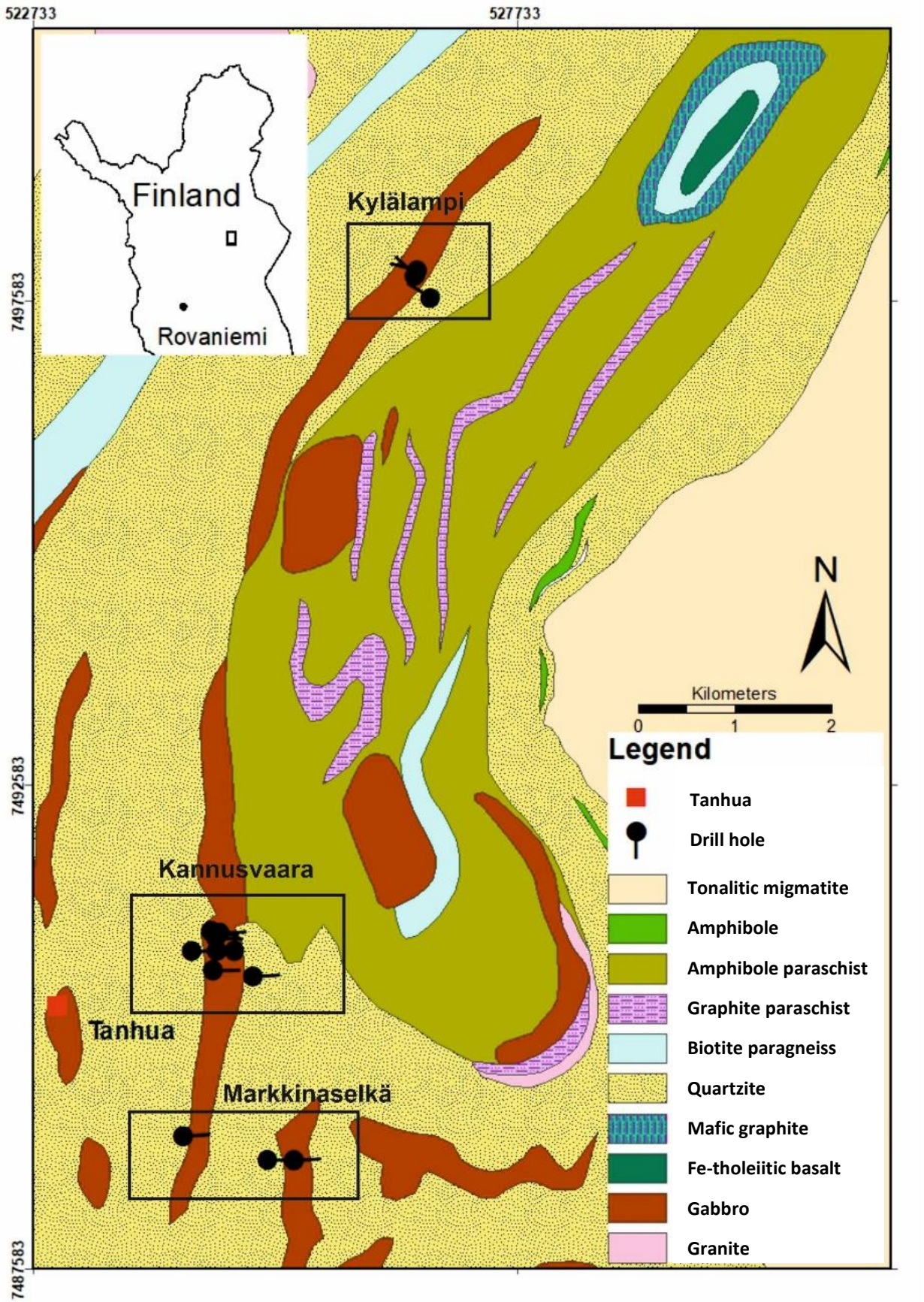

Figure 5. Geological map from the area of the Tanhua mafic complex. Coordinate system ETRS-TM35FIN (Modified after DigiKP and Konnunaho et al. (2022))

4.3 Tanhua mafic complex

The Tanhua mafic complex consist of three parts, southern part contains Kannusvaara and Markkinaselkä and northern part contains Kylälampi (Fig. 5). The different parts are considered to be one larger dyke-type intrusion which is cut by faults based on aeromagnetic map (Konnunaho, personal communication, 12.9.2023). Kannusvaara gabbro age is estimated to be 2148 ± 7 Ma using the laser ablation multi-collector inductively coupled plasma source mass spectrometer (LA-MC-ICPMS) U-Pb analyses from zircon. Two zircon samples were analysed, one granophyre and other magnetite-bearing gabbro. Kylälampi gabbro age determination gives 2137 ± 5 Ma with LA-MC-ICPMS U-Pb analyses as one zircon-bearing sample was analysed from gabbro. No age determination is made from Makkinaselkä (Huhma et al., 2018).

The main country rocks of the Tanhua mafic complex belong to Sodankylä groups (Fig. 5) and are strongly albitized quartzite, although minor amount of amphibolites and mafic vulcanic rocks is found in drill cores. The drill core loggings evidenced intrusive rocks from mafic to felsic in composition with variable textures. The positive magnetic anomaly is caused by oxide gabbros which contain magnetite as dissemination and mobilized veinlets, but the distribution of magnetic mineral is uneven through the intrusion. Magnetite bearing rocks have similar attributes like non-magnetic rocks of the intrusion (Konnunaho et al., 2022). Magnetite is found also as dissemination in felsic rock referred as albite in Korvuo (1977) meaning probably tonalite which has suffered albitization as plagioclase is mainly albite.

Major part of rocks of the intrusion shows significant albitization and biotitization. In parts of the intrusion that show the strongest biotitization, biotite has formed large biotite crystals (a.k.a. mottled gabbro or biotite gabbro). Mottled texture refers spots of different colour compared to the major colour of the sample (Neuendorf et al, 2011). These large biotite crystals are found generally together with albitization. Additionally, the mottled gabbro areas are lack of magnetite (Konnunaho et al., 2022). The Tanhua mafic complex is metamorphosed, and major part of the rocks are recrystallized. Uralite grains are found in previous studies, indicating the alteration of pyroxene to amphibole. Also, minor plagioclase has altered to scapolite and sericite (Mattila, 1974; Korvuo, 1977). Uralite is secondary amphibole as hornblende which is altered from pyroxene (Neuendorf et al., 2011).

Inside of the intrusion, chilled margins have been observed at places, likely indicating multiples internal magmatic pulses. In mineralized rock, moderate amount of pyrite, chalcopyrite and pyrrhotite locate as dissemination, veinlets and veins typically in magnetite -bearing gabbros, but minor amount of sulphides can be found as weak disseminations in gabbros without magnetite throughout the intrusion. Disseminated sulphides locate also in more felsic parts of the intrusion as diorites and granites (Konnunaho et al., 2022).

5 Materials and methods

5.1 Materials

This study's research material consists of 14 drill cores from Tanhua area. The holes were drilled by GTK in 2019 and 2020 with a total length of 2640.6 m (Table 1). For this study 83 polished thin section were made from different rock units by GTK (Appendix 2). To support petrographic studies, unpublished whole-rock geochemical analyses were used to support the data.

Table 1. Diamond drill hole drilled by GTK in 2019 and 2020.

Diamond drill hole	x-coordinate (ETRS-TM35FIN)	y-coordinate (ETRS-TM35FIN)	z (m)	Dip (°)	Azimuth (°)	depth (m)	Target
U5212019R6	7488972	524366	213	50	85	189.15	Markkinaselkä
U5212020R15	7488718	525234	207	50	89	147.35	Markkinaselkä
U5212020R10	7488714	525508	194	50	86	169.25	Markkinaselkä
U5212020R9	7490621	525091	218	50	86	150	Kannusvaara
U5212020R16	7490671	524672	204	45	89	299.4	Kannusvaara
U5212019R3	7490865	524449	204	55	88	349.2	Kannusvaara
U5212019R8	7490872	524714	209	65	268	234	Kannusvaara
U5212019R4	7490872	524715	209	60	91	109.5	Kannusvaara
U5212020R14	7491022	524712	211	45	92	75	Kannusvaara
U5212019R5	7491068	524648	206	50	98	350.8	Kannusvaara
U5212019R7	7491069	524751	211	60	87	124.05	Kannusvaara
U5212020R11	7497686	526756	225	45	302	269.2	Kylälampi
U5212020R13	7497922	526617	235	50	314	194.4	Kylälampi
U5212020R12	7497924	526613	235	45	284	29.2	Kylälampi

5.2 Methods

5.2.1 Petrographic studies

The revision logging was made for drill cores in Rovaniemi in spring 2022. Principal method for this study was polarization microscopy for petrography. It was used to identify minerals, textures and grain size from polished this section. Both polarization and reflected microscopes were used distributed by University of Turku. The modal compositions of main minerals were estimated visually using comparison chart for visual percentage estimation (after Terry & Chilingar, 1955).

5.2.2 Benchtop micro-XRF

Benchtop micro-XRF was used to make chemical element maps. Scanned four rock samples were U5212019R5 171.05-171.20 tonalite, U5212019R7 44.40-44.50 gabbro, U5212019R8 32.55-32.75 gabbro, U5212020R10 141.85-142.00 gabbro. The used instrument was M4 TORNADO at university of Turku, Geohouse. Each sample was first scanned as whole with analyses parameter of measured area of 100 µm and measured time of 2 msec. After the overall scan the sulphide and zircon bearing spot was scanned in more detail with measurement parameters of 20 µm and 15 ms. The samples were cut cores and the chemical element map was made from cut plane of the drill core.

5.2.3 Modelling softwares

Maps were made with Arc-map (ESRI) GIS software available at the University of Turku. 3D-modelling software MOVE was used to make three cross-sections (Kylälampi, Kannusvaara, and Markkinaselkä).

6 Results

6.1 Petrography of the Tanhua mafic complex

The studied rock samples from the Tanhua mafic complex can be divided into three different major rock groups based on the estimated modal amounts of hornblende, plagioclase, quartz, and their mutual ratios in the thin sections. I propose the following division for the intrusion rock types: tonalite, diorites and gabbros. Peridotites are also found in drill cores (U5212020R13 in Kylälampi) and studied thin sections, but peridotites possibly do not belong to the Tanhua mafic complex. Mafic vulcanic rocks are also present in drill cores and thin sections but belong to the country rocks of the intrusion. The gabbro is the most voluminous rock type present in the Tanhua mafic complex and major part of the mineralization locates in gabbro. Occasionally, the gabbros are melagabbros as they contain >65% dark minerals. In mafic vulcanic rocks the recrystallization is the most advanced and the granoblastic texture is abundant compared to other rock types is the Tanhua mafic complex.

6.1.1 Petrography of the gabbro

Gabbro

Macroscopically gabbros appear as igneous rocks with fine to medium grain size (Fig. 6). The texture varies from non-oriented to moderate orientation. The colour of the samples is generally pale greenish grey to dark greenish grey. Minor amount of sulphides is observed in gabbroic samples. The oxide-bearing gabbro samples do not contain generally as dark greenish grey samples as gabbros without oxides. In drill core samples sulphides are localised as dissemination and veinlets.

Figure 6. Photograph of drill core from the Tanhua mafic complex. A) Gabbro sample U5212019R14 64.30, B) Oxide gabbro sample U5212020R16 41.40

In thin section the texture of gabbros is generally granoblastic as plagioclase, hornblende and if present biotite intends to form triple points grain boundaries of 120°. The average grain size varies from smaller than 0.1 mm to approximately to 0.4 mm in diameter. (Fig. 7) in different samples. The grade of orientation varies from strong to non-existent. The oriented minerals are biotite together with hornblende (Figs. 7E and 7F). The main minerals in studied gabbro samples are hornblende and plagioclase with moderate amounts of biotite. In gabbroic rocks, the modal amount of hornblende varies from 35% to 80% (Fig. 7) and plagioclase varies from 15% to 55%. If biotite is present in gabbroic samples, the modal composition varies from accessory mineral up to 35%. Accessory mineral of gabbros in the Tanhua mafic complex are quartz, magnetite, scapolite, pyrite, chalcopyrite, chalcocite, bornite, ilmenite, titanite, calcite, zircon, chlorite, sericite, leucoxene, and augite.

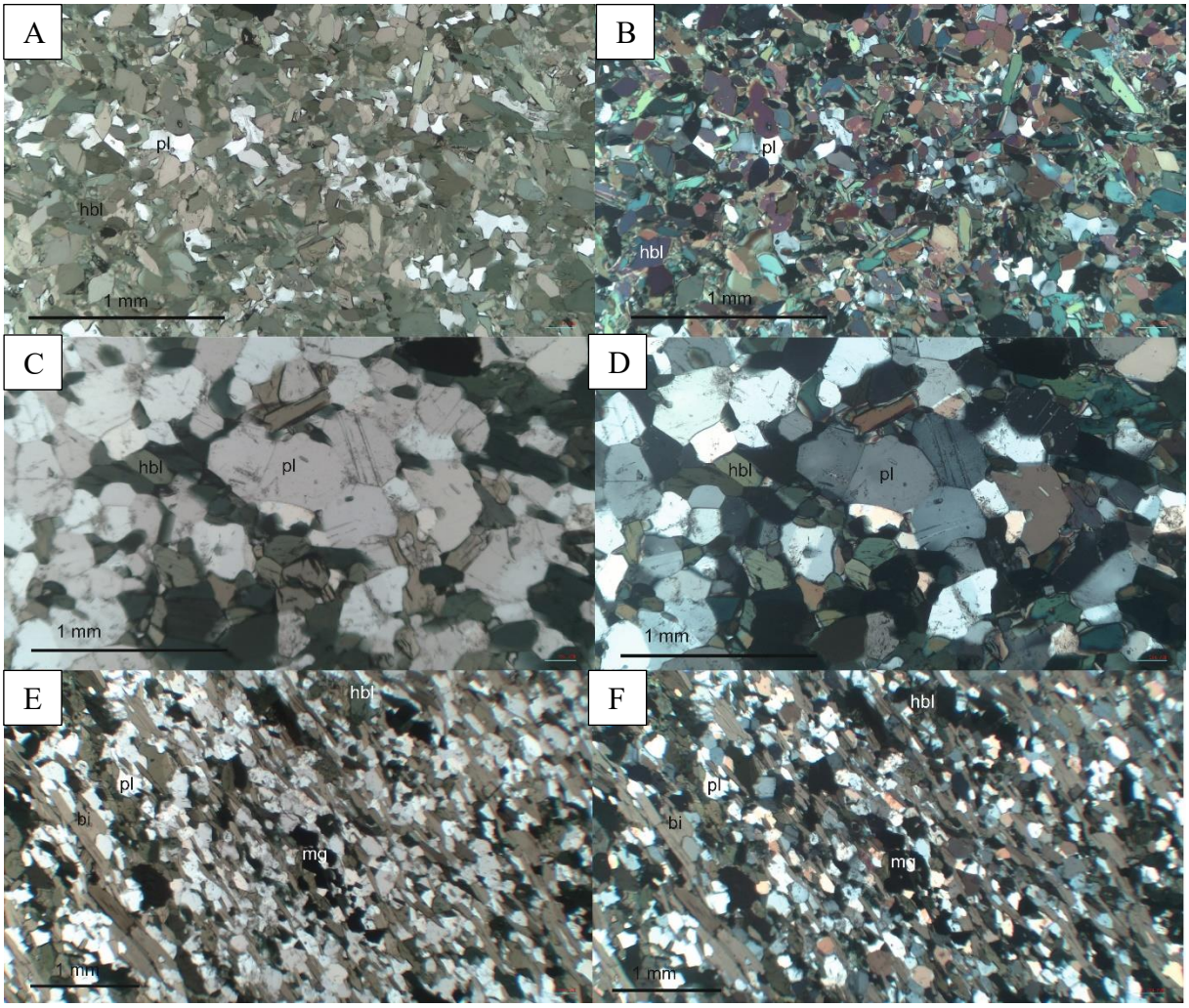

Figure 7. Microphotograph presenting general texture and grain size of gabbro in the Tanhua mafic complex. A) and B) Sample U5212019R13 159.80, A) PPL 5x. B) XPL 5x and D) sample U521019R14 22.20 C) PPL 5x, D) XPL 5x. E) and F) gabbro sample U5212019R6 176.30, E) PPL 2x, F) XPL 2x. Abbreviations hbl – hornblende, pl – plagioclase, bi – biotite and mg – magnetite.

Hornblende can commonly be observed with quartz as exsolution texture (Fig. 8A). The quartz is in very small grains inside of hornblende grain. In some gabbroic samples, some hornblende forms uralite grains (Fig. 8B). In these grains, the remained textures of pyroxene are still possible to observe as cleavage as well as quartz inclusions.

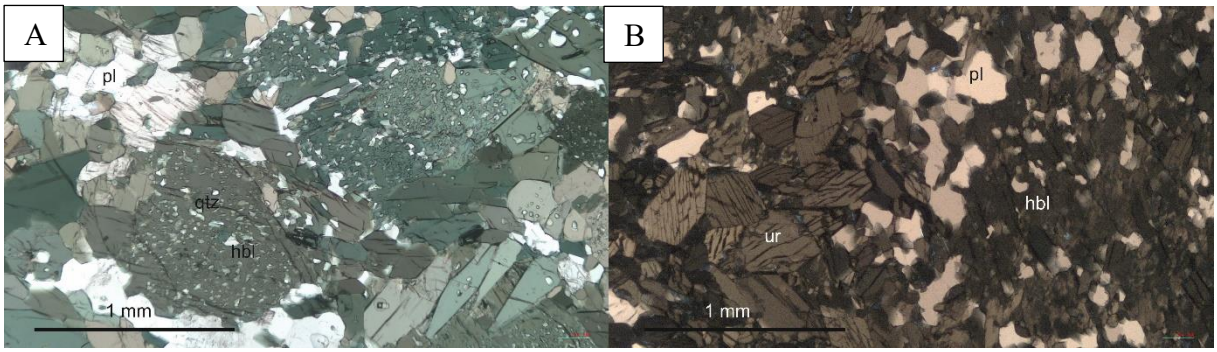

Figure 8. Microphotograph presenting A) exsolution texture of quartz in hornblende PPL 5x gabbro sample U5212020R16 298.40. B) uralite in the Tanhua mafic complex. PPL 5x remained mottled sample U5212019R6 131.35. Abbreviations hbl – hornblende, pl – plagioclase, qtz – quartz and ur – uralite.

Plagioclase is occasionally observed as poikilitic texture as plagioclase encloses hornblende crystals (Fig. 9). Various plagioclase grains are zoned as the centre of the grain extinguished in different time than the outer part of the crystal. The centre of the plagioclase is also more altered than the outer part of the grain (Fig. 9). The alteration product of plagioclase varies and is either albite, sericite, or scapolite depending on the sample. Multiple alteration products can also be present in the same thin section. Scapolite can be found as independent mineral or together with plagioclase as altered part of the plagioclase grain. The scapolite has high interference colours indicating meionite endmember and therefore high calcium content. Minor amount of plagioclase grains are albite law twinned or Carlsbad twinned, but major part of the plagioclase grains are not twinned.

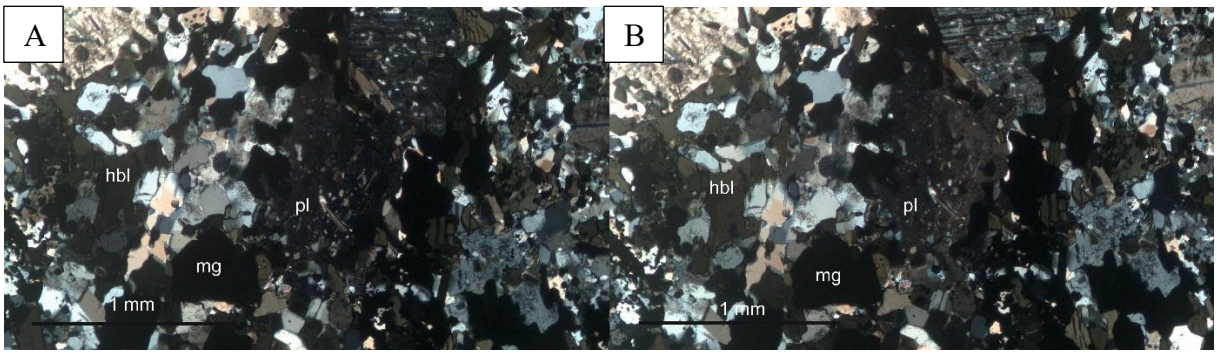

Figure 9. Microphotograph presenting poikilitic and zoned texture in gabbros in the Tanhua mafic complex. A) and B) XPL 5x gabbro sample U5212019R14 64.30. Abbreviations hbl – hornblende, pl – plagioclase and mg – magnetite.

In mineralized gabbros of the Tanhua mafic complex, the sulphides are found commonly as dissemination and veinlets (Fig. 10). The thin section samples were selected to represent typical rock in the Tanhua mafic complex and not sulphide-rich rocks. In thin sections, the most common sulphides are pyrite and chalcopyrite. Minor amount of chalcopyrite grains are found altered to bornite and chalcocite forming rim textures (Fig. 11). Outside of the grain consist of chalcopyrite, next rim consists of bornite and in the middle is formed of chalcocite. In thin section, also remotely grains of pyrrhotite are found.

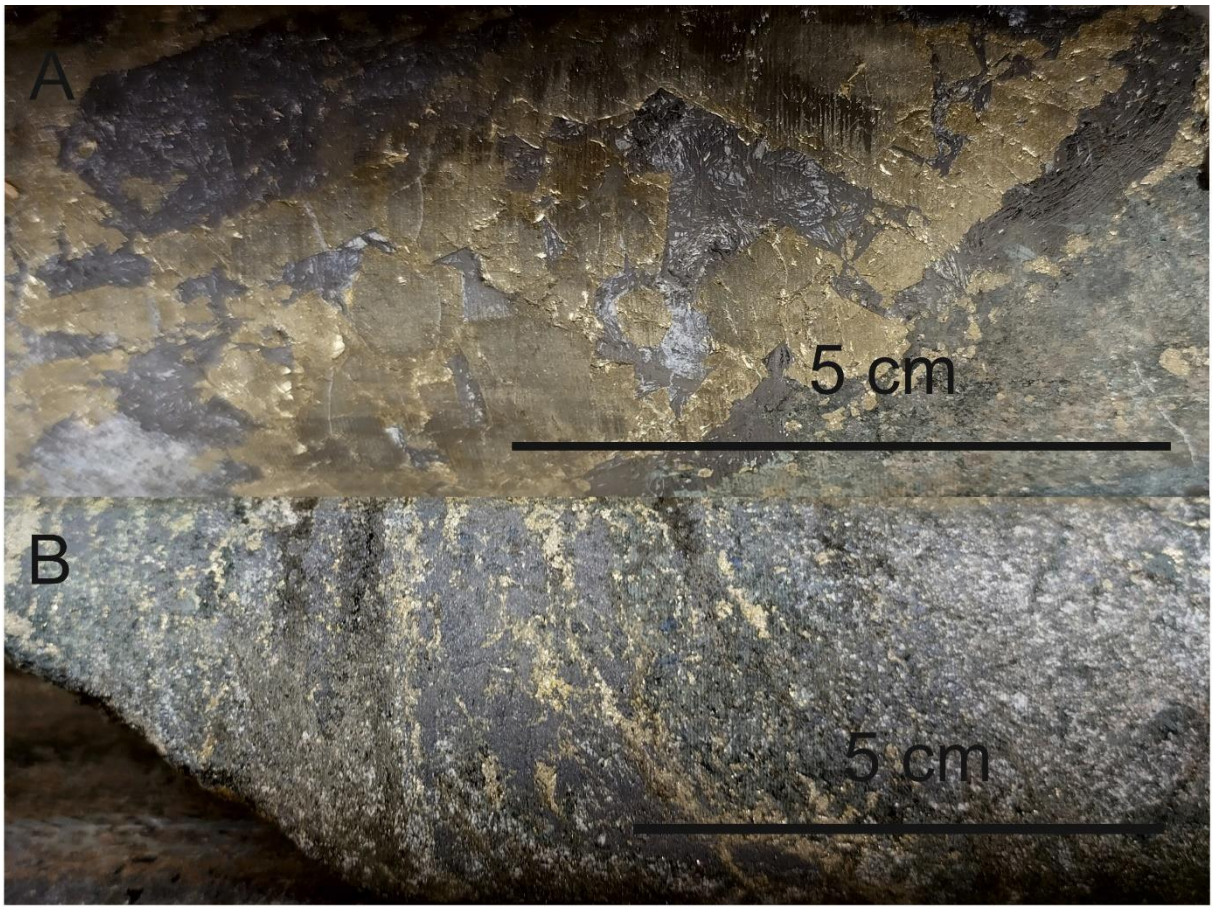

Figure 10. Photographs of drill core presenting the occurrence of sulphide minerals in gabbros in the Tanhua mafic complex as dissemination and veinlets. A) U2512019R8 116.70. B) U5212019R14 17.50.

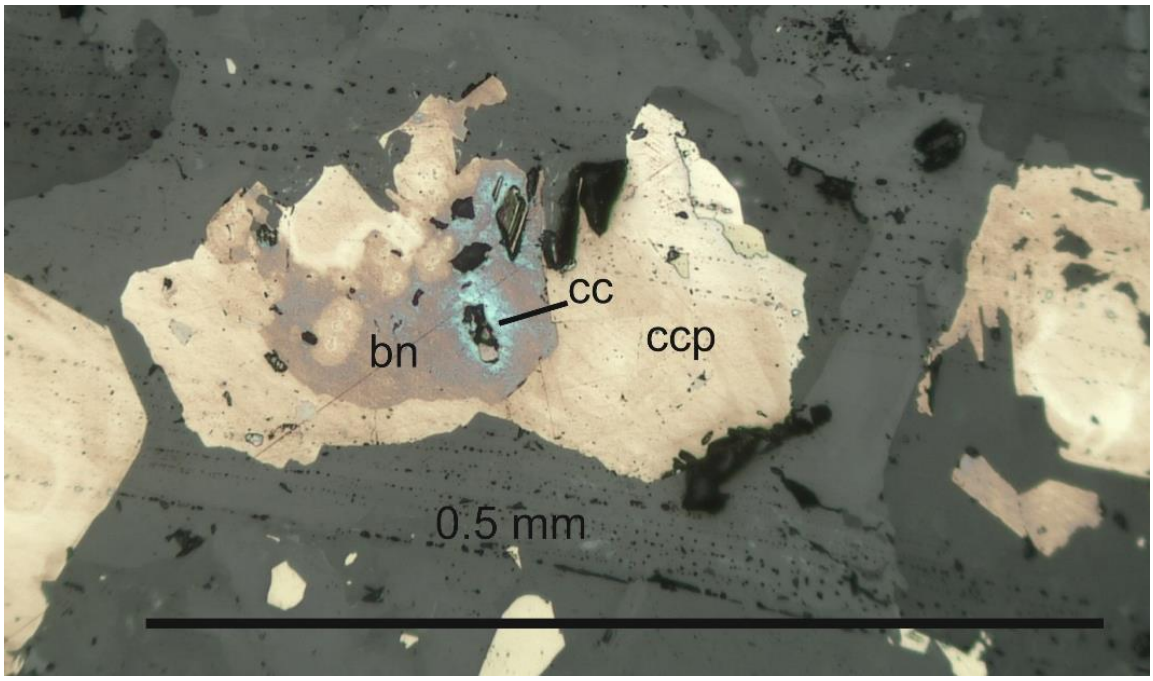

Figure 11. Microphotograph presenting occurrence of chalcopyrite, bornite and chalcocite in gabbros in the Tanhua mafic complex. The chalcocite has been altered to bornite which has been altered to chalcocite. Reflected PPL 20x gabbro sample U5212020R10 112.55. Abbreviations ccp – chalcopyrite, bn – bornite and cc – chalcocite.

Magnetite is present in 19 gabbro samples as main mineral and the modal composition varies from 5% to 30. These magnetite-bearing gabbros are referred as oxide gabbros and the modal compositions of hornblende and plagioclase varies from 20 to 45% of hornblende and 25 to 50% of plagioclase. Magnetite can be found mainly as dissemination (Fig. 12) and veinlet in studied gabbroic samples. The magnetite is commonly altered to leucoxene in grain boundaries of magnetite (Fig. 13). In majority of the samples, the magnetite occurs alone, but it is possible to observe magnetite forming core rim textures with titanite. In these cases, the magnetite forms the core and titanite forms the rim around. In minor amount of samples, the magnetite is located together with sulphides as ultimate rim of altered sulphides. Oxide minerals are present also, as accessory minerals in gabbros in the Tanhua mafic complex. Minor amount of magnetite is found as dissemination in 12 other gabbroic samples. Minor ilmenite is found together with magnetite or in core-rim texture with titanite replacing magnetite in the core. Titanite is found as core-rim texture together with other oxide minerals or as solely mineral.

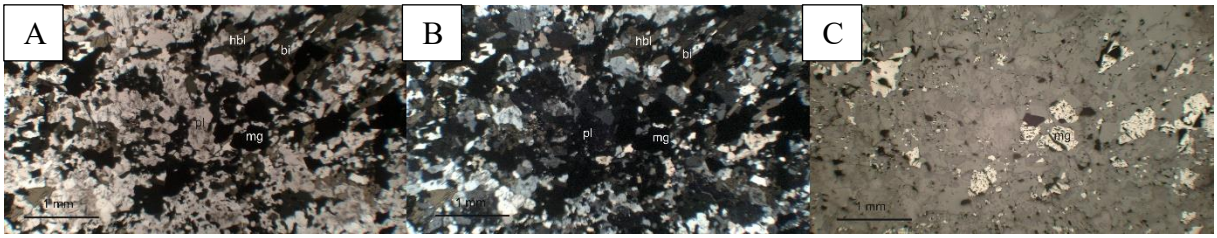

Figure 12. Microphotograph presenting occurrence of magnetite in gabbros in the Tanhua mafic complex. Sample U5212020R10 112.55 A) PPL 2x, B) XPL 2x, C) Reflected PPL 2x. Abbreviations hbl – hornblende, pl – plagioclase, mg – magnetite and bi – biotite.

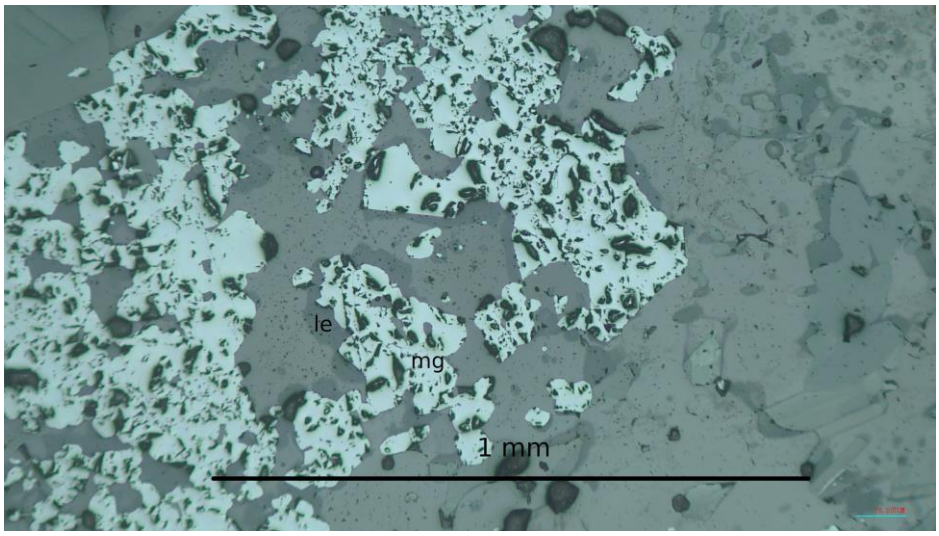

Figure 13. Microphotograph presenting alteration of magnetite to leucoxene. Biotitized mottled gabbro Sample U5212019R3 253.20. Reflected 10x. Abbreviations mg – magnetite, le – leucoxene.

Chlorite is found along on the cutting veins in minor number of samples (Fig. 14). Near of these veins also the grade of the metasomatic alteration of plagioclase is the strongest. In gabbroic samples, the zircon locates together with plagioclase either in the border or inside of the grain.

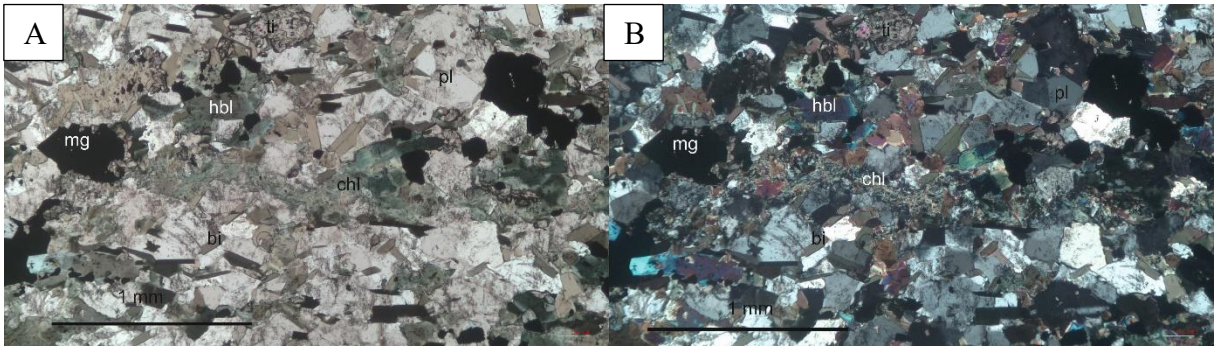

Figure 14. Microphotograph presenting chlorite vein in gabbro in the Tanhua mafic complex. A) PPL 5x, B) XPL 5x, both oxide gabbro sample U5212019R3 210.40 Abbreviations hbl – hornblende, pl – plagioclase, mg – magnetite, chl – chlorite and ti – titanite

One sample U5212020R11 219.19 is macroscopically medium grained, and no orientation is possible to observe. The colour of the drill core sample is pinkish grey with green dots as

pyroxene minerals. In thin section, the grain size of major minerals in in average 0.9 mm, but can be up to 2.2 mm. The sample contains plagioclase and augite, and there is no hornblende in this thin section (Fig. 15). In this sample, the quartz has been recrystallized to small grains between larger plagioclase and augite grains, but the granoblastic texture is not possible to observe. The sample contains accessory magnetite, calcite, and chlorite.

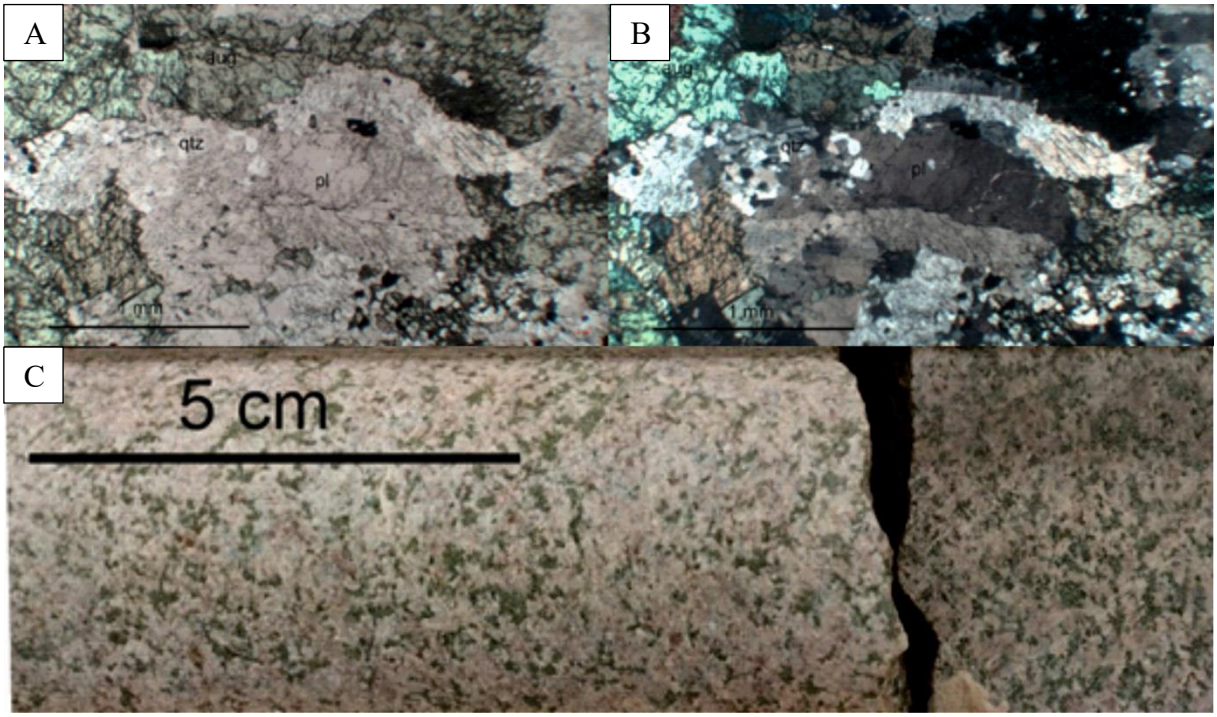

Figure 15. Microphotographs and photograph presenting general texture and presence of augite in gabbro in the Tanhua mafic complex. Sample U5212020R11 219.19 A) Microphotograph PPL 5x B) MicrophotographXPL 5x, C) Photograph of drill core. Abbreviations of A) and B) aug – augite, pl – plagioclase and qtz – quartz.

Mottled gabbro

Mottled texture is present in 21 samples. The mottled gabbro can be either a remained without biotitization or altered with biotitization. The drill core samples of remained mottled gabbros have dark grey colour with greenish tone (Fig. 16). The pale minerals as plagioclase are separated partly from dark mineral as hornblende and therefore the texture is mottled as the rock samples contain partly pale part and partly darker parts. The samples are weakly oriented.

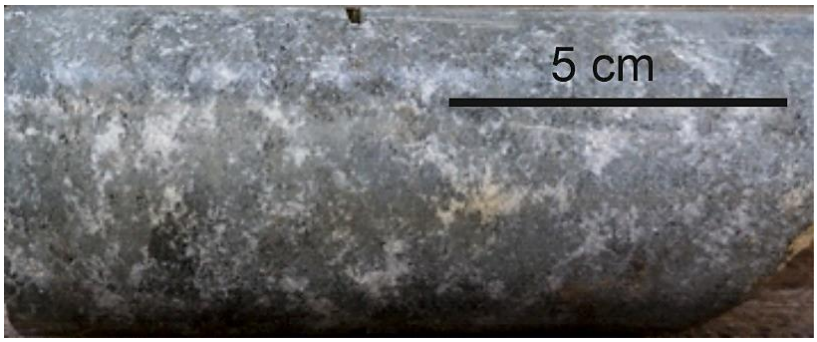

Figure 16. Photograph of drill core near of the sample U5212019R6 131.35 presenting remained mottled gabbro.

In thin sections, the remained mottled gabbro samples contain mainly granoblastic hornblende, plagioclase, and moderate amount of scapolite as alteration product of plagioclase (Fig. 17). The hornblende contains quartz exsolution and minor number of grains remain the cleavage of pyroxenes and therefore are referred as uralite mineral.

Plagioclase grains present zoned texture as centre of the grains is more altered and extinguish in different time than outside border of the grain. The poikilitic texture is observed as plagioclase as phenocryst with tiny hornblende grains. In remained mottled gabbros, the plagioclase and hornblende are partly separated from each other.

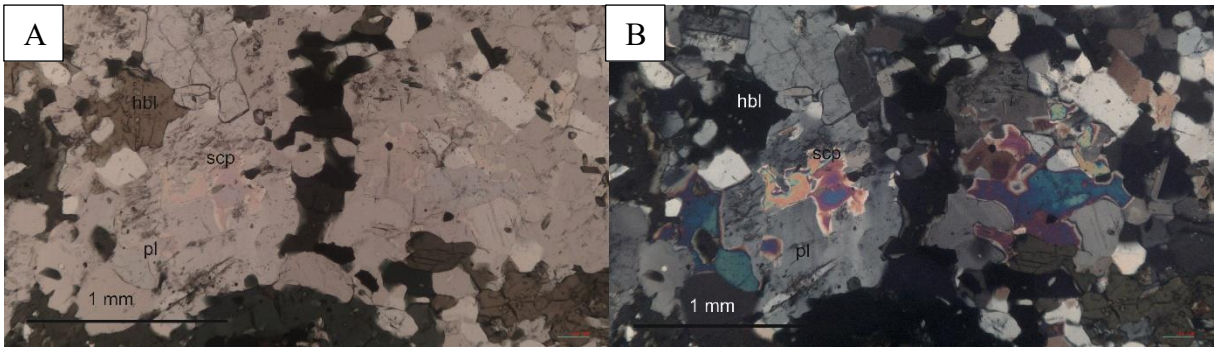

Figure 17. Microphotograph presenting scapolite as alteration product of plagioclase in gabbros in the Tanhua mafic complex. Sample U5212019R3 210.40 A) PPL 5x, B) XPL 5x. Abbreviations hbl – hornblende, pl – plagioclase and scp – scapolite.

In biotitized mottled samples the biotite grains have been accumulated and formed mottled texture (Fig. 18). These mottled biotite textures are strongly oriented. The accumulation of biotite is well observed in both hand samples and in thin sections. In the hand samples the colour is generally grey apart of the dark biotite accumulations. These accumulations can be up to 2 cm long and ca. 0.4 cm width. Well-formed biotitized mottled textures are present in ten studied thin sections and in addition minor accumulation of biotite grains are present in four other samples. Samples with biotitized mottled texture, the area outside of the mottled texture are mostly similar to gabbros without the mottled texture.

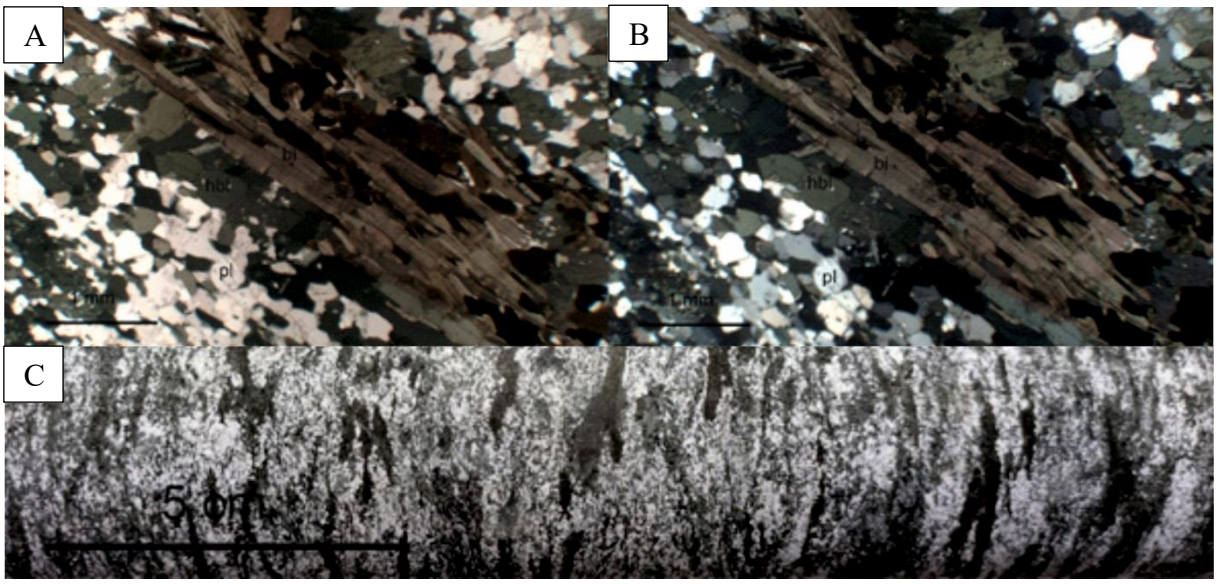

Figure 18. Microphotographs and photograph presenting general texture of biotitized mottled gabbro in the Tanhua mafic complex. A) PPL 2x, B) XPL 2x. Sample U5212019R5 83.30 C) Photograph of drill core sample U5212019R3 95.45. Abbreviations of A) and B) hbl – hornblende, pl – plagioclase and bi – biotite.

Hornblende is present as slightly oriented with granoblastic texture, but hornblende is also found with exsolution texture as the quartz has been suffered exsolution. Majority of plagioclase is recrystallized to form granoblastic texture. Minor plagioclase gains have poikilitic texture as hornblende occurs inside of the plagioclase phenocryst. The modal composition of hornblende varies from 10% to 45% and the model composition of plagioclase varies 30% to 45% in biotitized mottled gabbro samples.

In both, preserved mottled sample and altered mottled samples there are minor amount of sulphides. The sulphides consist of mainly of pyrite, but also chalcopyrite. Chalcopyrite is commonly altered first to bornite, which is also altered occasionally to chalcocite. Minor number of pyrrhotite grains have been observed in mottled samples. Magnetite is found in altered mottled samples, but it is more abundant in remained mottled samples. In remained mottled samples, magnetite forms symplectic core rim textures with titanite where the rim does not cover all sides of the core, but the form of the grains is more complex. The magnetite-titanite grains form elongated grains in two opposite directions. The resulted texture appears as net formed by elongated magnetite-titanite grains. The spaces between elongated magnetite-titanite grains are fulfilled with plagioclase or hornblende grains. In biotitized mottled gabbros the titanite is absent and magnetite is located as minor dissemination.

6.1.2 Petrography of the diorite

A total of ten samples were classified as diorites. In hand samples, the diorite texture is phaneritic and the grain size is medium (Fig. 19). The colour of the drill core samples is medium grey with greenish tint. Diorites in the Tanhua mafic complex consist mainly of plagioclase and hornblende. Moderate to minor amount of quartz is present in diorite samples. The modal composition of hornblende varies from 10% to 30% and the composition of plagioclase from 40% to 55%. All studied diorite samples contain magnetite between 20 and 30%. The amount of quartz changes from accessory mineral up to 25%. The average grain size of diorites is between 0.3 mm to 0.7 mm, but the maximum grain size is 2.2 mm.

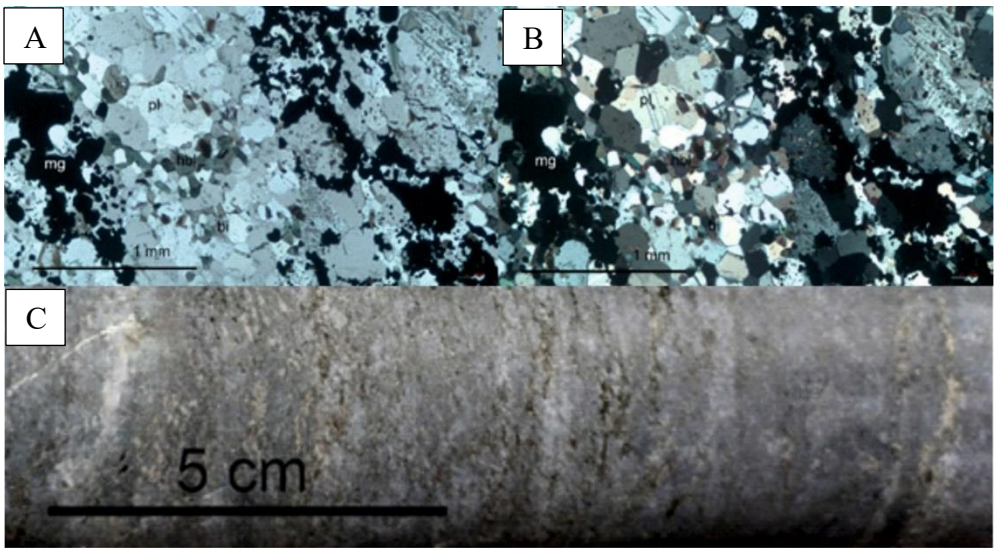

Figure 19. Microphotographs and photograph presentinggeneral texture of diorite in the Tanhua mafic complex. Sample U5212019R7 56.85 A) Microphotograph PPL 5x, B) Microphotograph XPL 5x. C) Photograph of drill core. Abbreviations of A) and B) hbl – hornblende, pl – plagioclase mg – magnetite and bi – biotite.

Texture of plagioclase and hornblende is mainly granoblastic. Minor amount of exsolution of quartz from hornblende is possible to observe. Poikilitic texture is common with plagioclase as phenocryst and hornblende as smaller grains. If biotite is present, it forms granoblastic texture together with plagioclase and hornblende. One sample (U5212019R8 162.40) present minor accumulation of biotite grains. The amount of biotite can be up to 10% in dioritic samples. Magnetite forms dissemination and veinlet in dioritic samples in the Tanhua mafic complex (Fig. 20). Magnetite is also found together with titanite forming core-rim texture. Minor amount of sulphides locates in diorites. Main sulphides are pyrite and chalcopyrite, but minor amount of pyrrhotite can be also found. Chalcopyrite is commonly altered to bornite and chalcocite. Other accessory mineral are apatite, chlorite, and zircon.

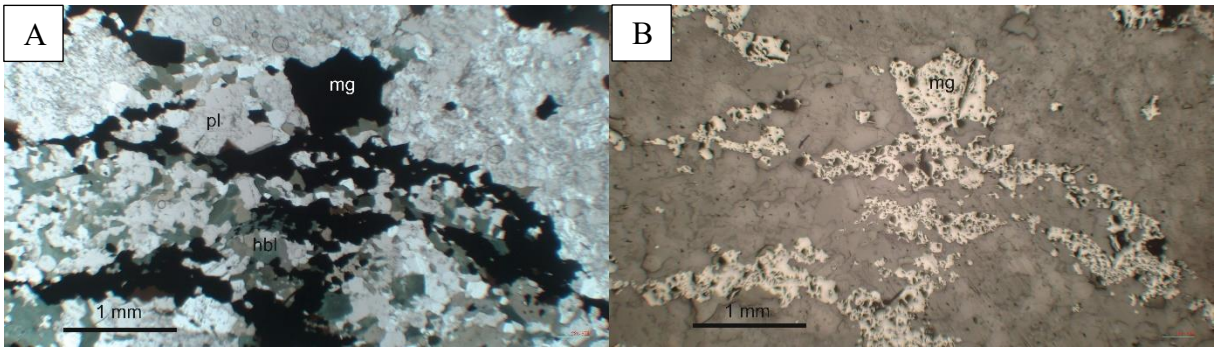

Figure 20. Microphotograph presenting occurrence of magnetite in diorite in the Tanhua mafic complex. Sample U5212019R3 277.15 A) PPL 2x, B) Reflected PPL 2x. Abbreviations hbl – hornblende, pl – plagioclase and mg – magnetite.

6.1.3 Petrography of the tonalite

The tonalite represent the most felsic material in the Tanhua mafic complex. The 11 sample of tonalitic material were studied. Macroscopic scale the colour of the drill core samples is either grey with dark parts of pinkish with dark parts, the texture is phaneritic with medium grain size (Fig. 21). The pinkish colour of in macroscopic scale can be easily confused with granite, but the pinkish colour is caused by albite as plagioclase is mainly albite in tonalites (Fig. 21). Minor amount of sulphides are visible. In thin section, tonalites consist mainly of plagioclase and quartz. The modal composition of plagioclase is between 40% and 70% and the composition of quartz is between 20% up to 40%. Hornblende is found mainly as accessory mineral, but the amount of hornblende can be up to 5%. The average grain size in different tonalitic samples varies from 0.4 mm to 0.8 mm, but the grain size can be up to 3.1 in tonalites.

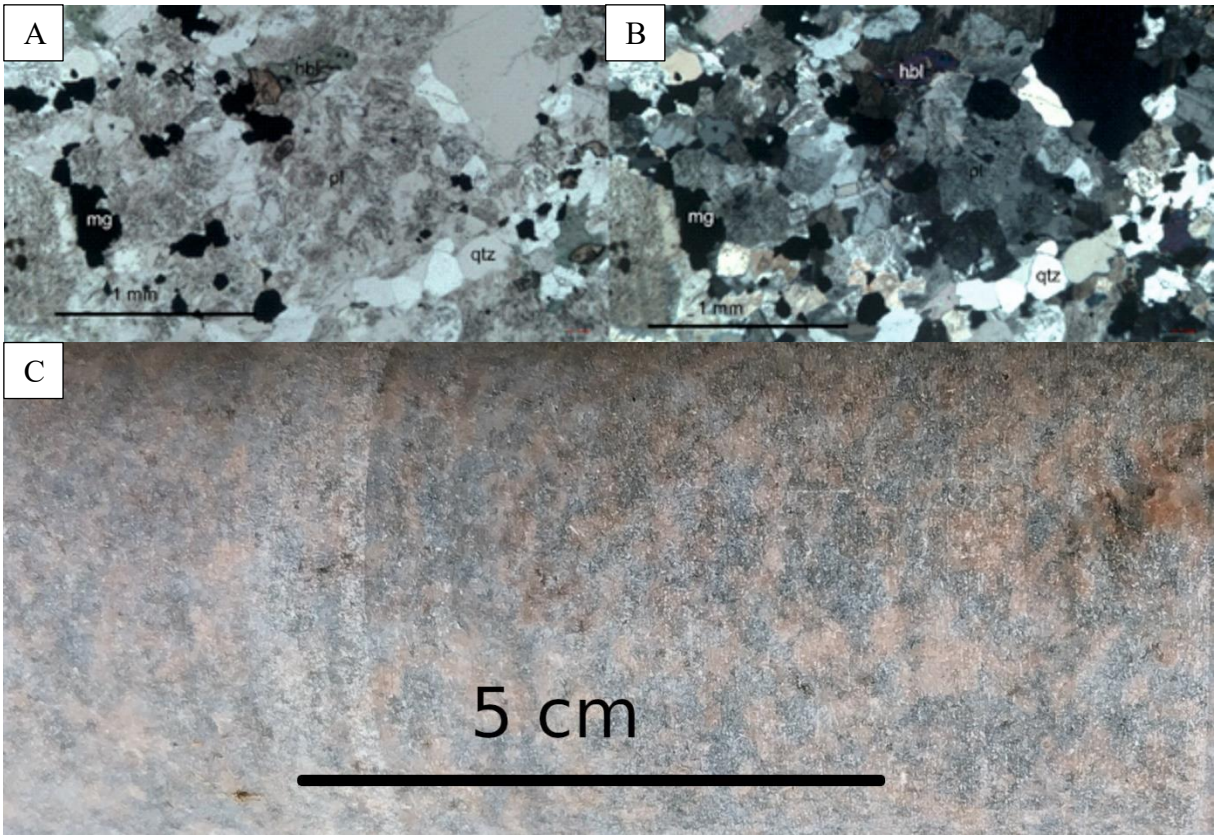

Figure 21. Microphotographs and photograph presenting general texture of tonalite in the Tanhua mafic complex. Sample U5212019R7 120.70 A) Microphotograph PPL 5x, B) Microphotograph XPL 5x. C) Photograph of drill core. Abbreviations of A) and B) hbl – hornblende, pl – plagioclase, mg – magnetite and qtz – quartz.

The general texture of tonalites is granoblastic. Plagioclase is found as porphyroblast with poikilitic textures. The minerals inside of the plagioclase phenocryst are hornblende and biotite. Commonly plagioclase has strong alteration mostly to albite, but also to scapolite and sericite. Minor plagioclase grains have zoned textures as the centre is more altered than outside. Minor amount of plagioclase grains are albite law twinned or Carlsbad twinned (Fig. 22A). All studied samples contain 5-30% of magnetite. Magnetite forms dissemination and veinlets in tonalite. Magnetite can be found also overprinting hornblende in tonalitic samples and in these places the hornblende is strongly altered (Fig. 22B). Zircon, calcite, and apatite are found as rare accessory minerals (Figs. 22C and 22D). Minor amount of pyrite and altered chalcopyrite are found. Chalcopyrite is altered to bornite and chalcocite.

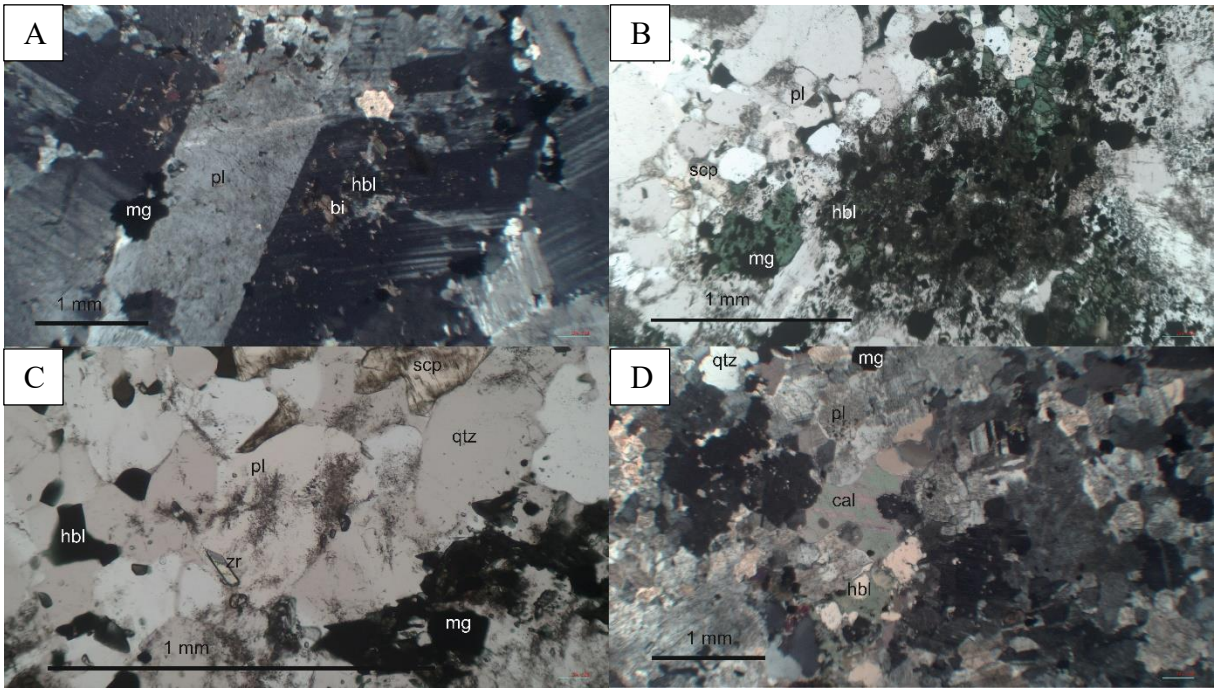

Figure 22. Microphotograph presenting A) poikilitic texture and albite twinning of plagioclase, sample U5212019R4 65.45 XPL 2x B) Magnetite overprint on hornblende, sample U5212019R3 330.35 PPL 5x, C) Occurrence of zircon, sample U5212019R3 330.35 PPL 10x D) Occurrence of calcite in tonalite in the Tanhua mafic complex, sample U5212019R3 330.35 XPL, 2x. Abbreviations hbl – hornblende, pl – plagioclase, bi – biotite, mg – magnetite scp – scapolite, qtz –quartz, zr– zircon and cal – calcite.

6.1.4 Petrography of the peridotite

Two samples U5212019R13 82.35 and U5212019R13 149.05 from the Tanhua mafic complex present peridotitic rocks. In macroscopic samples the peridotite's colours is pale grey with minor dark dots. The samples are not oriented, and the grain size is fine. In the thin section the main mineral is white amphibole, which extinguish oblique, about 12° c ∧ γ and have high interference colours up to third order blue (Fig. 23). Accessory minerals of peridotite are magnetite as dissemination and minor amount of pyrite. The samples are not oriented, and the texture is desccussate. The average grain size is ca. 0.3 mm, and the maximum grain size is 1.2 mm.

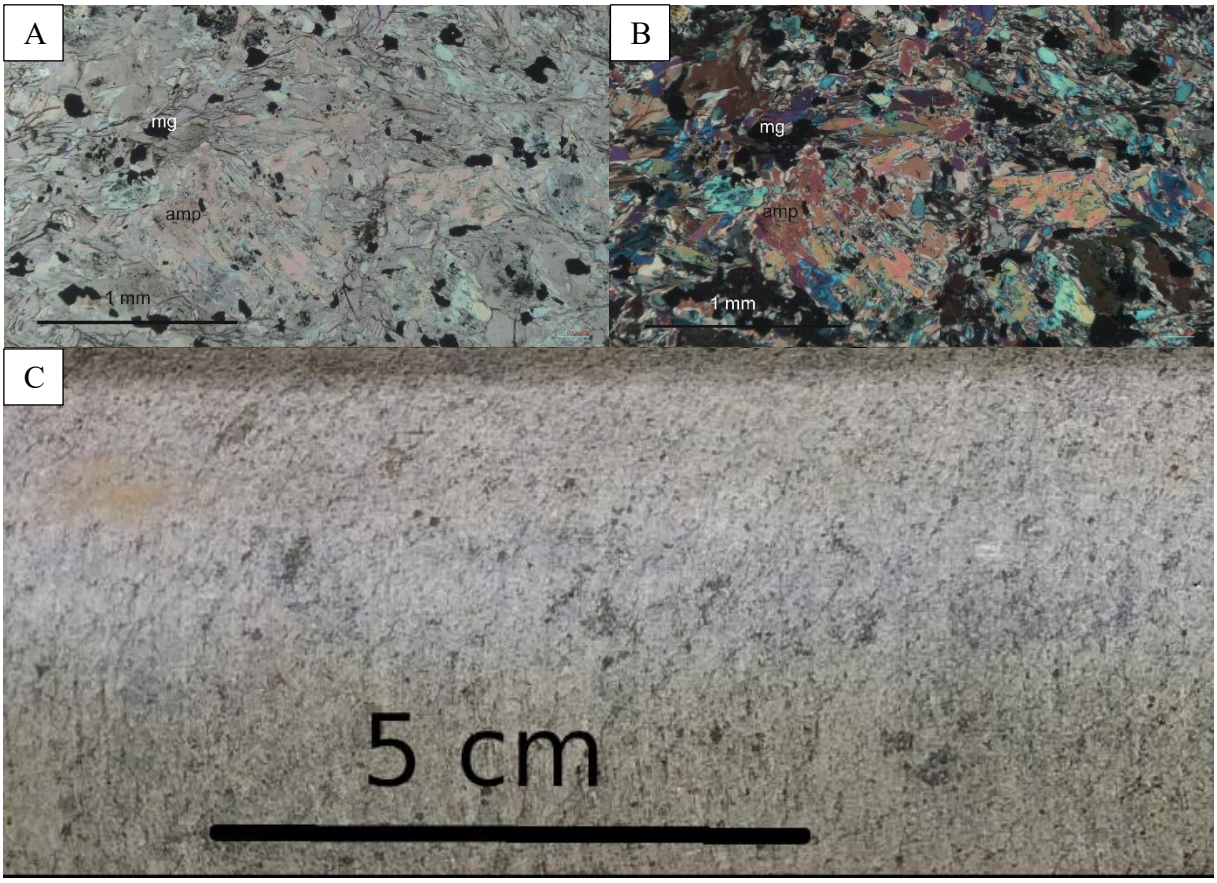

Figure 23. Microphotograph presenting general texture of peridotite in the Tanhua mafic complex. A) PPL 5x, B) XPL 5x. Sample U5212019R13 82.35, C) Photograph of drill core near of the sample U5212019R13 149.05 presenting pyroxene in the Tanhua mafic complex. Abbreviations of A) and B) amp – amphibole and mg – magnetite.

6.1.5 Petrography of the mafic vulcanic rock

Mafic vulcanic rocks are dark greenish greys in macroscopic samples (Fig. 24). The grain size of the samples is fine, and the drill core samples are moderately to strongly oriented. In thin sections the mafic vulcanic rocks are strongly recrystallized, and the texture is strongly granoblastic (Fig. 24). The average grains size is 0.1 mm and grains up to 0.7 mm are found in mafic vulcanic rock samples. The main minerals are hornblende which model composition varies between 50 to 55 %, and plagioclase which model composition varies between 45 to 50 %. Minor amount of accessory minerals are present as magnetite, ilmenite, pyrite, chalcopyrite, chalcocite, bornite, chloride, scapolite and quartz. The mafic vulcanic rocks are weak to strongly oriented as hornblende grains are elongates and oriented to same direction. The plagioclase grains are not twinned. The grade of the hydrothermal alteration of plagioclase varies on different samples from intact to strongly altered. The alteration product is mainly albite, but minor amount of scapolite is found. Veins cut the vulcanic material and the hydrothermal alteration is strong along the vein. The chlorite is observed in the vein.

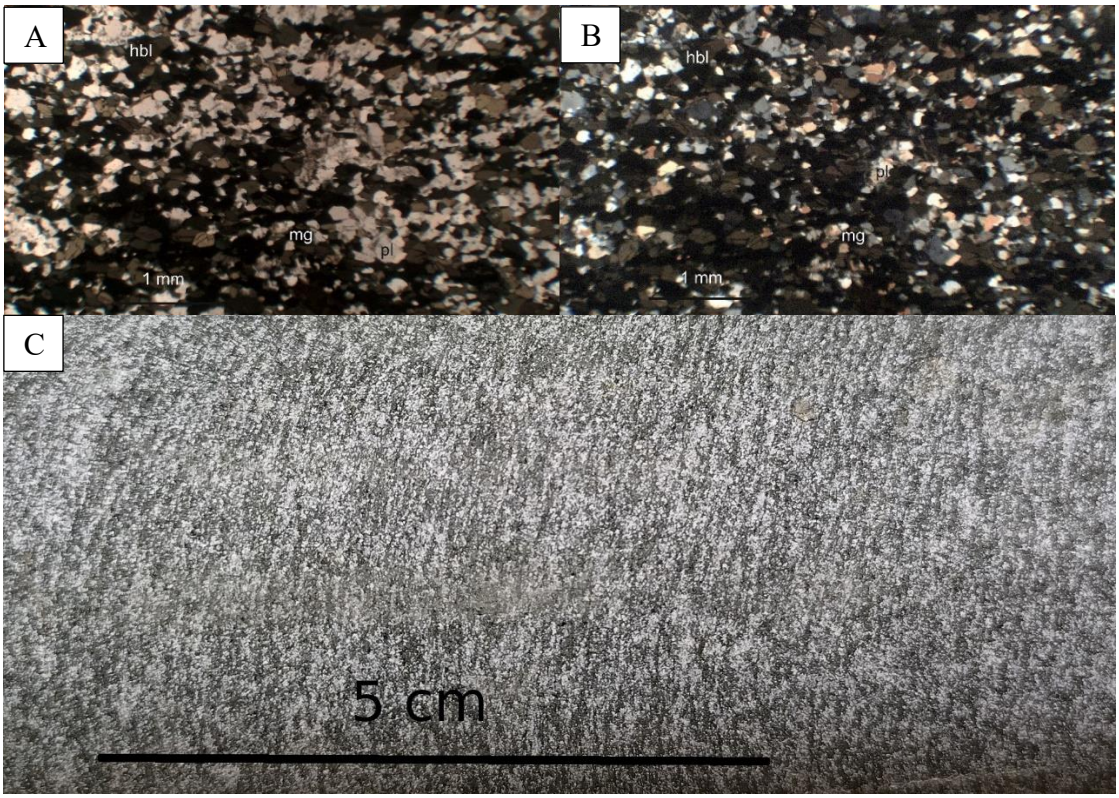

Figure 24. Microphotograph presenting general texture and grain size of mafic vulcanic rock in the Tanhua mafic complex. A) PPL 2x, B) XPL 5x. Sample U5212019R14 84.50 C. Photograph of drill core near of the sample U5212019R14 84.50 presenting vulcanic rock in the Tanhua mafic complex. Abbreviations of A) and B) hbl – hornblende, pl – plagioclase and mg – magnetite.

6.2 Benchtop Micro-XRF results

Benchtop Micro-XRF elementary maps were made from four samples, which contained three gabbro samples and one tonalite sample. The scanned elementary maps support the thin section studies as like found minerals and textures. The benchtop micro-XRF studies also revealed the location of Co and Zr in the Tanhua mafic complex. The Co is found in pyrite mineral (Fig. 25).

6.2.1 Sample U5212019R8 32.55-32.75

The elementary map made from gabbro sample U5212019R8 32.55-32.75 (Fig. 25) present well the occurrence of Co in the Tanhua mafic complex. In elementary map, the Co is located in places where also S is present, but the Cu is not. Indicating that the Co is not in chalcopyrite, but it is in pyrite. The same spots contain also Fe, but because the majority of the mineral present in sample U5212019R8 32.55-32.75 contain Fe the elementary map of Fe is not informative apart to confirm the pyrite mineral. The ratio of pyrite/chalcopyrite in the sample U5212019R8 32.55-32.75 is high and the pyrite is more common mineral than chalcopyrite.

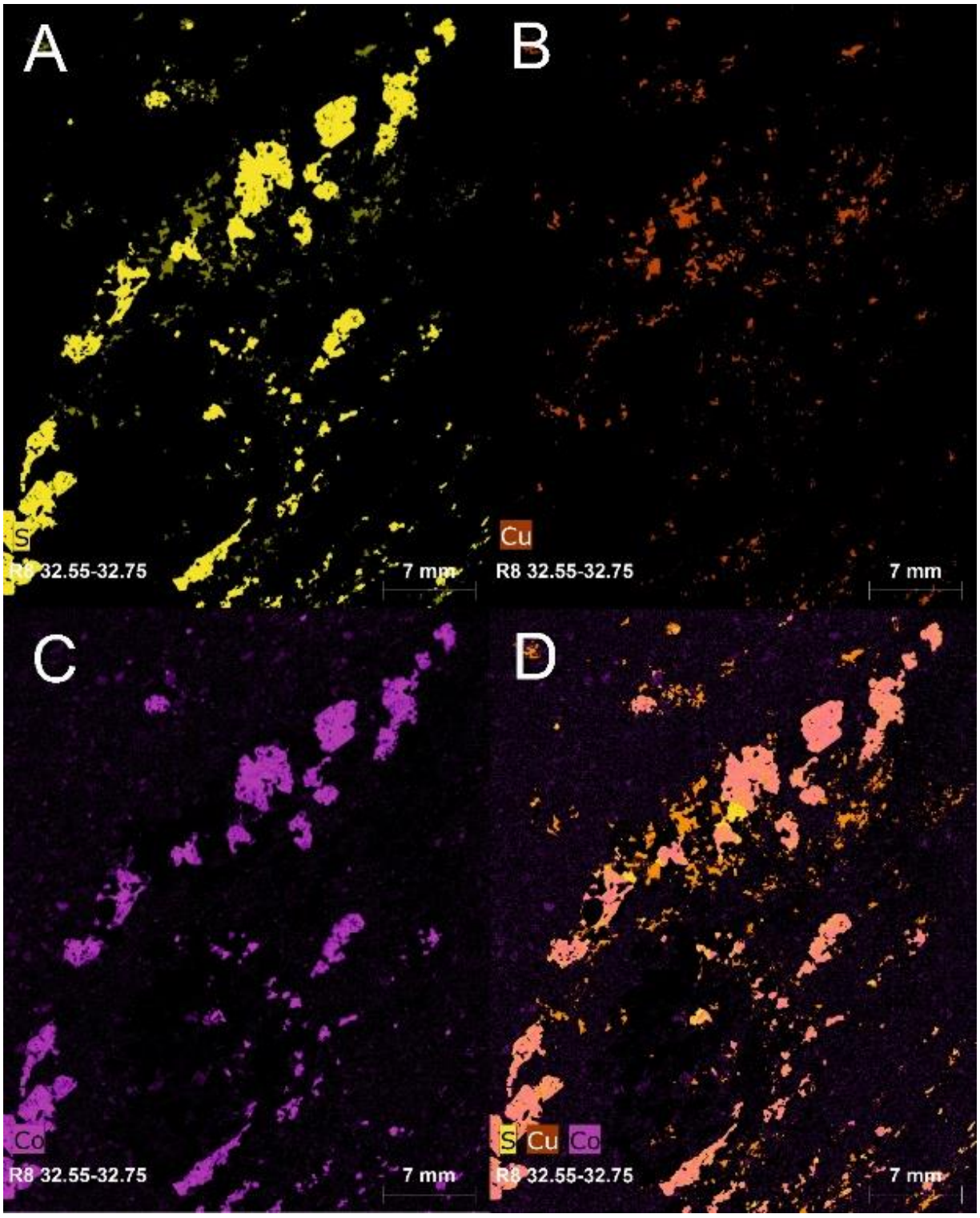

Figure 25. XRF elementary maps of sample U5212019R8 32.55-32.75 presenting the occurrence of pyrite and chalcopyrite. In addition, present the occurrence of Co in pyrite. A) sulphur presented, B) copper presented, C) cobalt presented, D) sulphur, copper and cobalt presented together.

6.2.2 Sample U5212019R7 44.40-44.50

The dissemination of magnetite in gabbro can be observed in elementary map from sample U5212019R7 44.40-44.50 (Fig. 26). In the elementary map, the red parts are proposed to be magnetite as these parts do not contain any other detectable element in benchtop micro-XRF. The instrument cannot detect oxygen and therefore it is suggested that these parts contain oxygen also. The map shows that the gabbro consists of mainly hornblende and plagioclase. Minor amount of biotite and calcite and sulphides are present. The minerals are proposed based on the elementary content and relative concentration of element in elementary map.

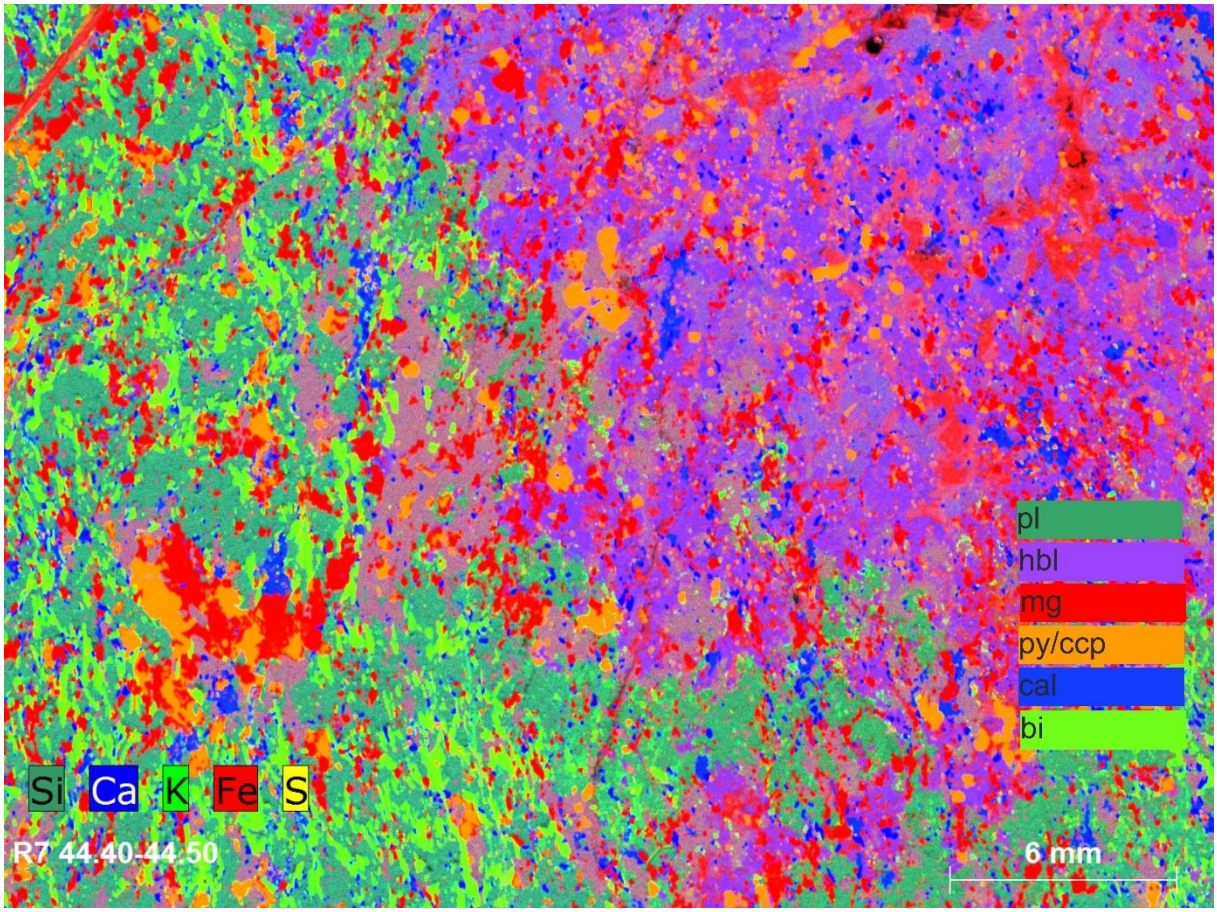

Figure 26. XRF-elementary maps presenting dissemination of magnetite in sample U5212019R7 44.40-44.50. The proposed minerals are based on common element content of minerals. Abbreviations pl – plagioclase, hbl – hornblende, mg –magnetite, py – pyrite, ccp – chalcopyrite, cal – calcite and bi – biotite.

6.2.3 Sample U5212020R10 141.85-142.00

Calcite is strongly present in sample U5212020R10 141.85-142.00 (Fig. 27). All blue parts are proposed to represent calcite as Ca is the unique detected element by benchtop micro-XRF. As O and C are not delectables with XRF-instrument, they are suggested to be present in blue parts and completing the calcite mineral. Biotite is proposed based on existence of K and other typical

mineral in the Tanhua mafic complex do not contain significant amount of K in chemical formula. In the sample U5212020R10 141.85-142.00 the spectrum gives spike for zirconium and the zircon is found in the Tanhua mafic complex and are shown in elementary map and microphotograph (Fig. 28). With the benchtop micro-XRF Si was the only other element detected together with zirconium. The zircon locates together with plagioclase either inside of mineral or in grain boundaries of the plagioclase mineral.

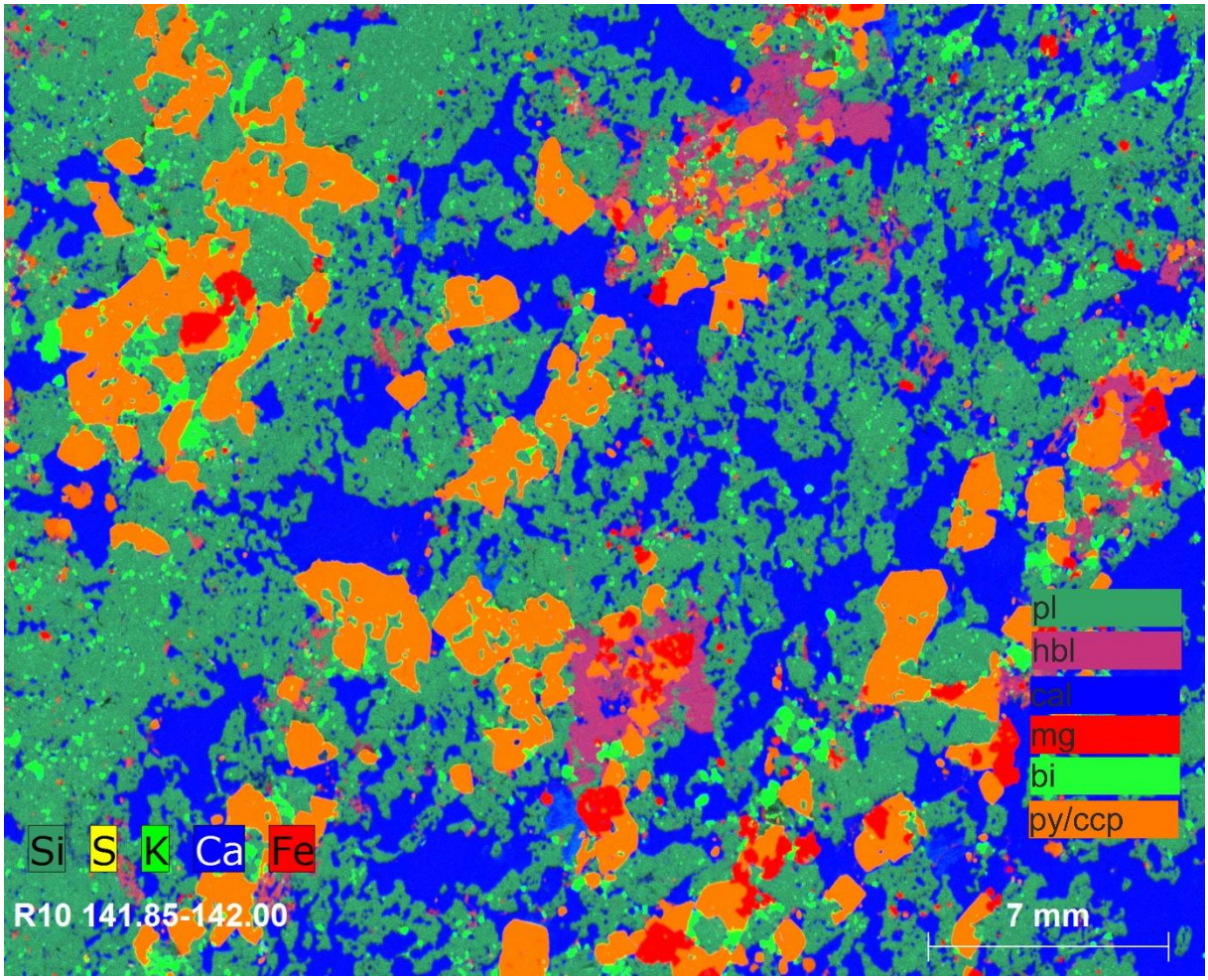

Figure 27. XRF-elementary maps of sample U5212020R10 141.85-142.00 presenting calcium alteration of the Tanhua mafic complex. The proposed minerals are based on common element content of minerals. Abbreviations pl – plagioclase, hbl – hornblende, mg –magnetite, py – pyrite, ccp – chalcopyrite, cal – calcite and bi – biotite.

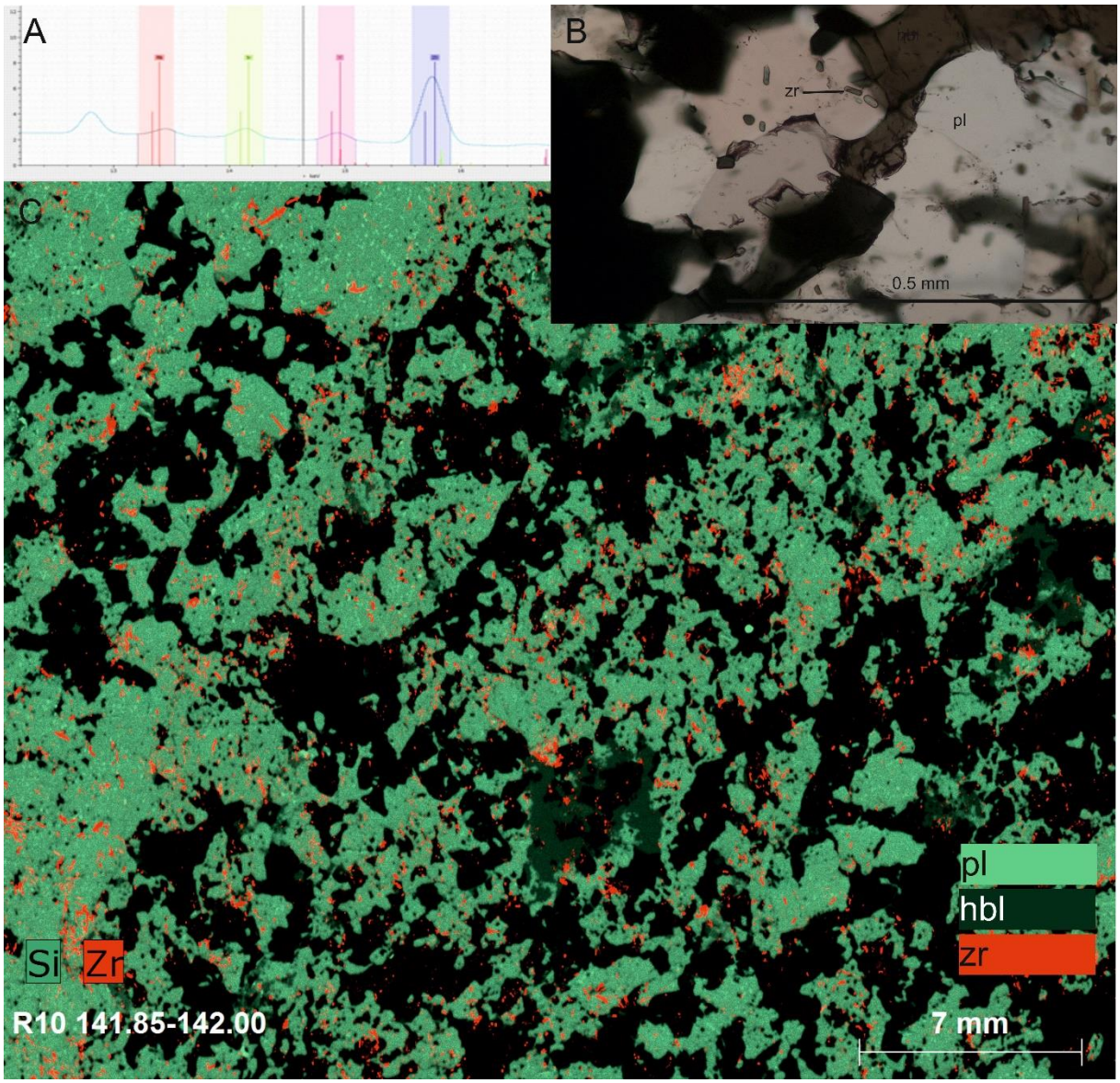

Figure 28. Sample U5212020R10 141.85-142.00 A) XRF spectrum of zirconium. B) Microphotograph of occurrence of zircon together within plagioclase PPL 20x C) XRF-elementary map presenting the location of zircon. The proposed minerals are based on common element content of minerals. abbreviations pl – plagioclase, hbl – hornblende and zr – zircon.

6.2.4 Sample U5212019R5 171.05.171.20

Elementary map made from tonalite sample U5212019R5 171.05.171.20 (Fig. 29) shows general texture of tonalite. It consists mostly of plagioclase with magnetite as dissemination. Minor amount of quartz in present. In the elementary map, sulphides can be either pyrite or chalcopyrite as copper is not show in the map. Sulphides are found as dissemination in tonalite Sample U5212019R5 171.05.171.20. As Ca together Fe is rare in elementary map, hornblende is not common in tonalite sample and is precent as accessory mineral as biotite, and calcite are also accessory minerals in the sample.

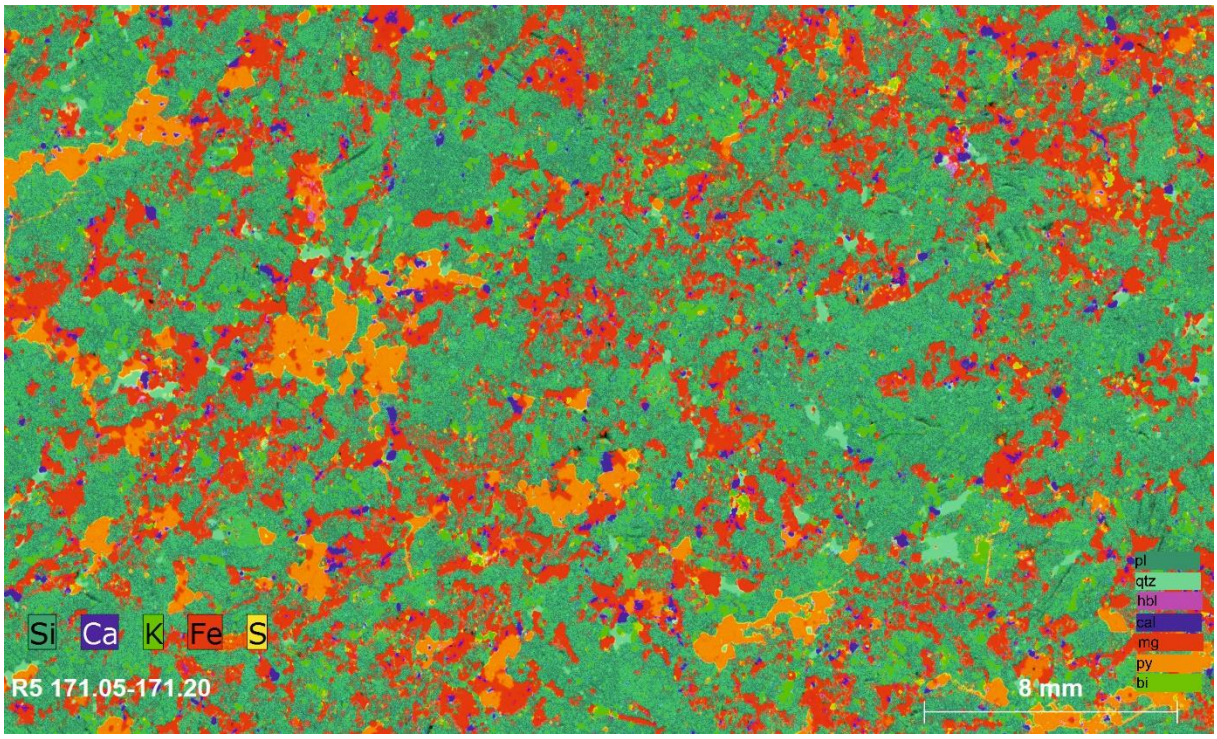

Figure 29. XRF-elementary maps of sample U5212019R5 171.05.171.20 presenting tonalite in the Tanhua mafic complex. The proposed minerals are based on common element content of minerals. Abbreviations pl – plagioclase, hbl – hornblende, mg –magnetite, py – pyrite, qtz – quartz, cal – calcite and bi – biotite.

7 Discussion

7.1 The Tanhua mafic complex emplacement and connection of the original geology

7.1.1 Multiple magma pulses as mechanism of placement

The Tanhua mafic complex has been formed by multiple different magma pulses. The clearest evidence of multiple magma pulses is the presence of chilled margins within drill cores (Konnunaho et al., 2022). The chilled margins were observed in revision logging and confirmed from thin sections. The grain size decreases gradually towards the chilled margin. When reaching the margin, the grain size is about 0.1 mm. Passing the chilled margin the grain size is significantly larger, about 0.4 mm. The chilled margins are visible in majority of the drill cores and example in the drill core U5212019R8 there are four cycles of gradual decreasing of grain size and chilled margins (Fig. 30). The cross-cutting relationships between the rock units of the Tanhua mafic complex support that the rock units are not intruded in same time as younger units cuts the older rock units (Konnunaho, personal communication 23.2.2022).

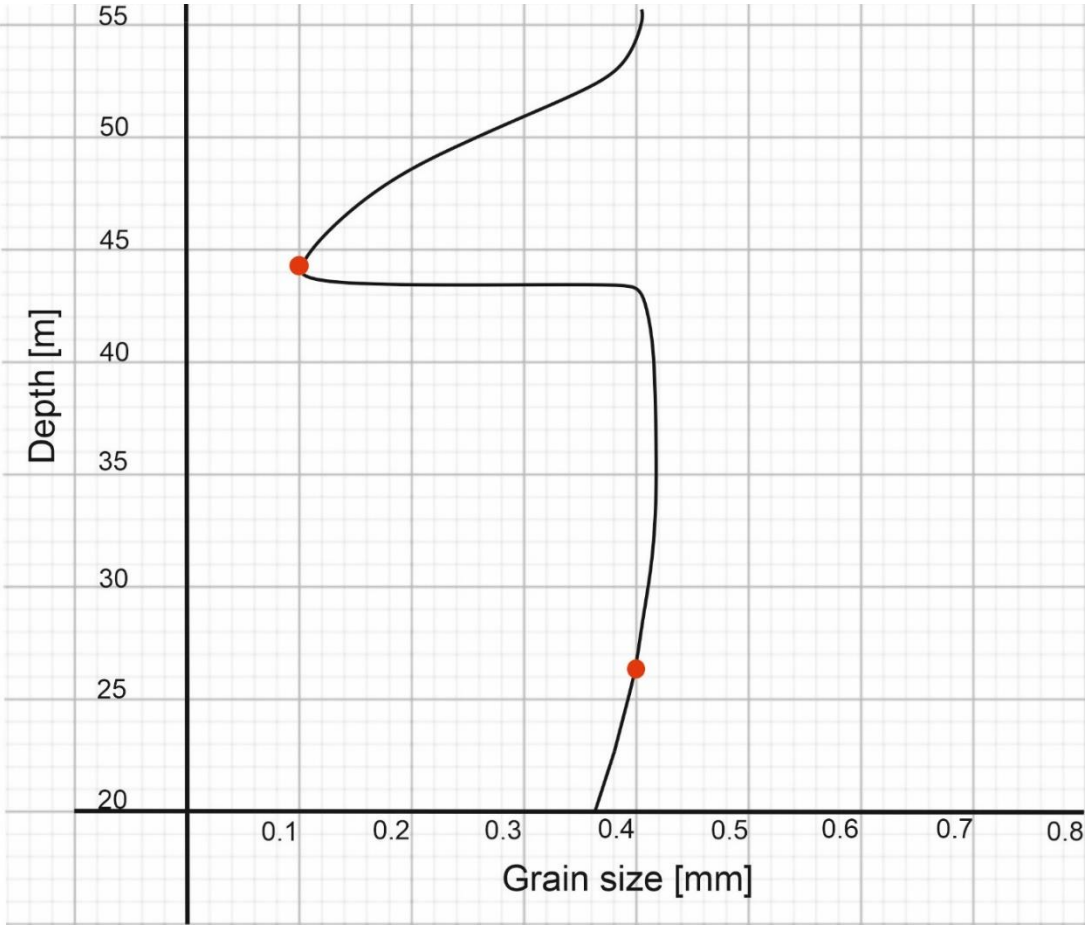

Figure 30. A draft presenting the estimated change of the grain size in drill core U5212019R8 between depths 20m and 55m. The red dots are measured points confirmed with thin sections. The black line is the estimated grain size along the drill core.

7.1.2 Local variation

In the Tanhua mafic complex (Fig. 31) the mineralogy is similar in Kylälampi (Fig. 32), Kannusvaara (Fig. 33), and Markkinaselkä (Fig. 34) intrusions. Not all rock types are present in all studied places, but described rock types are similar regardless of the place. Gabbros and oxide gabbros are present in all three places and are similar very similar always as they consist of hornblende, plagioclase and occasionally of magnetite. In Kannusvaara the stratigraphy is the most complex (Fig. 33) and it is only places where diorite is found, but remained mottled gabbro is absent. Kannusvaara contains skarn, vulcanic rocks and supracrustal rocks as xenoliths within the central part of the intrusion. Kylälampi contains ultramafic peridotite but is probable that the ultramafic part does not belong to the Tanhua mafic complex and is formed separately (Fig. 31). Apart of that it has similar mineralogy than Kannusvaara apart from minor presence of remained mottled gabbro that is absent in Kannusvaara. The supracrustal rock are stacked in Kylälampi also as in Kannusvaara, but no skarns or vulcanic rocks are logged. Markkinaselkä has the simplest stratigraphy as it consists only of four different rock types as felsic tonalite and intermediate diorite part of the intrusion are absent (Fig. 34). The rock units are also formed clear units. The most sulphide rich parts of the Tanhua mafic complex are related to magnetite bearing units as oxide gabbros and tonalites (Fig 33; Konnunaho, personal communication 23.2.2022). Remained mottled gabbros and biotitized mottled gabbros are poor in sulphides as well as in magnetite.

7.1.3 Zircon

The elevated Zr content (500-1300 ppm) described by Konnunaho et al., (2022) can be explained with the presence of zircon mineral (Fig. 28). Benchtop micro-XRF displays, that in the places where Zr is elevated, Si is detected without other detectable elements in the same place. That eliminates the other common Zr bearing minerals as monazite as P is absent and Baddeleyite as Si exist. No-detectable O fulfils the zircon mineral.

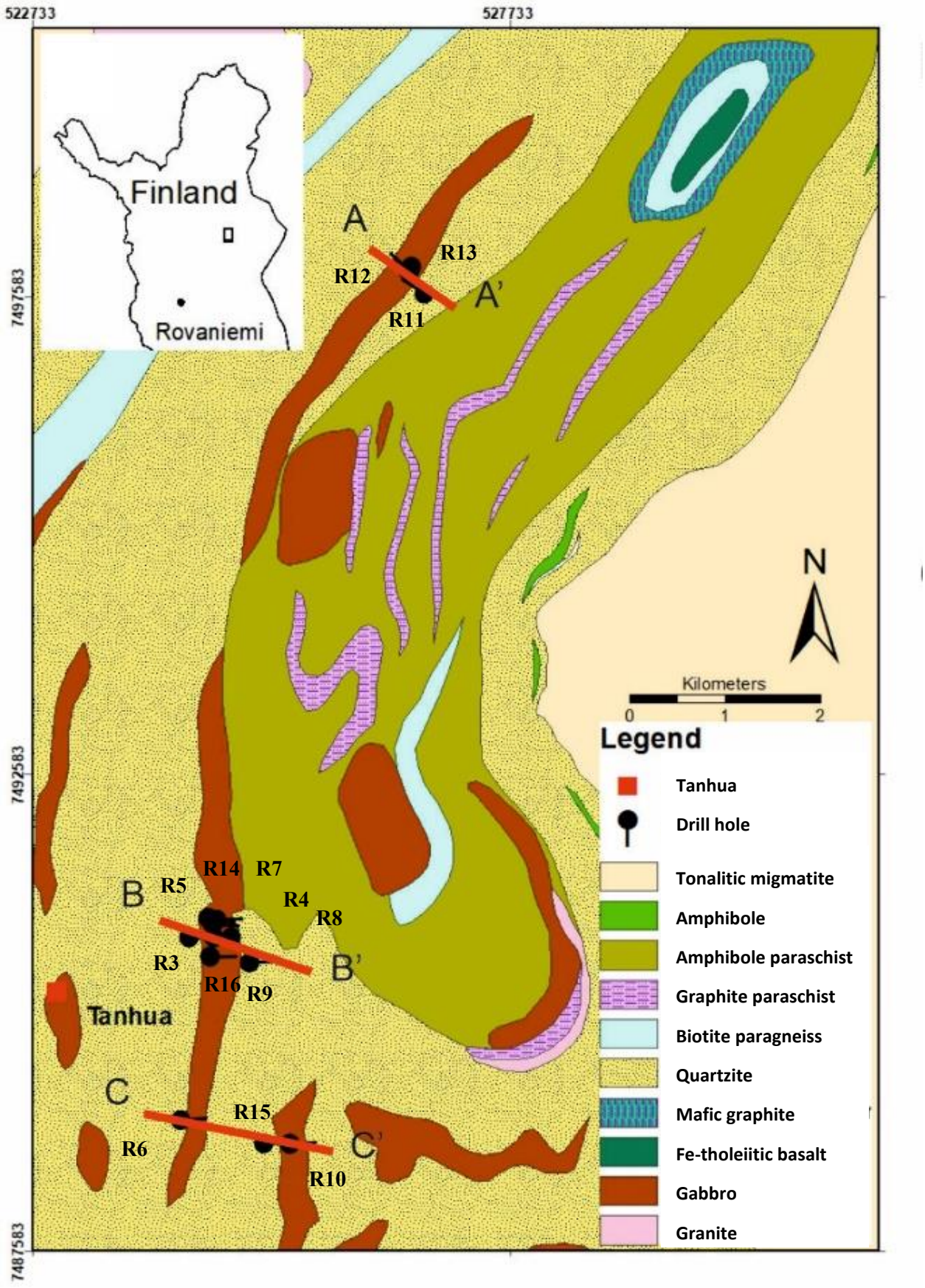

Figure 31. Geological map presenting the localization of three cross-sections (A – A' Kylälampi, B – B' Kannusvaara, C – C' Markkinaselkä) and drill hole of the Tanhua mafic complex. Coordinate system ETRS-TM35FIN. (Modified after DikiKP and Konnunaho et al. (2022)).

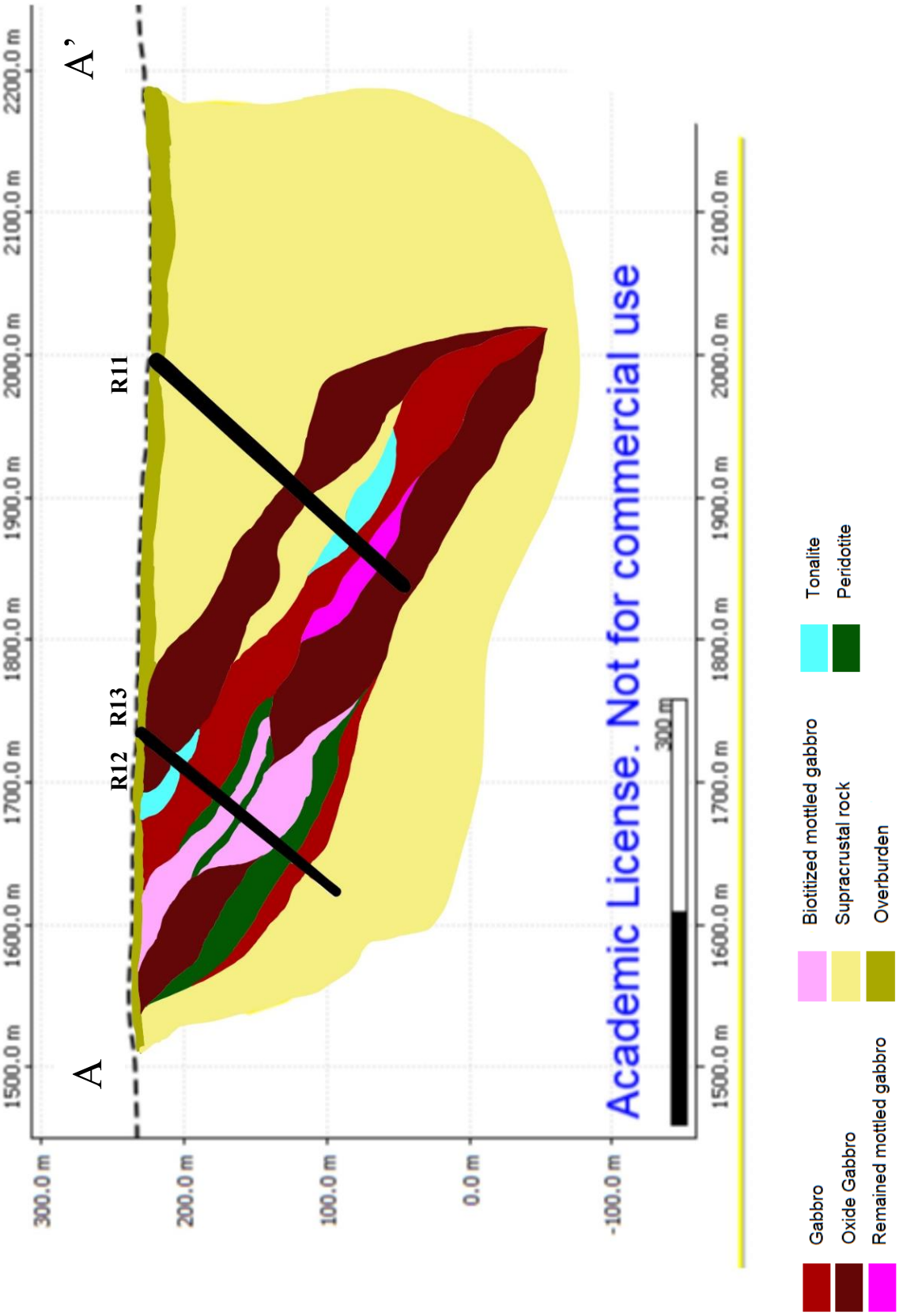

Figure 32. Simplified cross section of Kylälampi.

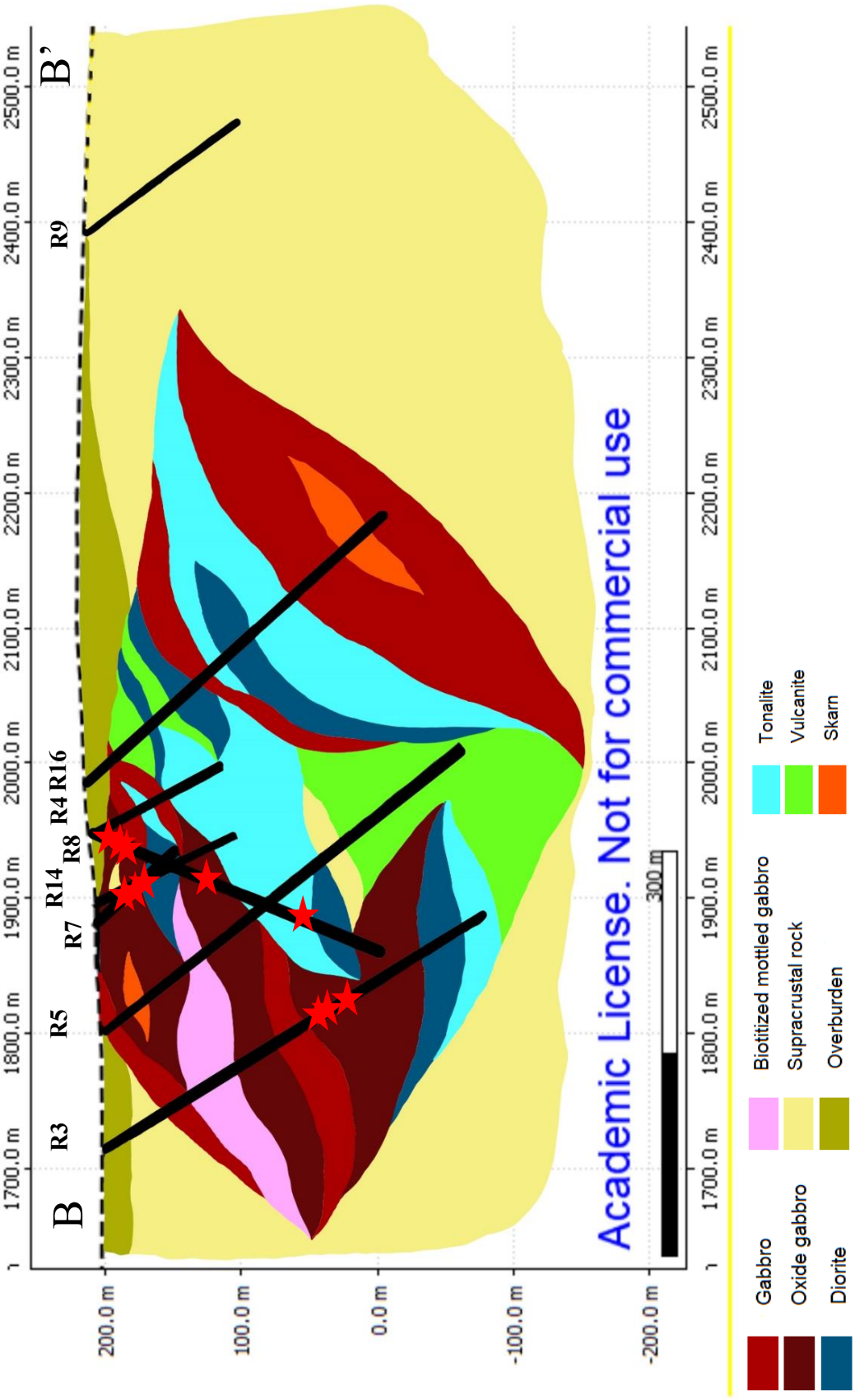

Figure 33. Simplified cross section of Kannusvaara. Red stars symbolize the most significant mineralizations in the Tanhua mafic complex after Konnunaho et al. (2022).

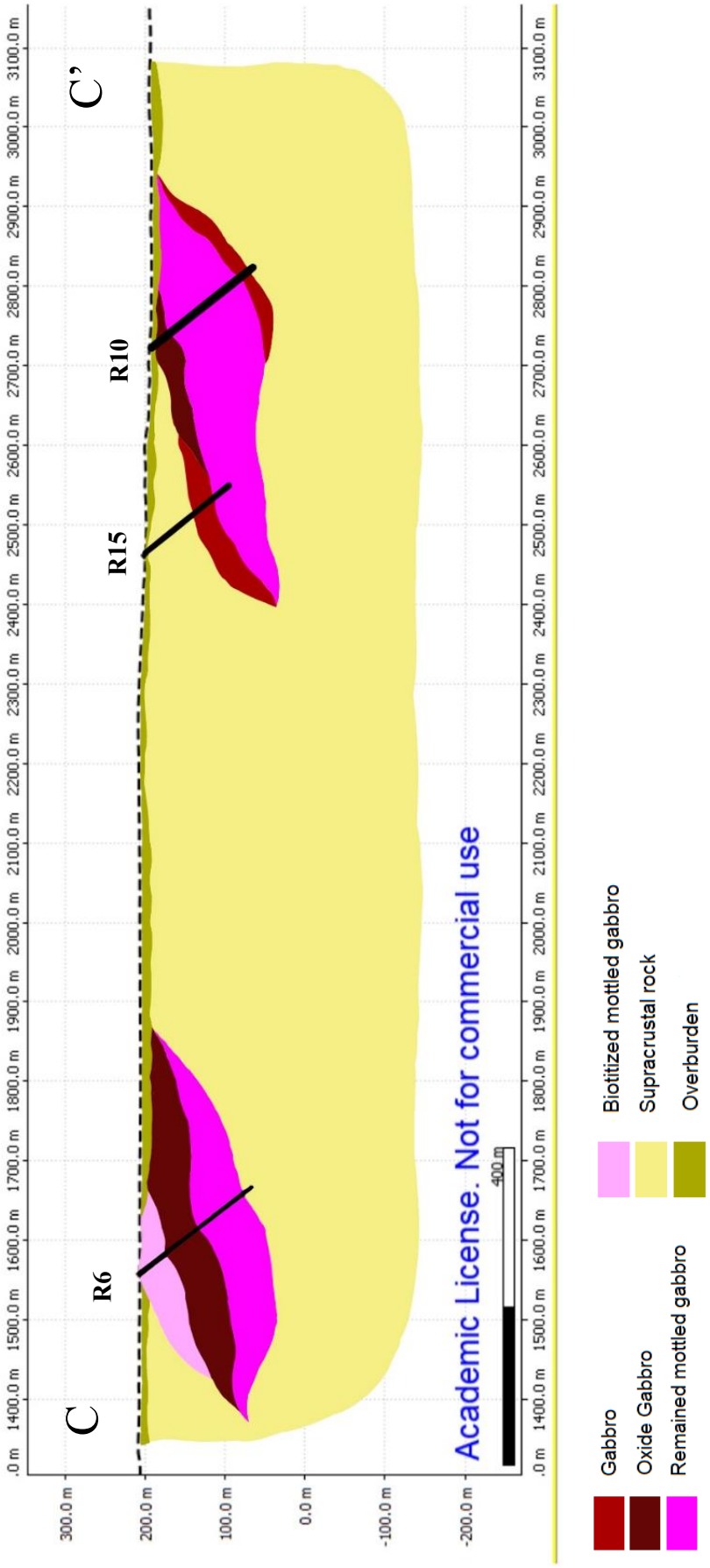

Figure 34. Simplified cross section of Markkinaselkä.

7.1.4 Differentiation of magma

High magnetite content of the Tanhua mafic complex indicates elevated Fe concentration in original magma. As the forming process of the Tanhua mafic complex has been by multiple magma pulses, the differentiation of magma has not occurred in situ but rather within the original magma chamber. The magma has been differentiated before the magma is erupted to the placement. Based on unpublished geochemical data, the differentiation trend has been tholeiitic. The Tanhua mafic complex does not bear evidence of layered structure except some larger petrographic units which can be followed to other drill cores. The different rock units of the Tanhua mafic complex are placed in disorder in different drill cores and same rock units are difficult to identified in other drill cores (Fig. 33). The same rock unit can be repeated various times in same drill core and different magma pulses of the same rock types can be seen following each other in same drill core. The differentiation trend cannot be followed upwards in the Tanhua mafic complex rather the more felsic material can be between two mafic rock units.

7.1.5 Effect of metamorphosis

The area of the Tanhua mafic complex is strongly metamorphosed in middle amphibole facies (Hölttä & Heilimo, 2017) and the results of this study support that as hornblende is common secondary mineral in the Tanhua mafic complex. Therefore, the original augite, which is present only in one sample, is metamorphosed to hornblende in conditions of amphibole facies. Also, the metasomatic processes have occurred as sulphides are found in the Tanhua mafic complex and it has been significantly hydrothermal altered. The common alteration processes of the Tanhua mafic complex for plagioclase are albitization, scapolitization, and calcitization as anorthite is altered to albite, scapolite or calcite, and for hornblende common alteration is biotitization. Also, leucoxene is common alteration product of magnetite. Therefore, the original textures and minerals of the Tanhua mafic complex are hardly seen and it increases the uncertainty of the interpretation. As the mafic vulcanic rock is also strongly metamorphosed and it appears as amphibolite, therefore it is hard to be sure of the protolith of the rock and some mafic vulcanic rock samples might be originally gabbros.

7.2 Comparation to other mafic intrusion types in northern Finland

7.2.1 Metasomatised mafic intrusives in northern Finland

The Tanhua mafic complex belongs to the metasomatized mafic Co-enriched intrusions in northern Finland as the similarities with Hietakero (Konnunaho et al., 2018), Iso-Povivaara (Karvinen, 1983), Kelujoki (Karvinen, 1982) are significant and the attributes of the Tanhua mafic complex support the hypothesis. Compared to the Hietakero mafic intrusion (Fig. 1), Tanhua mafic complex has several similarities as both the Tanhua mafic complex and Hietakero mafic intrusion contain elevated Co-Cu content and the Co is located in pyrite mineral lattice although in Hietakero Co is located also in pentlandite. Both deposits are associated with oxide enriched gabbroic bodies and contain veinlets and net-textures of sulphides like pyrrhotite, pyrite and chalcopyrite. The dissemination of sulphides is rare in Hietakero mafic intrusion, but relative common in the Tanhua mafic complex. Both Hietakero mafic intrusion as well as the Tanhua mafic complex has been metamorphosed in middle amphibole facies (Hölttä & Heilimo, 2017) and significantly hydrothermal altered. The albitization and scapolitization have been observed in both. The primary magmatic silicate minerals are rare in both intrusions. The country rocks of both intrusions consist of supracrustal rocks formed in basin environment, but country rocks of Hietakero mafic intrusion represents more deep sea environmental as it consists mainly of graphite-sulphide-bearing schist and felsic to intermediate vulcanic rocks. However, country rocks of the Tanhua mafic complex represent shallower basin environment with limited amount of deep-sea environmental rock as quartzite and biotite-schist and mafic to intermediate vulcanic rocks. The Hietakero mafic intrusion itself contain ultramafic parts which are absent in the Tanhua mafic complex at least current erosion level and drill holes. Instead the Tanhua mafic complex contains felsic and intermediary parts as tonalites and diorites. The cumulate texture is observed in Hietakero mafic intrusion, but it is not observed in the Tanhua mafic complex as the primary textures are not reserved. Mineralogically both intrusions are similar, with some difference. The main minerals in both are hornblende and plagioclase, but clinopyroxene and actinolite are absent in the Tanhua mafic complex and scapolite is not as common as in Hietakero mafic intrusion. The Hierakero mafic intrusion does not contain the mottled texture (Konnunaho et al., 2018). The intrusions of Kelujoki and Iso-Povivaara have similarities with the Tanhua mafic complex as Co-bearing pyrite is related to metasomatized gabbro intruded to Paleoproterozoic supracrustal rocks. As both intrusions remain poorly studied, the larger comparations are not possibles. The age determinations are made only from the Tanhua mafic complex and Iso-Povivaara giving the same age. Thet

indicates that they are related to same magmatism. Even there are no age determination made from Hietakero and Kelujoki, they probably are related to same magmatism 2.14 Ga ago because similarity of gabbros and geological location in CLGB.

7.2.2 Mafic-ultramafic 2.5-2.4 Ga layered intrusions in northern Finland

Compared to the layered intrusions formed by magmatism of 2.5-2.4 as Koitelainen intrusion the Tanhua mafic complex has several differences. The Tanhua mafic complex lacks the characteristic layered structure that is present in Koitelainen mafic intrusion. Mineralogically the Koitelainen intrusion consists of the ultramafic part, the mafic part and felsic part, but lacks intermediate rocks (Fig. 31). In the Tanhua mafic complex lacks ulramafic part, but the mafic part is mineralogically different compared to the Koitelainen intrusion as gabbro of Koitelainen contains cumulates of plagioclase, orthopyroxene and clinopyroxene, but gabbro of Tanhua does not contain cumulates and the pyroxenes has been metamorphosed to mainly hornblende. Also, then felsic part of Koitelainen intrusion is different than the tonalites of the Tanhua mafic complex as in Koitelainen the felsic part consists of anorthosites compared to tonalites. The main potentially economical metals of Koitelainen are Cr and PGE, but the Tanhua mafic complex contain instead Co-Cu mineralization.

7.2.3 Ni-Cu-Co-PGE deposits in mafic-ultramafic intrusives in northern Finland

The Tanhua mafic complex differs significantly when compared to example Kevitsa mafic-ultramafic intrusion, which is example of Ni-Cu-Co-PGE deposit in mafic-ultramafic intrusive in northern Finland. Kevitsa mafic-ultramafic intrusion is little younger than the Tanhua mafic complex. Kevitsa consists mostly of ultramafic rocks as poikilitic olivine websterite and the ore is mainly located in ultramafic rocks (Fig. 32). As mentioned earlier, the Tanhua mafic complex lacks ultramafic rocks. Both complexes have been metamorphosed and pyroxenes have been altered to amphiboles. The Kevitsa intrusion is metamorphosed in middle amphibole facies (Hölttä & Heilimo, 2017). Hydrothermal processes are caused amphibole and serpentine-chlorite alteration to Kevitsa intrusion (Luolavirta, 2018). Gabbroic part of the Kevitsa intrusion contains minor amount of magmatic olivine, which is not present in the Tanhua mafic complex, and clinopyroxene, which is rare in the Tanhua mafic complex. In the Tanhua mafic complex, the boundaries between different rock types are generally chilled margins, but in Kevitsa intrusion the boundaries normally are gradual and sharp contact are absent. As the Kevitsa intrusion is Ni-Cu-PGE deposit, the ore contain mainly pentlandite and chalcopyrite with

moderate amount of pyrrhotite and magnetite, which are found mainly as dissemination in interstitial spaces between cumulates. The location and type of ore is different in the Tanhua mafic complex as pentlandite is not found and the ore is located as dissemination and veinlets without textural control (Santaguida et al., 2015, Makkonen et al., 2017).

7.3 Mineralization types and indication to ore forming processes, ore potentiality and exploration

7.3.1 Cobalt

Cobalt is found inside of the pyrite crystal lattice. As the chemical formula of pyrite is FeS_2 and in this case the Fe-ion occurs with oxidation state +2. Co-ion has been found with oxidation states of -3, -1, 0, +1, +2, +3, +4 and +5, but normally Co occurs in oxidation states of +2 and +3. Co^{2+}-ion has similar attributes with Fe^{2+}-ion as the oxidation state is same and the radius of these two ions are quite similar. Therefore, the Co^{2+} substitutes Fe^{2+} as cation in lattice of pyrite (Greenwood & Earnshaw, 1997; Rollinson, 1993). The Co/Ni ratio has not been calculated from pyrite, but as the Co content of the Tanhua mafic complex is high and Ni content is low (Konnunaho et al., 2022), the Co/Ni in pyrite should be higher than 1, indicating hydrothermal mineralization rather than sedimentary origin (Raymond, 1995). Vasilopoulos et al. 2020 suggests that in later ca. 1.93-1.76 Ga, strongly altered Au-Co deposit of Juomasuo in Paleoproterozoic greenstone belt the mineralization have occurred in different stages. In the mineralization the Co locates also in pyrite as in the Tanhua mafic complex, but also in pyrrhotite. The first stage has been strong albitization as majority of the rock has been altered. The second stage has been chloritization-biotization, which has formed the part of the Co mineralization. The third stage has been sericitization, which has formed the main part of Au-Co mineralization. Even Juomasuo deposit has differences with the Tanhua mafic complex e.g., host rock of Juomasuo is not limited to rocks within igneous origin and the presence of Au, the similar processes could have brought the Co to the Tanhua mafic complex. Vasilopoulos et al. 2020 propose that the Co of Juomasuo deposit (Fig. 1) is from mafic metavulcanic rocks which has been moved by highly saline, reduced hydrothermal fluids. Therefore, the origin of Co might be vulcanic from older Paleoproterozoic rock and moved by fluid activism to the Tanhua mafic complex itself (Bralia et al., 1979).

7.3.2 Source of sulphur

The source of sulphur of the Tanhua mafic complex is suggested not to be magmatic origin rather than delivered from country rock (Konnunaho et al., 2022). The schists are generally thought to be source of sulphur. There are not available sulphur isotope analyses from the Tanhua mafic complex, therefore the more complex indication of the source of sulphur are hard to make. But based on the information that the Tanhua mafic complex is mainly surrounded by quartzites, and the schist are more prominent source of sulphur, the sulphur source has been in deeper crust below the Tanhua mafic complex. As the Paleoproterozoic CLGB contains large portion of schist, it seems possible that below the Tanhua mafic complex and country rocks locates schists. The sulphur would have come to the Tanhua mafic complex either by hydrothermal processes from schist or the magma channel would have penetrated the schist and bring the sulphur to the Tanhua mafic complex. The sulphide-bearing liquids are dense and therefore hard to transport vertically upwards (Barnes et al., 2015). Therefore, the source of S should be relative imminent below the Tanhua mafic complex itself if S is brought upwards through magma channel. Other option is downward injection (Barnes et al., 2015), the S source would have been above the Tanhua mafic complex, but it would not exist anymore with current erosion level.

7.3.3 Ore potential of metasomatized mafic intrusives in northern Finland

Four mineralized metasomatized mafic intrusives are known in northern Finland. Neither of these deposits are economical important, but the existence of these deposits indicates that other similar intrusion can exist in northern Finland. Probably the most important element of this type of deposits would be Co-(Cu-Ni). If the size of the mineralization is larger than in the Tanhua mafic complex or Hietakero and the concentration of Co is higher, together with associated Cu and Ni, the deposit could be economical. As Co is important element in green transition, and it is listed as critical raw material in EU, the metasomatized mafic intrusives might be potential source of these elements in future.

The information known by this day suggest that the original mafic magma should be around 2.15 Ga. To be formed this type of deposits need to have source of Co and S as Co is locates in pyrite and pyrrhotite. All known deposits are intruded in supracrustal rocks of CLGB. Similar country rock might be requisite to form this type of deposits as schist would be needed as the source of sulphur and the Co is also probably came in hydrothermal processes from country

rock as vulcanic rocks. As the S and Co are results from hydrothermal process, the hydrothermal activity should have been high to enable this type of deposit. Therefore, the intrusion would be strongly altered along the entire intrusion.

8 Conclusions

1. The rocks of the Tanhua mafic complex can be divided into three different rock types: gabbro, diorite, and tonalite based of the ratio of hornblende, plagioclase and quartz. Additionally, the gabbros of the Tanhua mafic complex can be further divided into four groups: gabbro, oxide gabbro, remained mottled gabbro, and biotitized mottled gabbro.

2. The Tanhua mafic complex is strongly metamorphosed in middle amphibole facies and strongly hydrothermal altered. Plagioclase is altered to albite, scapolite, sericite, and calcite. Pyroxene is restabilized to hornblende and quartz. Hornblende is further altered to biotite.

3. The Tanhua mafic complex has been emplaced by multiple magma pulses based of existing chilled margins and lack of layered structure. Different rock units of the Tanhua mafic complex are in nonspecific order.

4. Co is located into lattice of pyrite replacing Fe^{2+} ion discovered by benchtop micro-XRF. The elementary map shows clear evidence of the relation of Co and S. Pyrite, and chalcopyrite are the major sulphide minerals in the Tanhua mafic complex, present as dissemination and veinlets.

5. Metasomatized mafic intrusives such as the Tanhua mafic complex can be potential economical source of Co-(Cu-Ni). The mafic magma together with supracrustal rock of CLGB and strong hydrothermal process can form economically important Co-enriched sulphide deposits.

6. Zirconium is present as zircon mineral, which explain the high Zr (up to 1300 ppm) content on some whole rock analyses samples. Zircon locates inside or in boundaries of plagioclase grains in the rock types of the Tanhua mafic complex.

Acknowledgements

I would like to thank my supervisors of master thesis PhD Esa Heilimo of University of Turku and PhD Jukka Konnunaho of GTK, who gave me guidance and invaluable advice through this writing process. Also, I would like to thank PhD Tuomo Karinen from GTK and PhD Pietari Skyttä from University of Turku for advice. Special thanks to GTK for the topic and material for my master thesis as well as University of Turku for petrographic microscopes and specially for benchtop micro-XRF instrument and PhD Timo Saarinen for using the micro-XRF instrument and guidance to analyze the results. Thanks also to the crew of GTK drill core archive of Rovaniemi and all other personals who has participated in this project. I want to acknowledge Petroleum Experts Ltd. for the use of MOVE^{TM} under the Academic Software Initiative.

References

Annen, C., 2009. Implications of incremental emplacement of magma bodies for magma differentiation. Tectonophysics 500, 3–10.

Annen, C., Blundy, J. D., Leuthold, J., Sparks, R. S. J., 2015. Construction and evolution of igneous bodies: Towards an integrated perspective of crustal magmatism. Lithos 230, 206221.

Barnes, S. J., Cruden, A. R., Arndt, N., Saumur, B., M., 2015. The mineral system approach applied to magmatic Ni–Cu–PGE sulphide deposits. Ore Geology Reviews 76, 296–316.

Begg, G. C., Hronsky, J. M. A., Griffin, W. L., O'Reilly, S. Y., 2018. Global- to deposit-scale controls on orthomagmatic Ni-Cu(-PGE) and PGE reef ore formation. Processes and Ore Deposits of Ultramafic-Mafic Magmas through Space and Time. Elsevier, 1–46

European Commission, Directorate-General for Internal Market, Industry, Entrepreneurship and SMEs, Grohol, M., Veeh, C., 2023. Study on the critical raw materials for the EU 2023: final report, Publications Office of the European Union. https://data.europa.eu/doi/10.2873/725585, [Online referred 04.09.2023].

Brownscombe, W., Ihlenfeld, C., Coppard, J., Hartshorne, C., Klatt, S., Siikaluoma, J.K., Herrinton, R.J., 2015. The Sakatti Cu-Ni-PGE sulfide deposit in northern Finland. Mineral deposit of Finland. Elsevier Inc, 211–252.

Eales, H. V., Cawthorn, R. G., 1996. The Bushveld Complex. Layered intursions. Elsevier, 181–229.

Fennoscandian Ore Deposits Database (FODD), GTK verkkojulkaisut, [Online referred 10.08.2023].

Greenwood, N. N., Earnshaw, A., 1997. Cobalt, Rhodium, Iridium. Chemistry of the Elements (Second Edition), Butterworth-Heinemann, 1113–1143.

Hanski, E., Huhma, H., 2005. Central Lapland Greenstone Belt. Precambrian Geology of Finland - Key to the Evolution of the Fennoscandian Shield. Developments in Precambrian geology 14, 139–194.

Himmelberg, G. R., Loney, R. A., 1995. Characteristics and Petrogenesis of Alaskan-Type Ultramafic-Mafic Intrusions, Southeastern Alaska. U.S. Geological Survey professional paper 1564, 55p.

Hoover, J. D., 1987a. Petrology of the Marginal Border Series of the Skaergaard Intrusion. Jamtal of Petrology. Vol. 30, Part 2, 399–439.

Huhtelin, T., 2015. The Kemi chromite deposit. Mineral Deposits of Finland. Elsevier, 165–187.

Huhma, H., Hanski, E., Kontinen, A., Vuollo, J., Mänttäri, I., Lahaye, Y., 2018. Sm–Nd and U–Pb isotope geochemistry of the Palaeoproterozoic mafic magmatism in eastern and northern Finland. Geological Survey of Finland, Bulletin 405, 153 p.

Hölttä, P., Heilimo, E., 2017. Metamophic map of Finland. Geological Survey of Finland, Special Paper 60, 77–128.

Iljina, M., Maier, W.D., Karinen, T., 2015. PGE-(Cu-Ni) deposit of the Tornio-Näränkävaara belt of intursions (Portimo, Penikat, and Koillismaa). Mineral deposit of Finland. Elsevier, 133–164.

Irvine, T. N., 1980. Magmatic density currents and cumulus process. American Journal of Sciance, vol. 208-A, 1–58.

Irvine, T. N., Andersen, J. C., Brooks, C. K., 1998. Included blocks (and blocks within blocks) in the Skaergaard intrusion: Geologic relations and the origins of rhythmic modally graded layers. Geological Society of America Bulletin 110, 1398–1447.

Karinen, T. 2010. The Koillismaa Intrusion, northestern Finland – evidence for PGE reef forming process in the layered series. Geological survey of Finland, Bulletin 404, 176 p.

Karinen, T., Konnunaho, J., Salmirinne, H., Taivalkoski, A., 2018. The Hietakero Co-Cu-Ni occurrence. GTK Open File Work Report 4/2018, 16 p.

Karvinen, A., 1982. Tutkimustyöselostus Sodankylän kunnassa valtausalueella Kelujoki 1, Kaiv. REk. N:o 3070 suoritetuista malmitutkimuksisata vuoisna 1980 – 1981. Geologinen tutkimuslaitos, M 06/3719/-82/1/10, 14 p. [In Finnish]

Karvinen, A., 1983. Kobolttitutkimukset Lokan Iso-Povivaarassa Sodamkylän kunnassa vuoisna 1979-1982. Geologinen tutkimuslaitos. M19 /3741/-83/1/10, 21 p. [In Finnish]

Keays, R. R., Lightfoot, P. C., 2004. Formation of Ni–Cu–Platinum GroupElement sulfide mineralization in the Sudbury Impact Melt Sheet. Mineralogy and Petrology 82, 217–258.

Konnunaho, J. P., Hanski, E. J., Bekker, A., Halkoajo, T. A. A., Hiebert, R. S., Wing, B. A., 2013. The Archean komatiite-hosted, PGE-bearing Ni–Cu sulfide deposit at Vaara, eastern Finland: evidence for assimilation of external sulfur and post-depositional desulfurization. Mineralium Deposita 48, 967–989.

Konnunaho, J. P., Halkoaho, T., Hanski, E., Törmänen, T., 2015. Komatiite-hosted Ni-Vu-PGE deposits in Finland. Mineral Deposits of Finland. Elsevier, 93–131.

Konnunaho, J. P., Karinen, T., Autio, U., Telkkälä, P., 2022. Mineral potential studies on Tanhua gabbro. Work report 66, 15 p.

Konnunaho, J. P., Hanski, E. J., Karinen, T. T., Lahaye, Y., Makkonen, H. V., 2018. The petrology and genesis of the Paleoproterozoic mafic intrusion-hosted Co-Cu-Ni deposit at Hietakero NW Finnish Lapland. Bulletin of the Geological Society of Finland, 90, 109–136.

Korvuo, E., 1975. Selostus Savukoski-Martti-Verriöjokivarsi aeromagneettisen anomaliajakson tunnustelututkimuksista syksyllä 1975 sekä käynti Tanhuan Kannusvaarassa. Rautaruukki Oy Malminetsintä raportti N:o RO15/75. 4 p. [In Finnish]

Korvuo, E., 1977. Kylälammen ja Kannusjängän magneettisten anomalioden tunnustelukairaus 1976. Rautaruukki Oy malminetsintä raportti N:o RO 9/77. 5 p. [In Finnish]

Korvuo, E., 1978. Orajärven-Tanhuam alueen emäksisten intrusiivien tutkimukset. Rautaruukki oy. Malminetsintä raportti N:o Ro 4/78. 41 p. [In Finnish]

Köykkä, J., Lahtinen, R., Huhma, H., 2019. Provenance evolution of the Paleoproterozoic metasedimentary cover sequences in northern Fennoscandia: Age distribution, geochemistry, and zircon morphology. Precambrian Research 331, 105364.

Köykkä, J., Luukas J., 2021. Keski-Lapin litostratigrafia ja paleoproterotsooisen Sodankylän ryhmän kivilajiyksiköiden määrittely. Geologian tutkimuskeskus. Tutkimustyöraportti 13/2021. 63 p. [In Finnish]

Latypov, R., Chistyakova, S., 2009. Phase equilibria testing of a multiple pulse mechanism for origin of mafic–ultramafic intrusions: a case example of the Shiant Isles Main Sill, NW Scotland. Geological Magazine. 146, 851–875.

Luolavirta, K., 2018. Magmatic evolution of the Kevitsa igneous complex, northern Finland, and its relation to the associated Ni-Cu-(PGE) mineralization. Res Terrae Publications in Geosciences, University of Oulu. Seria A 37, 62 p.

Maier, W. D., 2005. Platinum-group element (PGE) deposits and occurrences: Mineralization styles, genetic concepts, and exploration criteria. Journal of African Earth Sciences 41, 165–191.

Maier, W. D., Groves, D. I., 2011. Temporal and spatial controls on the formation of magmatic PGE and Ni–Cu deposits. Mineralium Deposita 46, 841–857.

Maier, W. D., Hanski, E. J., 2017. Layered mafic-ultramafic intrusions of Fennoscandia: Europe's treasure chest of magmatic metal deposits. Elements 13, 415–420.

Makkonen, H. V., Halkoaho, T., Konnunaho, J., Rasilainen, K., Kontinen, A., Eilu, P., 2017. Ni-(Cu-PGE) deposits in Finland – Geology and exploration potential. Ore Geology Reviews 90, 667–696.

Mattila, H., 1973. Tanhuan alueen kallioperä kartoitus v. 1973. Rautaruukko Malminetsintä raportti N:o RO 19/73, 14 p. [In Finnish].

Mattila, H., 1974. Karelidit Savukosken Tanhuan alueella, Keski-Lapissa. Pro Gradu. Rautaruukki Oy, Malminetsintä, 89 p. [In Finnish].

McBirney, A.R., 1996. The Skaergaard Intrusion. Layered Intrusions. Elsevier, 147–180.

McCallum, I. S., 1996. The Stillwater Complex. Layered Intrusions. Elsevier, 441–483.

Mondal, S. K., Griffin, W. L., 2018 Introduction. Processes and ore deposits of ultramafic-mafic magmas through space and time. Elsevier, 15–18.

Mutanen, T., 1989a. Koitelaisen malmitutkimukset vuosina 1979-1989. Geologian tutkimuskeskus M19/37/-89/1/10, 81 p. [In Finnish].

Mutanen, T., 1989b. Koitelainen Intrusion and Keivitsa – Satovaara complex. Geological survey of Finland guide 28. 5th Internacional Platinun Symposium, 49 p.

Mutanen, T., 1997. Geology and ore petrology of the Akanvaaraand Koitelainen mafic layered intrusions and the Keivitsa-Satovaara layered complex, northern Finland. Geological Survey of Finland Bulletin 395, 233 p.

Mutanen, T., 2005. The Akanvaara intrusion and the Keivitsa – Satovaara complex, with stops at kaikkivaltiaanlehto and Rantavaara intrusions. Geological Survey of Finland, Guide 51b, 124 p.

Naslund, H.R., McBirney, A.R., 1996. Mechanisms of Formation of Igneous Layering. Elsevier, Layered Intrusions, 1–43.

Neuendorf, K. E., Mehl, J. P., Jackson, J. A., 2011. Glossary of geology. Fifth edition, revised. American Geosciences Institute, 779 p.

Nielsen, T. F. D., Andersen, J. C. Ø., Holness, M. B., Keiding, J. K., Rudashevsky, N. S., Rudashevsky, V. N., Salmonsen, L. P., Tegner, C., Veksler, I. V., 2015. The Skaergaard PGE and Gold Deposit: The Result of in situ Fractionation, Sulphide Saturation, and Magma Chamber-scale Precious Metal Redistribution by Immiscible Fe-rich Melt. Journal of Petrology 56N, 1643–1679.

Orvik, A. A., Slangtad, T., Sørensen, B. E., Millar, I., Hansen, H., 2022. Evolution of the G´alloj´avri ultramafic intrusion from U-Pb zircon ages and Rb-Sr, Sm-Nd and Lu-Hf isotope systematics. Precambrian Research 379, 106813.

Puchtel, I. S., Mundl-Petermeier, A., Horan, M., Hanski, E. J., Blichert-Toft, J., Walker, R. J., 2020. Ultra-depleted 2.05 Ga komatiites of Finnish Lapland: Products of grainy late accretion or core-mantle interaction? Chemical Geology 554, 119801.

Ripley, E. M., Li, C., 2018. Metallic ore deposits associated with mafic to ultramafic igneous rocks. Processes and Ore Deposits of Ultramafic-Mafic Magmas through Space and Time. Elsevier, 79–111.

Rollinson H. R., 1993. Using geochemical data: evaluation, presentation, interpretation. Pearson Education Limited. Longman Scientific and Technical, 352 p.

Santaguida, F., Luolavirta, K., Lappalainen, M., Ylinen, J., Voipio, T., Jones, S., 2015. The Kevitsa Ni-Cu-PGE deposit in Central Lapland Greenstone Belt in Finland. Mineral deposit of Finland. Elsevier, 195–210.

Terry, R. D., Chillingar, G. V., 1955. Comparison charts for visual estimation of percentage composition. Journal sedimentary petrology 25, 229–234.

Thakurta, J., Ripley, E. M., Li, C., 2008a. Geochemical constraints on the origin of sulfide mineralization in the Duke Island Complex, southeastern Alaska. Geochemistry geophysics geosystem 9, Q07003.

Thakurta, J., 2018. Alaska-type complexes and their associations with economic mineral deposits. Processes and ore deposits of ultramafic-mafic magmas through space and time. Elsevier, 269–302.

Vartiainen, H., 1971. Tanhuan suunnan kenttätyöt 1971. Rautaruukki Oy Malminetsintä raportti N:o RO 9/71, 3 p.

Vasilopoulos, M., Molnár, F., O'Brien, H., Lahaye, Y., Lefèbvre, M., Richard, A., André-Mayer, A-S., Ranta, J-P., Talikka, M. 2020. Geochemical signatures of mineralizing events in the Juomasuo Au–Co deposit, Kuusamo belt, northeastern Finland. Mineralium Deposita 56, 1195–1222.

Vernon, R. V., 2004. A Practical Guide to Rock Microstructure. Cambridge University Press. 578 p.

Vuollo, J., Huhma, H., 2005. Paleoproterozoic mafic dikes in NE Finland. Precambrian Geology of Finland- Key to the Evolution of the Fennoscandian Shield. Elsevier, 195–236.

Wager, L. R., 1963. The mechanism of adcumulus growth in the layered series of the Skaergaard intrusion. Mineralogical society of America, Special paper 1, 9 p.

Wager, L.R., & Brown, G.M., 1968. Layered Igneous Rocks. Edinburgh Oliver and Boyd, 558 p.

Wilson, A.H., 1996, The Great Dyke of Zimbabwe. Layered Intrusions. Elsevier, 365–402.

Wyche, N.L., Eilu, P., Koppström, K., Kortelainen, V.J., Niiranen, T., Välimaa, J., 2015. The Suurikuusikko gold deposit (Kittilä mine), Northern Finland. Mineral deposit of Finland. Elsevier, 411–433.

Yilanci, V., Turkmen, N. C., Shah, M. I., 2022. An empirical investigation of resource curse hypothesis for cobalt. Resources Policy 78, 102843.

Appendices

Appendix 1 Resources of deposits of northern Finland

Source Fennoscandian ore deposit database. Referred in 10.08.2023.

Deposit	Commodities	Resources (Mt)	Resources (%/ppm)	Calc method	Calc year
Kemi	Cr_3O_2	130.9	28.935%	PERC Code	2020
Penikat (Kirakkajuppura)	Total	0.011		Non-compliant	1990
	PGE		35.29 ppm		
	Pd		23.5 ppm		
	Pt		10.7 ppm		
	Au		0.13 ppm		
	Rh		1.09 ppm		
Penikat (Sompujärvi)	Total	0.115		Non-compliant	1990
	PGE		32.52 ppm		
	Pd		19.8 ppm		
	Pt		11.3 ppm		
	Au		0.15 ppm		
	Rh		1.42 ppm		
Penikat (Sompuoja)	Total	0.072		Non-compliant	1996
	PGE		34.82 ppm		
	Pt		12.54 ppm		
	Pd		20.69 ppm		
	Au		0.13 ppm		
	Rh		1.59 ppm		
Penikat (Sompujärvi Reef	Total	6.7		Non-compliant	1990
	PGE		8.82 ppm		
	Pd		5.36 ppm		
	Pt		3.08 ppm		
	Au		0.1 ppm		
	Rh		0.38 ppm		
Penikat (Ala-Penikkavaar	Total	3.5		Non-compliant	1990
	PGE		7.95 ppm		
	Pd		6.16 ppm		
	Pt		1.68 ppm		
	Cu		0.210%		
	Au		0.28 ppm		
	Ni		0.100%		
	Rh		0.11 ppm		
Penikat (Paasivaara)	Total	5		Non-compliant	1990
	PGE		6.7 ppm		
	Pd		2.58 ppm		
	Pt		4.04 ppm		
	Cu		0.280%		
	Au		0.61 ppm		
	Rh		0.08 ppm		
	S		0.630%		

Portimo (Siika-Kämä Reef	total	49.4		JORC code	2004
	Pd		2.448 ppm		
	Ni		0.082%		
	Pt		0.665 ppm		
	Cu		0.100%		
	Au		0.07 ppm		
Portimo (Nutturalampi)	Total	0.4		non-compliant	1990
	PGE		7 ppm		
	Pd		5.5 ppm		
	Pt		1.5 ppm		
	Cu		0.090%		
	Au		0.15 ppm		
Portimo (Kilvenlatvalamp	Total	3.2		non-compliant	1995
	Pd		1.419 ppm		
	Cu		0.500%		
	Pt		0.475 ppm		
Portimo (Koivukivalonaap	Total	0.84		non-compliant	1990
	PGE		8.1 ppm		
	Cu		0.100%		
	Au		0.17 ppm		
	Pd		6 ppm		
	Pt		2.1 ppm		
Portimo (Kilvenjärvi offse	total	0.7		non-compliant	1986
	PGE		8.39 ppm		
	Pd		7.27 ppm		
	Cu		2.740%		
	Pt		1.12 ppm		
	Au		0.8 ppm		
	Ag		6.7 ppm		
	S		3.370%		
Portimo (Kivijoki Offset)	Total	0.175		non-compliant	1987
	PGE		2.56 ppm		
	Pd		2.5 ppm		
	Cu		6.110%		
	Au		0.84 ppm		
	Ni		0.280%		
	Pt		0.06 ppm		
Portimo (Yli-Portimojärvi	total	29.8		non-compliant	2000
	PGE		1.3 ppm		
	Pd		1.12 ppm		
	Au		0.11 ppm		
	Pt		0.18 ppm		
Portimo (Niittylampi)	total	1.037		non-compliant	1986
	PGE		0.95 ppm		
	Ni		0.670%		
	Pd		0.68 ppm		
	Pt		0.27 ppm		
	Cu		0.490%		
	Co		460 ppm		
Portimo (Vaaralampi)	total	32		Ni 43-101	2011
	PGE		0.93 ppm		
	Ni		0.310%		
	Pd		0.68 ppm		
	Pt		0.25 ppm		
	Cu		0.200%		
	Au		0.07 ppm		

Portimo (Suhanko)	total	1		non-compliant	1986
	PGE		1.1 ppm		
	Ni		0.200%		
	Cu		0.310%		
	Au		0.03 ppm		
	Pd		0.9 ppm		
	Pt		0.2 ppm		
Portimo (Ahmavaara)	total	187.77		Ni 43-101, UNFC Code	2006
	Pd		0.825 ppm		
	Ni		0.069%		
	Cu		0.175%		
	Pt		0.17 ppm		
	Au		0.1 ppm		
	Co		0.007%		
Portimo (Konttijärvi)	total	75.24		CIM standarts, UNFC Cc	2006
	Pd		0.953 ppm		
	Ni		0.046%		
	Cu		0.097%		
	Pt		0.271 ppm		
	Au		0.073 ppm		
	Co		0.004%		
Koillismaa (Murtolampi)	total	3		Ni 43-101	2022
	Pd		0.4 ppm		
	Pt		0.22 ppm		
	Au		0.05 ppm		
	Cu		0.110%		
	Ni		0.140%		
	Co		94 ppm		
Koillismaa (Kaukua)	total	66		Ni 43-101	2022
	Pd		0.578 ppm		
	Ni		0.121%		
	Pt		0.21 ppm		
	Au		0.073 ppm		
	Cu		0.136%		
	Co		73.095 ppm		
Koillismaa (Haukiaho)	total	18.9		Ni 43-101	2022
	Pd		0.27 ppm		
	Pt		0.11 ppm		
	Ni		0.140%		
	Au		0.1 ppm		
	Cu		0.180%		
	Co		54.3 ppm		
Koillismaa (Lavotta)	total	3		non-compliant	1980
	PGE		0.4 ppm		
	Ni		0.210%		
	Pd		0.3ppm		
	Pt		0.1 ppm		
	Au		0.05 ppm		
	Cu		0.260%		
	Ag		0.07 ppm		
Koillismaa (Rusamo)	Total	1.5		non-compliant	1983
	PGE		0.65 ppm		
	Ni		0.240%		
	Cu		0.360%		
	Au		0.15 ppm		
	Pd		0.46 ppm		
	Pt		0.19 ppm		

Koillismaa (Mustavaara)	Total	145.9		CIM standarts	2020
	V		1383 ppm		
	Fe		96110 ppm		
	Ti		5640 ppm		
Sakatti	Total	44.4		JORC code	2016
	Ni		0.959%		
	Cu		1.902%		
	Co		0.046%		
	Pt		0.639 ppm		
	Pd		0.489 ppm		
	Au		0.33 ppm		
Kevitsa	Total	138.74		PERC code	2021
	Ni		0.223%		
	Cu		0.349%		
	Pd		0.084 ppm		
	Pt		0.132 ppm		
	Co		0.011%		
	Au		0.074 ppm		
Koitelainen (Koitelainen '	V	5.817	1.260%	JORC code	2019
Koitelainen (Koitelainen	total	70		non-compliant	1997
	Cr_3O_2		21.000%		
	V		0.400%		
	PGE		1.1 ppm		
Koitelainen (Koitelainen	total	2		non-compliant	2002
	Cr_3O_2		23.000%		
	Pd		0.9 ppm		
	Pt		0.48 ppm		
	PGE		1.38 ppm		
Akanvaara (Akanvaara UC	total	18.1		non-compliant	1998
	Cr_3O_2		22.800%		
	V		0.400%		
	PGE		0.92 ppm		
Akanvaara (Akanvaara Ga	total	20		non-compliant	1998
	V		0.340%		
	Cu		0.100%		
	Ag		2.5 ppm		
Akanvaara (Akanvaara UL	Cr_3O_2	10	15.260%	non-compliant	2006
Akanvaara (Akanvaara LC)	total	27		non-compliant	1998
	Cr_3O_2		15.650%		
	Pd		0.08 ppm		
	Pt		0.52 ppm		
	PGE		0.6 ppm		
Kelujoki	total	1.5			
	Cu		0.200%		
	Co		0.030%		

Appendix 2 Thin section chart

number	drillcore number	hornblende	plagioclase	quartz	biotite	magnetite	scapolite	amphibole	augite	average g	maximum	texture	2. texture	3. texture	4. texture	oriented	rock type	notes
201394	U5212019R13 76.25	80	20							0.2	0.6	granoblastic				none	gabbro	strogly altered
201395	U5212019R13 78.75	80	20							0.1	0.5	granoblastic	exsolution			none	gabbro	strogly altered
201400	U5212019R13 152.60	80	20							0.2	0.7	granoblastic				none	gabbro	
201401	U5212019R13 159.80	65	35							0.1	0.8	granoblastic				none	gabbro	
201408	U5212019R3 73.35	70	30							0.4	0.9	granoblastic	exsolution	zoned pl		none	gabbro	
201412	U5212019R3 125.35	40	35		20	5				0.4	2.1	granoblastic	exsolution			strong	oxide gabbro	
201428	U5212020R15 101.50	85	15							0.4	0.9	granoblastic	exsolution			none	gabbro	
201429	U5212020R15 115.20	75	25							0.4	1.5	granoblastic	exsolution	ti-mg rim		none	remained mottlec	strogly altered
201439	U5212020R16 41.40	55	45							0.3	1.3	granoblastic	exsolution	ti-mg rim		weak	gabbro	
201443	U5212020R16 105.30	80	5				15			0.4	1	granoblastic	exsolution			none	gabbro	
201450	U5212020R16 298.40	70	15		5		10			0.4	1.9	granoblastic	exsolution	mottled		weak	gabbro	minor accumulation of bi
201376	U5212019R7 56.85	15	55		10	20				0.3	1.1	granoblastic	poikilitic			weak	diorite	mg dissemination/veinlets
201417	U5212019R3 210.40	30	35		20	15				0.2	1	granoblastic	mottled			moderate	oxide gabbro	minor accumulation of bi
201423	U5212019R3 277.15	10	55	5		30				0.7	2.2	granoblastic	exsolution	poikilitic		none	diorite	cl vein
201424	U5212019R3 297.10	10	55	10	5	20				0.6	1.1	granoblastic	exsolution	poikilitic		weak	diorite	
201425	U5212019R3 314.25	10	45	15		30				0.5	1	granoblastic	exsolution	overprint	ti-mg rim	none	diorite	
201433	U5212019R8 162.40	5	70		10	15				0.4	0.7	granoblastic	mottled			weak	mottled diorite	minor accumulation of bi
201434	U5212019R8 172.65	25	55			20				0.5	1	granoblastic	poikilitic	exsolution	ti-mg rim	none	diorite	
201435	U5212019R8 199.50	30	50			20				0.3	1.1	granoblastic	poikilitic	exsolution		none	diorite	
201445	U5212020R16 129.80		40	40	10	10				0.7	1.9	granoblastic	poikilitic			weak	magnetite tonalite	
201378	U5212019R6 105.50	45	45				5			0.4	1	granoblastic	ti-mg rim	zoned pl	exsolution	weak	remained mottled	
201379	U5212019R6 131.35	55	40				5			0.4	1	granoblastic	poikilitic	ti-mg rim	exsolution	weak	remained mottled	
201380	U5212019R6 169.95	55	40							0.3	0.7	granoblastic	poikilitic	ti-mg rim	exsolution	weak	remained mottled	
201381	U5212019R6 176.30	30	35		35					0.2	0.5	granoblastic	exsolution			strong	gabbro	minor amout mg
201382	U5212019R14 6.50	45	45			10				0.4	1.3	granoblastic	poikilitic	ti-mg rim	exsolution	none	oxide gabbro	
201383	U5212019R14 22.20	45	45			10				0.3	0.7	granoblastic	exsolution			weak	oxide gabbro	
201384	U5212019R14 30.25		25			5		70		0.2	1	granoblastic				strong	oxide gabbro	Hbl cut is colourless
201385	U5212019R14 41.85	40	40		15	5				0.2	0.6	granoblastic	exsolution			moderate	oxide gabbro	minor accumulation of bi
201386	U5212019R14 64.30	35	50			15				0.2	2	granoblastic	poikilitic	zoned pl	exsolution	none	oxide gabbro	
201387	U5212019R14 84.50	50	50							0.1	0.2	granoblastic				moderate	vulcanite	
201389	U5212019R11 153.65	45	45			10				0.1	0.5	granoblastic	ti-mg rim	exsolution		moderate	oxide gabbro	
201390	U5212019R11 226.75	45	35			20				0.3	0.8	granoblastic	exsolution			weak	remained mottled	
201404	U5212019R5 110.65	35	45			20				0.3	0.6	granoblastic	poikilitic	exsolution		weak	oxide gabbro	
201405	U5212019R5 127.30	35	40		25					0.2	0.5	granoblastic				moderate	gabbro	
201406	U5212019R5 145.30	45	45			10				0.1	0.3	granoblastic				weak	oxide gabbro	strogly altered
201413	U5212019R3 155.15	45	45		15	5				0.3	1	granoblastic	exsolution			moderate	remained mottlec	minor accumulation of bi
201414	U5212019R3 160.85	55	45							0.1	0.6	granoblastic				strong	gabbro	veins
201415	U5212019R3 180.20	55	45							0.1	0.7	granoblastic				strong	gabbro	veins
201416	U5212019R3 193.70	40	45			15				0.2	0.5	granoblastic	exsolution			weak	oxide gabbro	
201418	U5212019R3 218.50	50	45		5					0.1	0.6	granoblastic				moderate	vulcanite	

number	drillcore number	quartz	biotite	calcite	pyrite	ilmenite	magnetite	titanite	zircon	calcite	apatite	chalcopyri	sericite	uralite	scapolite	honrblenc	chlorite	chalcocite	bornite	pyrrhotite
201394	U5212019R13 76.25				py			ti				ccp	ser	ur						
201395	U5212019R13 78.75	qtz			py			ti					ser							
201400	U5212019R13 152.60				py		mg					ccp								
201401	U5212019R13 159.80				py		mg					ccp						cc	br	
201408	U5212019R3 73.35	qtz			py		mg	ti				ccp		ur						
201412	U5212019R3 125.35	qtz			py	il						ccp						cc	br	
201428	U5212020R15 101.50	qtz				il	mg	ti												
201429	U5212020R15 115.20	qtz			py	il	mg	ti				ccp	ser		scp					
201439	U5212020R16 41.40	qtz			py		mg	ti				ccp		ur				cc	br	
201443	U5212020R16 105.30	qtz			py			ti						ur						
201450	U5212020R16 298.40	qtz			py			ti												
201376	U5212019R7 56.85				py						ap	ccp						cc	br	
201417	U5212019R3 210.40				py	il		ti				ccp								
201423	U5212019R3 277.15											ccp					cl			
201424	U5212019R3 297.10	qtz			py			ti				ccp								ph
201425	U5212019R3 314.25				py	il		ti				ccp						cc	br	ph
201433	U5212019R8 162.40	qtz			py			ti				ccp								ph
201434	U5212019R8 172.65	qtz	bi		py			ti				ccp						cc	br	
201435	U5212019R8 199.50	qtz	bi		py															ph
201445	U5212020R16 129.80				py							ccp				hbl				
201378	U5212019R6 105.50	qtz			py		mg	ti				ccp		ur						
201379	U5212019R6 131.35	qtz			py		mg	ti				ccp		ur				cc	br	
201380	U5212019R6 169.95	qtz			py		mg	ti				ccp	ser		scp			cc	br	
201381	U5212019R6 176.30				py		mg		zr			ccp		ur				cc	br	
201382	U5212019R14 6.50	qtz	bi		py			ti				ccp						cc	br	ph
201383	U5212019R14 22.20	qtz	bi		py							ccp		ur				cc	br	
201384	U5212019R14 30.25		bi		py							ccp								
201385	U5212019R14 41.85	qtz			py		mg		zr			ccp	ser	ur						
201386	U5212019R14 64.30	qtz			py		mg					ccp						cc	br	ph
201387	U5212019R14 84.50		bi		py		mg					ccp						cc	br	
201389	U5212019R11 153.65	qtz						ti				ccp								
201390	U5212019R11 226.75	qtz	bi		py							ccp	ser					cc	br	
201404	U5212019R5 110.65	qtz	bi		py							ccp						cc	br	ph
201405	U5212019R5 127.30						mg	ti				ccp							br	
201406	U5212019R5 145.30																			
201413	U5212019R3 155.15				py	il		ti				ccp								
201414	U5212019R3 160.85				py	il	mg					ccp					cl	cc	br	
201415	U5212019R3 180.20		bi		py	il											cl			
201416	U5212019R3 193.70	qtz			py	il		ti				ccp								
201418	U5212019R3 218.50														scp					

201419	U5212019R3 223.30	20	35		15	30				0.2	0.6	granoblastic	exsolution			strong	oxide gabbro	qtz vein
201427	U5212020R15 85.40	60	35		5					0.3	0.9	granoblastic	exsolution			weak	gabbro	metasomatosed vein
201430	U5212020R15 136.95	55	45							0.5	1.4	granoblastic	exsolution			weak	remained mottled	
201431	U5212019R8 26.20	35	40		5	10				0.4	0.9	granoblastic	exsolution			none	oxide gabbro	
201432	U5212019R8 44.35	45	45			10				0.1	0.6	granoblastic	exsolution			moderate	oxide gabbro	black vein and qtz vein
201436	U5212019R8 219.65	35	40			25				0.2	0.9	granoblastic	poikilitic	exsolution	ti-mg rim	none	oxide gabbro	
201437	U5212019R8 226.75	30	40			30				0.3	1.5	granoblastic	poikilitic	exsolution		none	oxide gabbro	
201438	U5212020R16 26.65	50	50							0.1	0.5	granoblastic	exsolution			moderate	vulcanite	
201440	U5212020R16 52.25	30	50			20				0.3	1.3	granoblastic	exsolution	poikilitic		weak	oxide gabbro	
201441	U5212020R16 91.25	15	40	25		20				0.4	0.8	granoblastic	exsolution			none	diorite	
201442	U5212020R16 97.80	10	50	10		30				0.4	2	granoblastic	poikilitic	exsolution		none	diorite	
201448	U5212020R16 210.45	55	45							0.3	1.4	granoblastic	exsolution	ti-mg rim		moderate	gabbro	
201449	U5212020R16 275.95	60	40							0.3	1.5	granoblastic	altered			weak	gabbro	
201881	U5212020R10 11.65	40	35			25				0.2	0.7	granoblastic	exsolution	zoned pl		none	oxide gabbro	
201882	U5212020R10 140.95	50	50							0.1	0.5	granoblastic				moderate	vulcanite	vein
201883	U5212020R10 34.70	45	50			5				0.2	2	granoblastic	exsolution			weak	remained mottled	
201884	U5212020R10 130.30	50	50							0.4	1.3	granoblastic	exsolution	zoned pl	ti-mg rim	weak	remained mottled	
201885	U5212020R11 219.19		55	5					40	0.9	2.2					none	gabbro	
201886	U5212020R10 112.55	50	50							0.3	0.8	granoblastic	exsolution			moderate	remained mottled	
201887	U5212020R10 74,25	50	50							0.4	1.7	granoblastic	exsolution	ti-mg rim		weak	remained mottled	
201398	U5212019R13 138.50	35	30		25	10				0.3	1.1	granoblastic	mottled	exsolution		weak	biotitized mottlec	accumulation bi
201402	U5212019R5 83.30	45	40		15					0.5	1.6	granoblastic	mottled	exsolution		moderate	biotitized mottlec	accumulation bi
201403	U5212019R5 98.65	35	35		30					0.4	0.6	granoblastic	mottled	exsolution		strong	biotitized mottlec	vein, accumulation bi
201409	U5212019R3 81.90	45	35		20					0.4	1.8	granoblastic	exsolution	mottled		weak	biotitized mottlec	accumulation bi
201410	U5212019R3 95.45	35	40		25					0.5	1.3	granoblastic	exsolution	mottled	mg-ccp-br-cc	moderate	biotitized mottlec	accumulation bi
201411	U5212019R3 110.20	35	35		30					0.6	1.5	granoblastic	exsolution	mottled	mg-ccp-br-cc	moderate	biotitized mottlec	accumulation bi
201397	U5212019R13 116.15	35	35		30					0.3	0.9	granoblastic	mottled	exsolution		moderate	biotitized mottlec	accumulation bi
201420	U5212019R3 234.10	25	35		15	25				0.3	1.1	granoblastic	exsolution	mottled		strong	oxide gabbro	
201421	U5212019R3 253.20	10	45		15	30				0.4	1.4	granoblastic	exsolution	mottled	poikilitic	strong	biotitized mottlec	qtz vein
201422	U5212019R3 264.15	25	30		20	25				0.4	1.6	granoblastic	exsolution	mottled	poikilitic	moderate	biotitized mottlec	accumulation bi
201377	U5212019R7 120.70	5	70	20		5				0.5	1.3	granoblastic				none	magnetite tonalite	altered
201388	U5212019R14 92.40		65	20		15				0.7	2	granoblastic				none	magnetite tonalite	
201391	U5212019R4 45.80		65	20	5	10				0.2	0.5	granoblastic	poikilitic			weak	magnetite tonalite	
201392	U5212019R4 65.45		70	20		25				0.7	2	granoblastic	poikilitic			none	magnetite tonalite	
201393	U5212019R4 88.25		65	20		25				0.4	1.5	granoblastic				none	magnetite tonalite	
201407	U5212019R5 151.55		45	25		30				0.5	1	granoblastic	overprint	zoned pl		none	magnetite tonalite	
201426	U5212019R3 330.35	5	45	40		10				0.6	1.2	granoblastic	overprint			none	magnetite tonalite	
201444	U5212020R16 115.80		45	35		20				0.5	1.2	granoblastic	poikilitic			none	magnetite tonalite	strogly altered
201446	U5212020R16 156.30		50	35		10				0.7	2	granoblastic	poikilitic	overprint		none	magnetite tonalite	
201447	U5212020R16 170.65		45	40		15				0.8	3.1	granoblastic	overprint			none	magnetite tonalite	strogly altered
201396	U5212019R13 82.35					10		90		0.3	1.2					none	pyroxenite	
201399	U5212019R13 149.05					10		90		0.3	0.7					none	pyroxenite	

201419	U5212019R3 223.30	qtz			py	il						ccp						cc	br	
201427	U5212020R15 85.40				py		mg	ti				ccp					cl	cc	br	
201430	U5212020R15 136.95	qtz			py							ccp								
201431	U5212019R8 26.20	qtz			py			ti				ccp						cc	br	
201432	U5212019R8 44.35	qtz			py							ccp					cl			
201436	U5212019R8 219.65	qtz	bi		py			ti												ph
201437	U5212019R8 226.75	qtz	bi		py				zr											ph
201438	U5212020R16 26.65	qtz	bi		py	il														
201440	U5212020R16 52.25	qtz	bi		py	il		ti				ccp							br	
201441	U5212020R16 91.25		bi		py	il		ti				ccp							br	
201442	U5212020R16 97.80		bi		py			ti	zr			ccp						cc	br	
201448	U5212020R16 210.45	qtz			py		mg	ti				ccp								
201449	U5212020R16 275.95		bi		py		mg													
201881	U5212020R10 11.65	qtz			py	il							ser							
201882	U5212020R10 140.95				py	il											cl			
201883	U5212020R10 34.70	qtz	bi			il														
201884	U5212020R10 130.30	qtz				il	mg	ti				ccp	ser		scp					
201885	U5212020R11 219.19			ca			mg										cl			
201886	U5212020R10 112.55	qtz			py		mg					ccp			scp			cc	br	
201887	U5212020R10 74,25	qtz			py		mg	ti				ccp			scp			cc	br	
201398	U5212019R13 138.50	qtz			py		mg				ap	ccp		ur				cc	br	
201402	U5212019R5 83.30	qtz			py		mg					ccp						cc	br	
201403	U5212019R5 98.65	qtz					mg					ccp						cc	br	
201409	U5212019R3 81.90	qtz			py		mg					ccp								ph
201410	U5212019R3 95.45	qtz			py		mg					ccp						cc	br	
201411	U5212019R3 110.20				py		mg					ccp						cc	br	
201397	U5212019R13 116.15		bi									ccp						cc	br	
201420	U5212019R3 234.10	qtz			py	il						ccp								ph
201421	U5212019R3 253.20	qtz			py	il						ccp						cc	br	ph
201422	U5212019R3 264.15	qtz			py	il														ph
201377	U5212019R7 120.70								zr	ca		ccp						cc	br	
201388	U5212019R14 92.40		bi		py			ti				ccp				hbl		cc		
201391	U5212019R4 45.80				py			ti				ccp						cc	br	
201392	U5212019R4 65.45		bi				mg	ti				ccp				hbl		cc	br	
201393	U5212019R4 88.25		bi		py							ccp				hbl		cc	br	
201407	U5212019R5 151.55							ti				ccp	ser			hbl				
201426	U5212019R3 330.35				py			ti	zr		ap				scp					
201444	U5212020R16 115.80				py			ti				ccp			scp					
201446	U5212020R16 156.30				py			ti				ccp			scp			cc	br	
201447	U5212020R16 170.65		bi		py			ti				ccp			scp	hbl		cc		
201396	U5212019R13 82.35				py		mg					ccp						cc	br	
201399	U5212019R13 149.05				py		mg													ph